ANALYSIS OF ACOUSTIC DAMPING IN DUCT TERMINATED BY POROUS ABSORPTION MATERIALS BASED ON ANALYTICAL MODELS AND FINITE ELEMENT SIMULATIONS

By

QIMING GUAN

A thesis submitted to the

Graduate School-New Brunswick

Rutgers, The State University of New Jersey

In partial fulfillment of the requirements

For the degree of

Master of Science

Graduate Program in Mechanical and Aerospace Engineering

Written under the direction of

Kimberly Cook-Chennault

And approved by

_____

_____

_____

New Brunswick, New Jersey

May, 2015

ABSTRACT OF THE THESIS

ANALYSIS OF ACOUSTIC DAMPING IN DUCT TERMINATED BY POROUS ABSORPTION MATERIALS BASED ON ANALYTICAL MODELS AND FINITE ELEMENT SIMULATIONS

By QIMING GUAN

Thesis Director:

Professor Kimberly Cook-Chennault

Acoustic absorption materials are widely used today to dampen and attenuate the noises which exist almost everywhere and have adverse impact upon daily life of human beings. In order to evaluate the absorption performance of such materials, it is necessary to experimentally determine acoustic properties of absorption materials. Two experimental methods, one is Standing Wave Ratio Method and the other is Transfer-Function Method, which also totally called as Impedance Tube Method, are based on two analytical models people have used to evaluate and validate the data obtained from acoustic impedance analyzers.

This thesis first reviews the existing analytical models of previous two experimental methods in the literature by looking at their analytical models, respectively. Then a new analytical model is developed is developed based on One-Microphone Method and Three-Microphone Method, which are two novel experimental approaches. Comparisons are made among these analytical models, and their advantages and disadvantages are discussed.

ACKNOWLEDGMENT

First of all, I would like to give my sincere thanks to my dear advisor, Dr. Kimberly Cook-Chennault. From her, I found the way and style to do my research about acoustic damping in Department of Mechanical and Aerospace Engineering at Rutgers University and I enthusiastically thank her for her patience, which allowed me enough time to complete my thesis. Prof. Cook-Chennault's scientific vision, knowledge and intelligence provided me with a wonderful graduate experience, also including her insightful advice on my research.

I also want to cordially thank Dr. Haim Baruh for his financial support these years for my graduate study. I am also very thankful for his thoughtfulness and encouragement for my daily life in the U.S. Also, I thank my committee members, Prof. Kimberly Cook-Chennault, Prof. Haim Baruh, and Prof. Xiaoli Bai, for their time, help, and assistance with my thesis defense.

Many thanks are also due to numerous people who helped me with my research work. First, I would like to thank my helpful buddy in our research group, Eric Bickford, for his discussions and help with the theory of impedance tube and finite element analyses. Thanks are also given to my excellent roommates and classmates, Bowen Huang, Rui Wang, Zhizhong Dong and Han Sun. I really appreciate all the time that we went through in the past three years in Rutgers University.

The love from the bottom of my heart is reserved for my Mom, Yejun Song, my Dad, Helou Guan and my girlfriend Ke Ke. You are the whole of my life. To Heaven, I thank God for the abundant blessings and graces He has bestowed on me.

CONTENTS

Chapter 1

1 Introduction

1.1 Background and Motivation

Sound, or the so called sound wave, is defined as the mechanical vibration in an elastic medium such as air, water and steel. Sound waves propagate as longitudinal or transverse waves that are audible or perceived by a hearing mechanism. Acoustic damping materials are used to dampen or absorb sound, i.e. absorb incident sound energy with their porosity, membrane or resonance. Materials such as these are ubiquitously used to eliminate or dampen noise pollution that can be generated by aircrafts, motor vehicles, and industrial machinery. Sound-absorbing materials have been widely used to reduce noise and vibration of the aircraft engine, and in the aircraft to protect passengers from noise and vibration.[1] Environmental noise has a financial impact on industrial, commercial and residential sectors of business, e.g., prices of homes, airlines, etc. NASA and the United States Air Force have established several initiatives aimed at reducing the noise generated from planes on surrounding communities, as noise pollutions negatively influences house price in addition to inhabitant health.[2] For example, in 2012, at the 48th AIAA Aerospace Science Meeting the Deputy Director of the Integrated Systems Research Program of the Aeronautics Research Mission Directorate, stated that noise reduction was one of the main challenges for the directorate[3], and it was the most significant hindrance to NASA capacity growth. Undoubtedly, noise, whether radiated outside or within the aircraft, is relevant to the aircraft industry, to the US Air Force and to NASA, in addition to the areas and communities exposed to the noise pollution.

Noise range	Obs.	OLS		Spatial	
		Estimated impact on house price	Probability	Estimated impact on house price	Probability
<=40 dB	1,259	2.1%	0.001	3.6%	0.000
41-45 dB	3,265	-1.0%	0.005	-0.7%	0.132
46-50 dB	11,638	-0.7%	0.002	-0.3%	0.195
51-55 dB	31,616	0.3%	0.043	-0.3%	0.050
56-60 dB	39,177	0.0%	*default*	0.0%	*default*
61-65 dB	20,669	-0.6%	0.001	0.2%	0.322
66-70 dB	5,064	-1.1%	0.000	-0.7%	0.040
71-75 dB	732	-3.2%	0.000	-3.9%	0.000
>=76 dB	154	-5.4%	0.000	-5.2%	0.001
Loglik		-475,894		-458,665	
rmse		0.196		0.162	
obs		113,574		113,574	

Table 1.1 Estimated price impact of noise, compared to 56-60 decibel (reproduced without permission with caption from [2]).

In Table 1.1, it can be noticed that with the growth of noise intensity compared to 56-60 decibel, the estimated impact on house price will be increased, which means that the noise has a negative impact upon house price.

Since noise pollution has an impact on the US national economy, researchers have focused investigation and development of materials that dampen and eliminate acoustic noise.

Acoustic damping materials are evaluated using several experimental techniques: Impedance Tube Method, Reverberation Room Method and Tone-Burst Method (schematic shown in Fig. 1.4). The acoustic impedance of a material describes the ability the acoustic material to absorb sound. There are primarily two analytical approaches used to estimate the acoustic impedance of a material. One approach is the Standing Wave Ratio (SWR) method (schematic depicted in Fig. 1.1), and the other is Transfer Function Method – so-called, Two-Microphone Method (schematic depicted in Fig. 1.2). More

types of experimental acoustic impedance tubes exist, such as the one-microphone and three-microphone method, though there are (to our knowledge) only two analytical approaches for the prediction of the Standing Wave Ratio Method and Transfer Function Method. There are two international standards used to describe the experimental methods used to evaluate the acoustic impedance, one is ISO 10534-1[5] and the other is ISO 10534-2.[6]

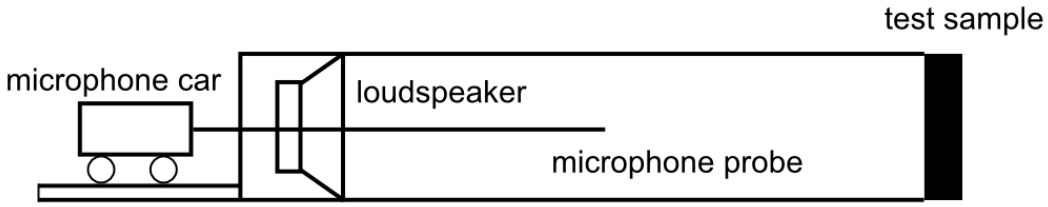

Fig 1.1 The impedance tube schematics for method using standing wave ratio (SWR).

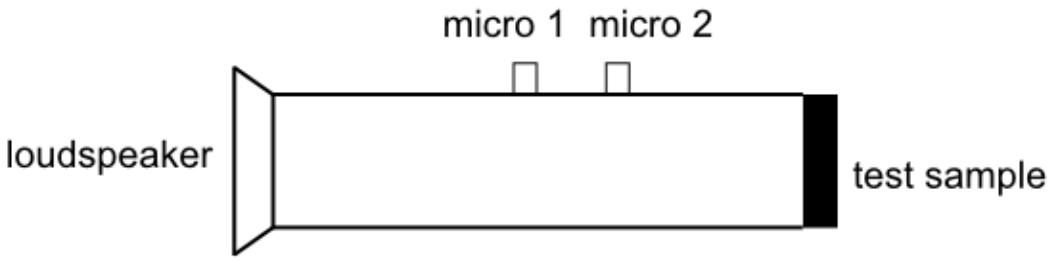

Fig 1.2 The impedance tube schematics for method using transfer-function (TMM).

Fig 1.3 The photograph for Reverberation Room Method (reproduced without permission with the caption from [13]).

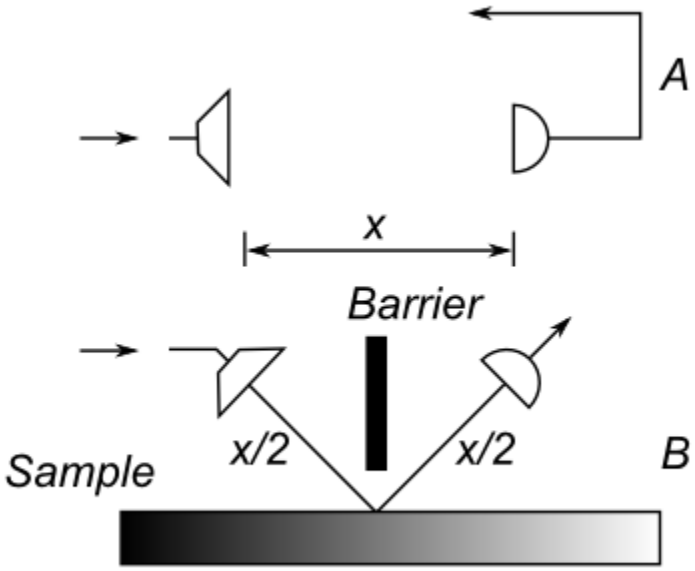

Figs 1.4 Determination of the absorption coefficients of materials by a Tone-Burst Method.[14]

In this thesis, two novel analytical approaches for prediction of the acoustic impedance from the one-microphone and three-microphone method are presented. These models will be derived and presented sequentially.

There are two components which constitute sound: amplitude and frequency. The amplitude of a sound wave is the measurement of the degree of change (positive or negative) in atmospheric pressure (the compression and rarefaction of air molecules) caused by acoustic waves. Amplitude is directly related to the acoustic energy or intensity of a sound. The frequency of a sound wave is the number of cycles per unit time, and directly related to wavelength. Decibel and hertz are used to interpret sound's amplitude and frequency, respectively.

As noise pollution becomes an important issue, especially in big cities, the government has begun to regulate noise pollution so as to prevent hearing loss, insomnia, and other health related issues influenced by environmental noise. Instruments such as acoustic impedance analyzers are used to evaluate the ability of specific materials to absorb and/or deflect sound. In particular, these instruments enable engineers and designers to make appropriate decisions pertaining to a material's effectiveness at absorbing sound, and over which frequency ranges the material is most effective.

1.2 Basic Concepts and Definitions

When a sound wave comes into contact with a material, sound energy can be: 1) dissipated or absorbed by the material and transformed into heat energy and/or 2) reflected by the surface of the material to generate a reflected sound wave. The sound wave can also penetrate the material if it has sufficient energy. To describe the acoustic properties of a material, two basic concepts need to be introduced: one is the acoustic impedance and the other is the absorption factor or absorption coefficient. The acoustic impedance is the amount of sound pressure needed to overcome the resistance for the vibration of molecules of a particular medium at a given frequency. The acoustic impedance is the ratio of the complex acoustic pressure, p, to complex acoustic volume velocity, vS, at the surface of material. As such, the acoustic impedance is a complex number, where the real part, which is the resistive part, represents the energy transfer of an acoustic wave, while the imaginary part, which is the reactive part, represents pressure that is out of phase with the motion. Since the reactive part causes no average energy transfer, it is associated with energy loss. The reflect factor r is the ratio of the reflected

sound energy (sound that comes from the surface of the material), to the incident sound energy (sound that enters the surface of the material). The absorption coefficient α is a measure of the efficiency of a surface or material in absorbing sound. For example, if 55% of the incident sound energy is absorbed, the absorption coefficient is said to be 0.55. The absorption coefficient α can be calculated when given the reflect factor r. The absorption coefficient α of a material varies with frequency and with the angle at which the sound wave impinges upon the material. Furthermore, the sound absorption of a material is a function of multiple variables, e.g. acoustic impedance and absorption coefficient, which are macroscopic properties; porosity, flow resistivity, tortuosity, characteristic length, which are microstructural properties and will be introduced in Chapter 3.

The above two macroscopic properties, acoustic impedance and absorption coefficient, are closely related to the sound absorption materials and it is necessary to measure them via experimental methods so as to evaluate the acoustic property of a certain material in a certain frequency range. There are several approaches to determining the acoustic impedance and absorption coefficient, such as the Standing Wave Ratio Method, Transfer-Function Method, Reverberation Room Method (schematic provided in Fig. 1.3), and Tone-Burst method. The first three methods have standards that are associated with them. The Standing Wave Ratio Method must adhere to the requirements provided in ISO-10534-1[5] (or ASTM C384-04[7]), and the Transfer-Function Method must adhere to the requirements established in ISO-10534-2[6] (or ASTM E1050-98[8]), which were developed in 1996 and 1998, respectively. Many of the methods require use of an acoustic impedance tube for measurement of critical acoustic impedance values.

The acoustic impedance tube is a common experimental apparatus that is used to measure the absorption coefficient and acoustic impedance of a porous sound absorbing material according to the theory of the standing wave. The standing wave is generated by the superposition of the incident and reflected sound waves in the impedance tube. These two methods are widely used to calculate the normal incident acoustic impedance and absorption factor, by measuring sound pressure differentials and recording sound frequency values. The reverberation room method is also used to evaluate the acoustic properties of a material. The difference in the reverberation time with and without the material yields the absorbing properties of the material[9], according to ISO-3547[10] (or ASTM C423[11]). This method is based on the comparison of the reverberation time t_1 (room with sample) with the time t_2 (room without sample), which yields the number of absorption units the sample adds to the room. The reverberation room method is widely used. Other methods, such as the Tone-Burst method, can be used to measure the inclined incident acoustic impedance and absorption coefficient. The Tone-Burst method has no standard associated with it, and is not commonly used in industry. The theory of this method hinges on the comparison of the reflected pulse with the un-reflected pulse at distance x to determine the absorption coefficient of the sample. In this method, it is assumed that if the is pulse short enough, the time gate can be opened only for the desired sound pulse, filtering the interfering pulses.

The method using standing wave ratio is well-established, but slow, so it was replaced by transfer-function method because of its quickness and accuracy[12]. Both standing wave ratio and transfer-function methods have the disadvantage of only being able to provide the normal incident acoustic impedance. However, they are relative

simple, and can quickly and accurately allow for the calculation of the acoustic coefficient. Also, these two methods only require a small sample, modest demands in terms of supporting equipment, which makes these methods preferable in comparison to the reverberation room method.

The advantage of the reverberation room method is that it can measure randomly incident acoustic impedance. However, this method requires much bigger samples of tested material and special lab facilities, which are not always available. Also the diffraction of sound from the edge of the sample makes the measurement of time not accurate, becoming primary drawbacks of this method.

The advantage of the Tone-Burst method's arrangement is that it can be used to measure the sound absorption coefficient of a material at any desired angle of incidence, which offsets the drawback of the impedance tube method.

1.3 Research Objective and Strategies

The objective of this thesis is to establish two analytical methods for two experimental approaches for the measurement of acoustic impedance properties, e.g. the one-microphone and three-microphone approach. To our knowledge, these approaches are new to the literature.

In this thesis, attention is paid to acoustic properties of the material, which is exposed to the normal incident sound wave. Fundamental concepts about wave and vibration will be reviewed together with some fluid mechanics as the foundation of the theoretical model. Main efforts are taken to look at the physical theory of the acoustic damping and sound attenuation in porous materials. A finite element model is created using ACTRAN

to simulate the real impedance tube in the laboratory. Acoustic properties of the porous materials are determined by analytical approaches, using data obtained from the finite element model using MATLAB. A new one-microphone method and three-microphone method are analytically modeled, and the results will be compared with the transfer-function method, one-microphone method, and three-microphone method based on the data obtained from finite element model in ACTRAN.

1.4 Outline of This Thesis

In Chapter 2, the analytical model of the standing wave ratio method and transfer-function method are described. In Chapter 3, analytical methods for the prediction of the one-microphone and three-microphone methods are detailed. Chapter 4 introduces microstructural properties of porous material and briefly presents the procedure of finite element modeling of an impedance tube in ACTRAN. In Chapter 5 the results are plotted according to calculation of the data obtained from the finite element model in MATLAB using the methods described Chapters 2 and 3. Chapter 5 presents comparison of results of different analytical models, the predictions from the analytical approaches will be compared to finite element models created by ACTRAN software to simulate the experiments. In Chapter 6, conclusions from the work and future research direction are provided.

References

1. Arenas, J. P.; Crocker, M. J., Recent trends in porous sound-absorbing materials. *Sound & vibration* **2010,** *44* (7), 12-18.
2. Theebe, M. A., Planes, trains, and automobiles: the impact of traffic noise on house prices. *The Journal of Real Estate Finance and Economics* **2004,** *28* (2-3), 209-234.
3. Wolfe, J. In *Aeronautics Research Mission Directorate Update with emphasis on Integrated Systems Research*, 48th AIAA Aerospace Science Meeting, Orlando, Florida, Orlando, Florida, 2010.
4. Muehleisen, R. T., Measurement of the acoustic properties of acoustic absorbers. *Illinois Institute of Technology, Muehleisen_plenary_acoustic_materials. pdf* **2007**.
5. ISO, ISO 10534-1, Acoustics---Determination of sound absorption coefficient and impedance in impedance tubes---Part 1: Method using standing wave ratio. International Standards Organisation. 1996.
6. ISO, ISO 10534-2, Acoustics-Determination of sound absorption coefficient and impedance in impedance tubes-Part 2: Transfer-function method. 1998.

7. ASTMC384-04(2011), Standard Test Method for Impedance and Absorption of Acoustical Materials by Impedance Tube Method, ASTM International, West Conshohocken, PA, 2011, www.astm.org.
8. ASTME1050-10, Standard Test Method for Impedance and Absorption of Acoustical Materials Using A Tube, Two Microphones and A Digital Frequency Analysis System, ASTM International, West Conshohocken, PA, 2010, www.astm.org.
9. Russell, D. A., Absorption coefficients and impedance. *Science and Mathematics, Department, GMI Engineering & Management Institute, www. gmi. edu, diakses Maret* **2004**.
10. ISO, ISO 354 Acoustics--Measurement of sound absorption in a reverberation room. 2003; Vol. 2003.
11. ASTM, ASTM C423-02a Standard Test Method for Sound Absorption and Sound Absorption Coefficients by the Reverberation Room Method. ASTM International: 2002.
12. Suhanek, M.; Jambrosic, K.; Domitrovic, H., Student project of building an impedance tube. *Journal of the Acoustical Society of America* **2008,** *123* (5), 3616.
13. ASTMC522-03(2009)e1, Standard Test Method for Airflow Resistance of Acoustical Materials, ASTM International, West Conshohocken, PA, 2009, www.astm.org.
14. Everest, F. A.; Pohlmann, K., *Master Handbook of Acoustics*. McGraw-Hill Education: 2009.

Chapter 2

2 Review of the Existing Analytical Models for Standing Wave Ratio (SWR) and Transfer-Function Methods

2.1 Introduction

In this chapter, the definitions of basic acoustic concepts are provided in 2.2 and two methods for the measurement of acoustic properties of absorbing materials are introduced in 2.3. These two methods can be used to measure the acoustic impedance and absorption coefficient of absorption materials. Also, both methods are based on international standards (ISO 10534-1[5] and ISO10534-2[6]). In this chapter, the theories of these two methods will be described in detail. Finally the advantages and disadvantages of these two methods will be discussed in section 2.5.

2.2 Basic Acoustic Concepts

2.2.1 Acoustic Impedance

The term acoustic impedance describes how much sound pressure is needed to overcome the resistance of molecules within particular medium to vibration at a given frequency. The expression of acoustic impedance is given as

$$Z = R + Xi \tag{2.2.1}$$

In equation (2.2.1) R and X are the real and imaginary parts of the impedance respectively, and represent the resistive and reactive parts of impedance respectively. The resistive part represents the energy transfer of an acoustic wave and the reactive part

represents pressure that is out of phase with the motion of molecules in the acoustic medium. The reactive part causes no average energy transfer[15]. The acoustic impedance is also frequency dependent.

Acoustic impedance may also be expressed as,

$$Z = \frac{p}{vS}, \tag{2.2.2}$$

where p is sound pressure, v is particle velocity, S is surface area of the cross-section through which an acoustic wave of frequency, f, propagates. The "volume velocity" is described using the variables, "vS".

In Figure 2.2.1, the propagation of a plane sound wave in a one dimensional duct is presented. The duct is filled with a homogenous medium with a density ρ. The horizontal x-axis denotes the position coordinate. In this figure, the speed of sound in this homogenous medium is v, the sound pressure at an arbitrary point x_n is p_n. The acoustic impedance at an arbitrary point x_n may be expressed as

$$Z_n = \frac{p_n}{vS_n}. \tag{2.2.3}$$

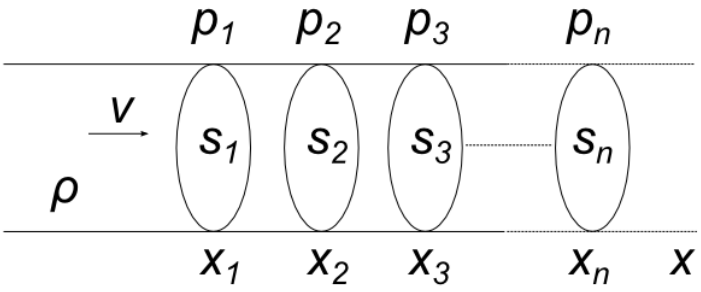

Fig 2.2.1. Propagation of a plane sound wave through a 1D duct

The mechanical impedance may be expressed as,

$$Z_m = \frac{pS_0}{v}, \tag{2.2.4}$$

where p is sound pressure at the surface of material, v is particle velocity at the material's surface, and S_0 is the surface area on which an acoustic wave impinges. pS_0 can be regarded as an "equivalent sound force," which is applied to the area.

2.2.2 Reflection Factor and Absorption Coefficient[12]

Sound waves can impinge on surface of a material at any angle that ranges from 0° to 180°. The interaction between the sound wave and the material is called the "normal incidence," which occurs when a sound wave impinged upon a material at right angle (90°). The acoustic properties of a material at normal incidence may be described in terms of the sound pressure reflection factor and sound absorption coefficient. The sound pressure reflection factor, *r*, is the complex ratio of the sound pressure reflected by the test object, and the incident sound pressure for a plane wave at normal incidence.

$$r = \frac{p_r}{p_i} \tag{2.2.5}$$

In equation (2.2.5) p_i and p_r are the incident sound pressure and reflected sound pressure, respectively.

The sound absorption coefficient, α, is the ratio of the incident sound power entering the surface of the test object (without return), to the incident sound power for a plane wave at normal incidence. The expression for the sound absorption coefficient, α can be written as,

$$\alpha = 1 - |r|^2 = 1 - \left|\frac{p_r}{p_i}\right|^2. \tag{2.2.6}$$

After the introduction of two acoustic properties of sound absorbing material in the current section, a description for how these two properties are measured is provided. This will be done by introducing two models which were prepared by the Technical Committee ISO/TC 43, Acoustics, Subcommittee SC 2, Building acoustics. The two models are the Standing Wave Ratio (SWR) method and the Transfer Function (TF) method, which is mentioned in ISO 10534-1:1996 and ISO 10534-2:1996 respectively. These two standards are described in detail in sections 2.3 and 2.4 of this chapter.

2.3 Standing Wave Ratio (SWR) Method

2.3.1 Introduction

When a sound wave propagates in a duct, it impinges upon a sound absorbing material at the end of it. As the incident wave reaches the surface of material, part of the energy is absorbed, while the remaining energy generates the reflected wave that travels in the opposite direction of the incident wave. By superposition, the incident sound wave and reflected sound wave together form a static wave in tube which is called the "standing wave". By measuring the sound pressure amplitude at a pressure maximum and sound pressure amplitude at an adjacent pressure minimum, the standing wave ratio can be determined and then used to analyze acoustic properties of the sound absorbing material in duct.

To measure the acoustic impedance and absorption factor at normal incidence, an impedance tube may be used. The impedance tube is a tube with a loudspeaker connected to one end of the tube and a test sample mounted at the other end of the tube. The

assumptions for the SWR method of analysis are that the impedance measurement tube is straight, rigid, smooth and also sealed.

2.3.2 Description of the Acoustic Impedance Tube

In Figure 2.3.1, a schematic of a simplified impedance tube is provided. The tube is cylindrical and made of metal with dimensions of *L* and *d* for the length and diameter respectively. In a real tube, support fixtures would be used to hold the tube in place thereby assuring its stability and horizontal alignment with the ground. Fixtures such as these are not portrayed in Figure 2.3.1. The loudspeaker is located at the left end of the impedance tube. The loudspeaker generates the incident plane sound wave at different frequencies. The right end of the tube is terminated with the test sample, which is cut into a circular shape of a certain thickness. The impedance tube is backed with a rigid end to make sure the sample remains fixed. Both sides of the tube are well sealed to prevent the sound waves from escaping from the tube. The metal wall of the tube is assumed to be rigid to isolate the acoustic disturbance from the outer environment.

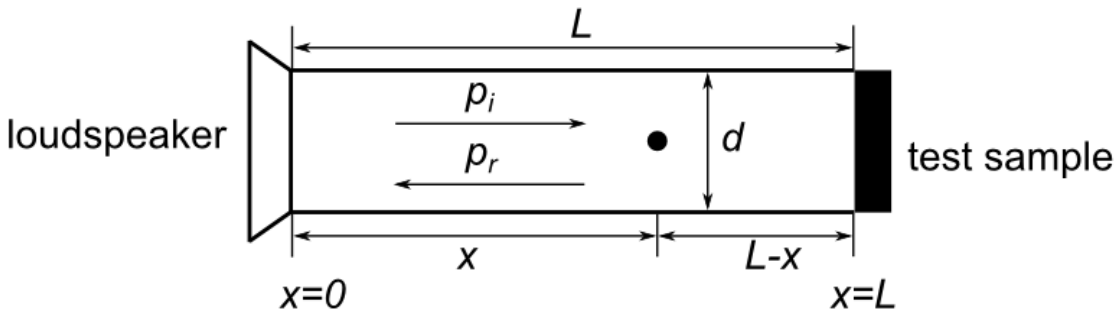

Fig 2.3.1 Schematic diagram of incident and reflected wave in impedance tube (the impedance tube's dimension is diameter *d* and length *L*).

2.3.3 Theory of Standing Wave Ratio (SWR) Method[9]

The phase interference between incident wave (generated by loudspeaker) and the reflected wave (generated by reflection of test sample), results in the formation of a standing wave in the impedance tube. The horizontal x coordinate system in this model spans from the origin, which is at the left end of tube, to the left surface of the test sample. The interaction generates a static wave in tube, which can be called the "standing wave" which is shown in Figure 2.3.2. The sound pressure, p about the position coordinate x, is a periodic function $p(x)$, e.g. sinusoid with local maximum and minimum pressure values at different intervals. The Standing Wave Ratio (SWR) is defined as:

$$SWR = \frac{P_{max}}{P_{min}}, \tag{2.3.1}$$

where P_{max} denotes the maximum sound pressure measured in tube, and P_{min} denotes the minimum sound pressure measured in tube.

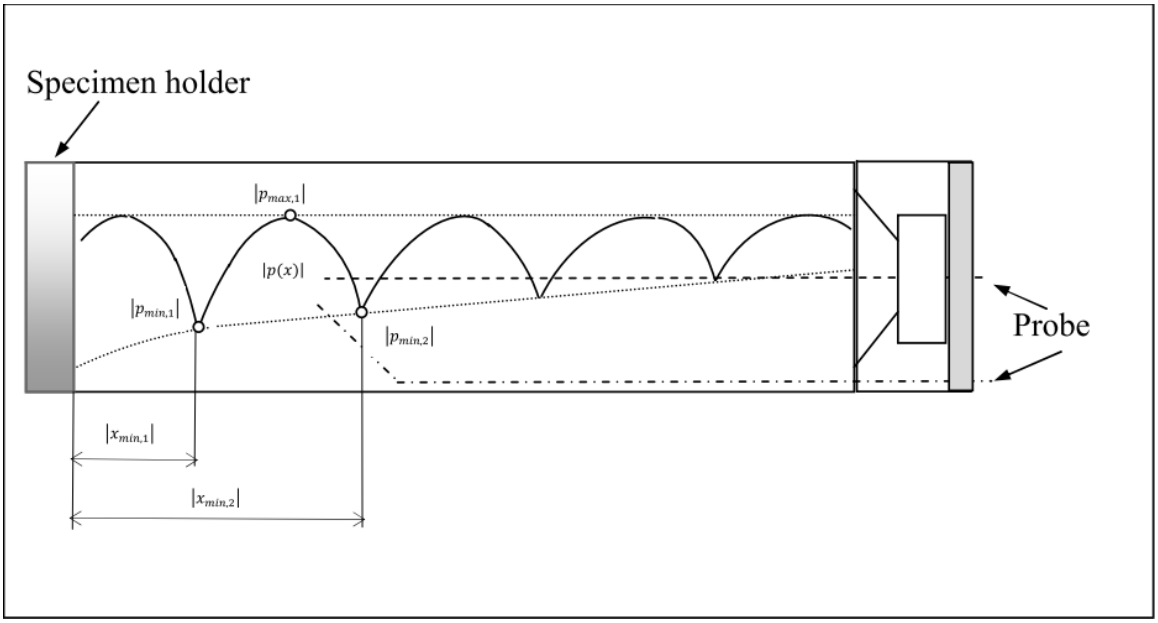

Fig 2.3.2 Schematic diagram of a periodic stand wave function of sound pressure p about position coordinate x in impedance tube.[16]

The incident sound pressure, $p_{i,}$ and the reflected sound pressure, $p_{r,}$ can be written respectively as:

$$p_i(x,t) = A(\theta_1)e^{i[\omega t - kx]} \tag{2.3.2}$$

and

$$p_r(x,t) = B(\theta_2)e^{i[\omega t + kx]}\,, \tag{2.3.3}$$

where ω is the angular frequency and equal to $2\pi f$, and f , k, and c are the sound frequency wave number (equal to $\frac{\omega}{c}$), sound and speed in the medium, respectively. $A(\theta_1)$ and $B(\theta_2)$ are the amplitude function of incident and reflected sound waves respectively, where θ_1 and θ_2 are the phase angle of incident and reflected waves respectively.

The composite sound pressure, p, in the tube is the sum of the incident wave and reflected wave, which when superposed result in:

$$p(x,t) = p_i(x,t) + p_r(x,t) = A(\theta_1)e^{i[\omega t - kx]} + B(\theta_2)e^{i[\omega t + kx]}. \tag{2.3.4}$$

For convenience of the following analysis, the variable in (2.3.4) is changed from "x" to "$L - x$", where "L" is the length of tube[9]. By doing that, the location of the origin is changed from left end side (loudspeaker) to the right end side (surface of test sample) within the impedance tube. Thus, equation (2.3.4) may be re-written as

$$p(x,t) = p_i(x,t) + p_r(x,t) = A(\theta_1)e^{i[\omega t + k(L-x)]} + B(\theta_2)e^{i[\omega t - k(L-x)]}. \tag{2.3.5}$$

The velocity of a fluid particle traveling through the tube can be determined with the aid of Euler's equation[9], which is expressed as

$$\rho \frac{\partial v(x,t)}{\partial t} = -\frac{\partial p(x,t)}{\partial x}\ . \tag{2.3.6}$$

In equation (2.3.6), ρ, is the density of medium, which is assumed to be constant in tube and $v(x,t)$ is particle velocity at x. By solving this PDE for $v(x,t)$, the origin is located at the surface of material. Based on this, the particle velocity may be expressed as,

$$v(x,t) = \frac{1}{\rho c}\left(A(\theta_1)e^{i[\omega t + k(L-x)]} - B(\theta_2)e^{i[\omega t - k(L-x)]}\right) \tag{2.3.7}$$

Substitution of equations (2.3.5) and (2.3.7) into (2.2.4) results in another expression for the impedance:

$$Z_m(x) = \frac{p(x,t)S_0}{v(x,t)} = \rho c S_0 \frac{A(\theta_1)e^{i[\omega t + k(L-x)]} + B(\theta_2)e^{i[\omega t - k(L-x)]}}{A(\theta_1)e^{i[\omega t + k(L-x)]} - B(\theta_2)e^{i[\omega t - k(L-x)]}}. \tag{2.3.8}$$

In equation (2.3.8), the e^{iwt} term in the denominator and numerator cancel each other, resulting in equation (2.3.9),

$$Z_m(x) = \rho c S_0 \frac{A(\theta_1)e^{i[k(L-x)]} + B(\theta_2)e^{-i[k(L-x)]}}{A(\theta_1)e^{i[k(L-x)]} - B(\theta_2)e^{-i[k(L-x)]}}. \tag{2.3.9}$$

To obtain the mechanical impedance at the surface of the test sample, that is the mechanical impedance of the material, the boundary conditions; $x = L$ in (2.3.9) and assignment of the variable x in (2.3.9) to L results in the following expression,

$$Z_m(L) = \rho c S_0 \frac{A(\theta_1) + B(\theta_2)}{A(\theta_1) - B(\theta_2)} = \rho c S_0 \frac{1 + \frac{B(\theta_2)}{A(\theta_1)}}{1 - \frac{B(\theta_2)}{A(\theta_1)}}. \tag{2.3.10}$$

Recall the definition of the reflection factor, r, in equation (2.2.5),

$$r = \frac{p_r}{p_i} = \frac{B(\theta_2)e^{i[\omega t - k(L-x)]}}{A(\theta_1)e^{i[\omega t + k(L-x)]}}. \tag{2.3.11}$$

When the boundary condition "$x = L$" is applied to equation (2.3.11), the reflection factor of test sample, is reduced to,

$$r = \frac{B(\theta_2)}{A(\theta_1)}, \tag{2.3.12}$$

which is the reflection factor of the test sample. Substitution of equation (2.3.12) into (2.3.10) renders the mechanical impedance of the test sample, which is:

$$Z_m(L) = \rho c S_0 \frac{1+r}{1-r} = \rho c S_0 \frac{1+\frac{B(\theta_2)}{A(\theta_1)}}{1-\frac{B(\theta_2)}{A(\theta_1)}}. \tag{2.3.13}$$

Assuming the phase shift angle is θ, e.g. $\theta_1 - \theta_2 = \theta$, and taking $\theta_2 = 0$, the functions for *A* and *B* may be expressed as,

$$A(\theta_1) = Ae^{i0} = A \quad B(\theta_2) = Be^{i\theta}\ , \tag{2.3.14}$$

where *A* and *B* are the amplitudes of the incident and reflected waves, respectively. Substitution of equation (2.3.14) into equation (2.3.13) results in the simplified mechanical impedance at the surface of the test sample, which is expressed as:

$$Z_m(L) = \rho c S_0 \frac{1+\frac{B}{A}e^{i\theta}}{1-\frac{B}{A}e^{i\theta}}\ . \tag{2.3.15}$$

Thus, the mechanical impedance can be calculated given the ratio of incident to reflected amplitude, $\frac{B}{A}$, and the phase shift angle θ. From equations (2.3.5) and (2.3.14), the amplitude function of sound pressure p in the acoustic impedance tube may be expressed as:

$$P = |p| = \left\{(A+B)^2 cos^2\left[k(L-x) - \frac{\theta}{2}\right] + (A-B)^2 sin^2\left[k(L-x) - \frac{\theta}{2}\right]\right\}^{\frac{1}{2}}. \tag{2.3.16}$$

In order to obtain the minimum value for the sound pressure, the following equation must be satisfied:

$$cos^2\left[k(L-x) - \frac{\theta}{2}\right] = 0 \tag{2.3.17.1}$$

$$sin^2\left[k(L-x)-\frac{\theta}{2}\right]=1. \qquad (2.3.17.2)$$

So, from equation (2.3.17.1) and equation (2.3.17.2), the minimum value for sound pressure, $P=P_{min}=A-B$,

In order to obtain the maximum value for the sound pressure, the following equation must be satisfied:

$$cos^2\left[k(L-x)-\frac{\theta}{2}\right]=1 \qquad (2.3.18.1)$$

$$sin^2\left[k(L-x)-\frac{\theta}{2}\right]=0. \qquad (2.3.18.2)$$

So, the maximum value for the sound pressure, $P=P_{max}=A+B$.

From equation (2.3.17.1) and equation (2.3.17.2), where n denotes the nth minimum value measured, starting from the surface of the test sample, the following may be concluded,

$$k(L-x)-\frac{\theta}{2}=\left(n-\frac{1}{2}\right)\pi \qquad n=1,2,3\ldots \qquad (2.3.19)$$

$$\theta=2k(L-x)-(2n-1)\pi=2\frac{2\pi f}{c}(L-x)-(2n-1)\pi \qquad (2.3.20)$$

$$n=1,2,3\ldots$$

From equation (2.3.18.1) and equation (2.3.18.2), where n denotes nth maximum value measured starting from the surface of the test sample, the following may be concluded,

$$k(L-x)-\frac{\theta}{2}=n\pi \qquad n=1,2,3\ldots\ldots \qquad (2.3.21)$$

$$\theta=2k(L-x)-2n\pi=2\frac{2\pi f}{c}(L-x)-2n\pi \qquad (2.3.22)$$

Recall the definition of Standing Wave Ratio in (2.3.1), the values form A and B may be substituted into (2.3.1) to render,

$$SWR = \frac{P_{max}}{P_{min}} = \frac{A+B}{A-B}. \tag{2.3.23}$$

The sound absorption coefficient of the test sample may be calculated the equation (2.3.24), which results from the application of equations (2.2.6), (2.3.12), (2.3.14) and (2.3.23).

$$\alpha = 1 - |r|^2 = 1 - \left|\frac{B(\theta_2)}{A(\theta_1)}\right|^2 = 1 - \left|\frac{B}{A}e^{i\theta}\right|^2 = 1 - \left(\frac{B}{A}\right)^2 \tag{2.3.24}$$

$$= 1 - \left(\frac{SWR-1}{SWR+1}\right)^2$$

Thus the sound absorption coefficient of test sample can be calculated by measuring the Standing Wave Ratio (SWR) first.

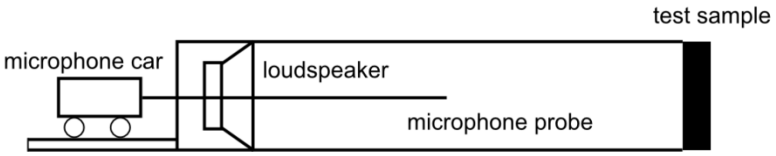

Fig 2.3.3 Schematic diagram of apparatus used to measure the absorption coefficients and acoustic impedance of samples of acoustic absorbing materials in laboratory according to Standing Wave Ratio (SWR) Method.

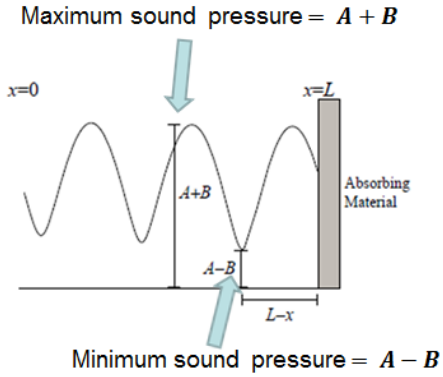

Fig 2.3.4 Schematic of standing wave in impedance tube.[4]

2.3.4 Procedure of Standing Wave Ratio (SWR) Method

The procedure of applying the Standing Wave Ratio method is depicted in Fig. 2.3.3. In this figure, a small car with its right side attached a long microphone probe that protrudes into the tube moves horizontally on a track. The track is parallel to the axial direction of the cylindrical tube, making the long microphone probe coincident with the center line of the tube. Hence, as the car moves along the horizontal line, the microphone probe measures the sound pressure at any location, *x*, in impedance tube. Once the sound pressure is measured as a function of x, which the tube, the phase shift angle θ, may be determined using equation (2.3.20), where the frequency, f, is the frequency of sound generated by loudspeaker and L is length of tube. Once the maximum and minimum sound pressure values are recorded, the SWR can be determined using equation (2.3.1), and $\frac{B}{A}$ can be determined from equation,

$$\frac{B}{A} = \frac{SWR-1}{SWR+1}. \tag{2.3.25}$$

The mechanical impedance and absorption coefficient may be calculated via combination of equations; (2.3.13), (2.3.15) and (2.3.24), resulting in equations (2.3.26) and (2.3.37).

$$Z_m(L) = \rho c S_0 \frac{1+\frac{B}{A}e^{i\theta}}{1-\frac{B}{A}e^{i\theta}} \tag{2.3.26}$$

$$\alpha = 1-|r|^2 = 1-\left|\frac{B}{A}e^{i\theta}\right|^2 = 1-\ (\frac{B}{A})^2 \tag{2.3.27}$$

The same procedure can be applied if the microphone probe is moved to a second, third, … , or *n*th local maximum or minimum value of sound pressure in impedance tube.

This Standing Wave Ratio method relies on the fact that there are only plane incident and plane reflected waves, which are propagating parallel to the axis of impedance tube in the test section. In other word, all kinds of waves in the form other than plane wave should be avoided during a test.

2.4 Transfer Function (Two-Microphone) Method

2.4.1 Introduction

The Transfer Function Method, which is also known as the two-microphone method, can be used to measure the acoustic impedance and absorption factor of test samples at normal incidence. This method employs the same impedance tube as was used for the Standing Wave Ratio method. As stated previously, the tube must be straight, rigid, smooth and airtight, with the test sample mounted at one end of it.

The two-microphone method is shown schematically in Figure 2.4.1. A sample of the material to be tested is placed in a sample holder and mounted to one end of a straight tube. A rigid plunger with an adjustable depth is placed behind the sample to provide a reflecting surface. A sound source, typically a high-output acoustic driver, is connected at the opposite end of the tube. A pair of microphones is mounted flush with the inner wall of the tube, near the sample end of the tube[17].

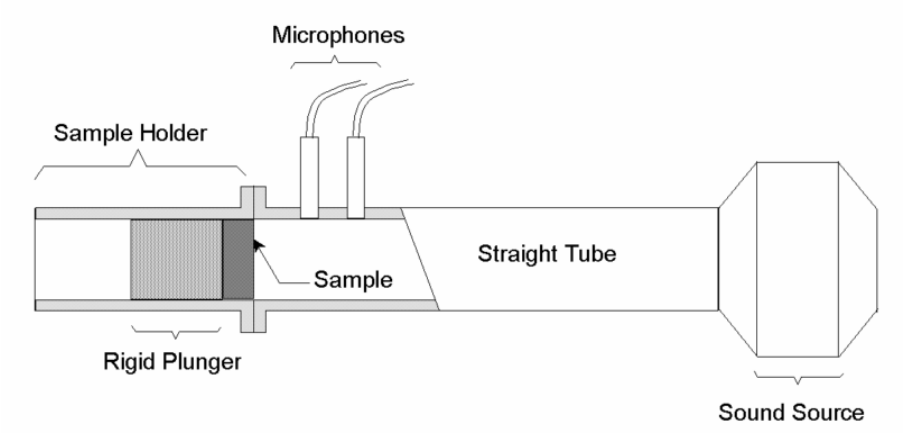

Figure 2.4.1 Schematic of apparatus used to measure the absorption coefficients and acoustic impedance of samples of acoustic absorbing materials according to Transfer Function Method.[17]

The difference between these two methods is that for the Transfer Function Method, two microphones are used. These microphones are fixed at the wall of the impedance tube with distance, s, from each other. These microphones replace the horizontally moving car, which attached the long microphone probe in SWR method. The two fixed microphones can measure the sound pressure at two fixed position in the same coordinate system defined for the SWR method.

2.4.2 Theory of Transfer-Function Method[18]

The schematic of transfer-function method is shown in Fig 2.4.2. This method incorporates the same dimensions and coordinate system for the tube as the SWR method. The distance between microphone 1 and microphone 2 is s. The sound pressure for the first microphone is derived with the use of equations (2.3.5) (2.3.4), where "x" is replaced with "$L - x$", and "L" is the length of tube. Hence, the sound pressure p_1, for

microphone 1, where the distance between the microphone and sample is X_1 is expressed as,

$$\begin{aligned} p_1 &= A(\theta_1)e^{i[\omega t+k(L-x_1)]} + B(\theta_2)e^{i[\omega t-k(L-x_1)]} \\ &= A(\theta_1)e^{i[\omega t+kX_1]} + B(\theta_2)e^{i[\omega t-kX_1]} \\ &= p_i(\theta_1,t)e^{jkX_1} + p_r\,(\theta_2,t)e^{-jkX_1} \end{aligned} \tag{2.4.1}$$

Similarly the sound pressure p_2 measured at microphone 2 with distance X_2 to the test sample is expressed as:

$$\begin{aligned} p_2 &= A(\theta_1)e^{i[\omega t+k(L-x_2)]} + B(\theta_2)e^{i[\omega t-k(L-x_2)]} \\ &= A(\theta_1)e^{i[\omega t+kX_2]} + B(\theta_2)e^{i[\omega t-kX_2]} \\ &= p_i(\theta_1,t)e^{jkX_2} + p_r\,(\theta_2,t)e^{-jkX_2} \end{aligned} \tag{2.4.2}$$

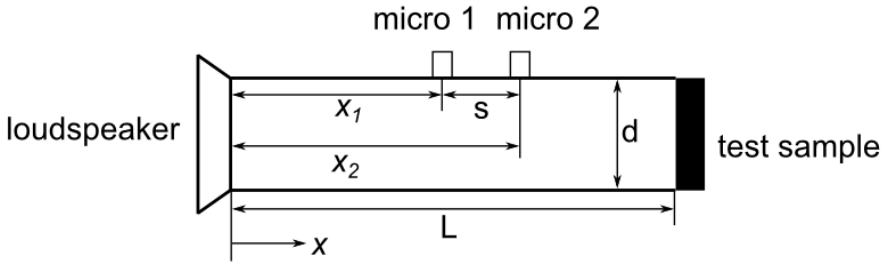

Fig 2.4.2 (a) Schematic of Transfer Function Method (before coordinate transformation).

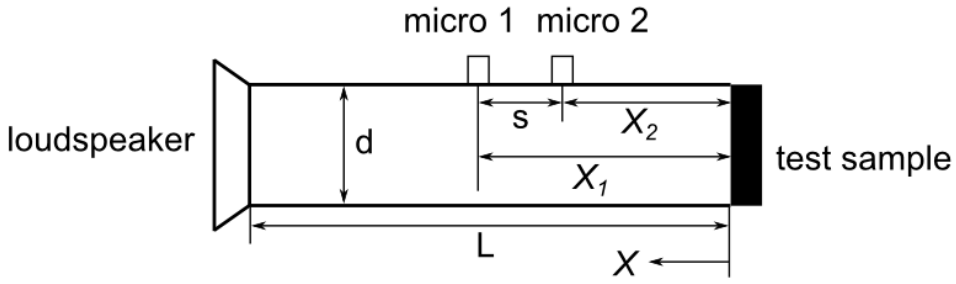

Fig 2.4.2 (b) Schematic of Transfer Function Method (after coordinate transformation).

Rewriting (2.3.11) the reflected sound pressure may be expressed as,

$$p_r = r * p_i \tag{2.4.3}$$

where,

$$B(\theta_2)e^{i[\omega t - k(L-x_2)]} = r * A(\theta_1)e^{i[\omega t + k(L-x_1)]}. \tag{2.4.4}$$

Recalling equations (2.4.1)*and* (2.4.2), yields equations (2.4.5) and (2.4.6), which are the reflected sound pressure at distances X_1 and X_2 respectively,

$$\begin{gathered} p_r(\theta_2, t)e^{-jkx_1} = r * p_i(\theta_1, t)e^{-jkx_1} \\ p_r\,(\theta_2)e^{-jkx_1} = r * p_i(\theta_1)e^{-jkx_1} \end{gathered} \tag{2.4.5}$$

$$\begin{gathered} p_r(\theta_2, t)e^{-jkx_2} = r * p_i(\theta_1, t)e^{-jkx_2} \\ p_r\,(\theta_2)e^{-jkx_2} = r * p_i(\theta_1)e^{-jkx_2} \end{gathered} \tag{2.4.6}$$

In equations, (2.4.5) and (2.4.6) r is the reflection factor. Substitution of (2.4.5) into (2.4.1), and of equation (2.4.6) into (2.4.2), produce expressions for the sound pressure at microphones 1 and 2 , in the form of :

$$\begin{aligned} p_1 = p_i(\theta_1, t)e^{jkx_1} + p_r\,(\theta_2, t)e^{-jkx_1} \\ = p_i\,(\theta_1, t)e^{jkx_1} + r \times p_i(\theta_1, t)e^{-jkx_1} \end{aligned} \tag{2.4.7}$$

and

$$\begin{gathered} p_2 = p_i(\theta_1, t)e^{jkx_2} + p_r\,(\theta_2, t)e^{-jkx_2} = p_i\,(\theta_1, t)e^{jkx_2} + \\ r \times p_i(\theta_1, t)e^{-jkx_2}. \end{gathered} \tag{2.4.8}$$

Defining the ratio of the pressure measured at microphone 2 to the pressure measured microphone 1, as H_{21}:

$$H_{21} = \frac{p_2}{p_1}, \tag{2.4.9}$$

And substitution of equations (2.4.7) *and* (2.4.8) into (2.4.9) renders,

$$H_{21} = \frac{p_i(\theta_1,t)e^{jkx_2} + r \times p_i(\theta_1,t)e^{-jkx_2}}{p_i(\theta_1,t)e^{jkx_1} + r \times p_i(\theta_1,t)e^{-jkx_1}}. \quad (2.4.10)$$

Equation (2.4.10) can now be used to solver for reflect factor, r, which can be defined as,

$$r = \frac{H_{21} - e^{jk(x_2-x_1)}}{e^{-jk(x_2-x_1)} - H_{21}} e^{2jkx_1}. \quad (2.4.11)$$

Because the distance s between microphones 1 and 2 is equal to $x_1 - x_2$, the reflection factor can be simplified as:

$$r = \frac{H_{21} - e^{-jks}}{e^{jks} - H_{21}} e^{2jkx_1}. \quad (2.4.12)$$

According to (2.2.6), the absorption coefficient α is a function of the reflection factor, r:

$$\alpha = 1 - |r|^2 = 1 - \left| \frac{H_{21} - e^{-jks}}{e^{jks} - H_{21}} e^{2jkx_1} \right|^2. \quad (2.4.13)$$

In addition, according to (2.3.13), the mechanical impedance of test sample can be determined by reflection factor, r:

$$Z_m(L) = \rho c S_0 \frac{1+r}{1-r} = \rho c S_0 \frac{1 + \frac{H_{21} - e^{-jks}}{e^{jks} - H_{21}} e^{2jkx_1}}{1 - \frac{H_{21} - e^{-jks}}{e^{jks} - H_{21}} e^{2jkx_1}}. \quad (2.4.14)$$

2.4.3 Procedure of Transfer Function (Two-Microphone) Method[622]

The Transfer Function Method is similar to the Standing Wave Ratio method presented in ISO 10534-1, because they both use an impedance tube with a loudspeaker connected to one end of the tube, and the test sample mounted at the other end of the tube.

However, the procedure of measurement is different. In the Transfer Function Method, plane waves are generated by a loudspeaker at different frequencies at one end

of the impedance tube. Second, two sound pressure values are measured at two fixed locations within the tube, using wall-mounted microphones. Third, this method enables the measurements of and subsequent calculation of the complex acoustic transfer function, H_{21}, the normal incidence absorption coefficient, α, and the mechanical impedance Z_m of the test specimen at different frequencies. There is no need to move the microphone probe horizontally for the Transfer Function Method, as with the Standing Wave Ratio Method, to detect the local maximum and minimum sound pressure values. Hence, this method is considered to an effectives and efficient alternative to the SWR method, and in general quicker.

2.5 Discussion and Comparison[9]

The Standing Wave Ratio method can make easy and reproducible measurements for the calculation of absorption coefficients. The Standing Wave Ratio method and Transfer Function Method are together called “impedance tube method”. However, although the Standing Wave Ratio method is well-established, the relative slower measurement time required to capture data over a wide frequency range limits it application in comparison to the Transfer-Function Method. Also there is a higher probability of operator error, in detection of the maximum and minimum sound pressures p_{max} and p_{min}. So the microphone car should be moved slowly and carefully to let microphone probe detecting p_{max} and p_{min} as accurately as possible, so as to minimize the error.

In this thesis, two new analytical models for another two experimental approaches will be developed, for the fixed one-microphone and three microphone approaches, to our knowledge, these approaches have not been used in the test. The fixed one-microphone

approach includes one microphone at a fixed location, which is used to measure the sound pressure within the impedance tube. The other analytical model provides predictions for an empirical method that incorporates three microphones.

The first analytical model is derived based on a fixed microphone is novel because only sound pressure value at one fixed location is needed for calculation of acoustic properties. Thus the procedure of looking for maximum or minimum sound pressure values at specific locations in the SWR method will become unnecessary. The second analytical model is based on a sound field in the impedance tube, where the equation set is overdetermined. A least-square method is employed to solve the equation set, which describes the sound field. The three-microphone method incorporates three microphones, compared to the transfer-function method.

References

1. ISO, ISO 10534-1, Acoustics---Determination of sound absorption coefficient and impedance in impedance tubes---Part 1: Method using standing wave ratio. International Standards Organisation. 1996.
2. ISO, ISO 10534-2, Acoustics-Determination of sound absorption coefficient and impedance in impedance tubes-Part 2: Transfer-function method. 1998.
3. Wikipedia, Acoustic impedance-Mathematical definitions. 2014.
4. Suhanek, M.; Jambrosic, K.; Domitrovic, H., Student project of building an impedance tube. *Journal of the Acoustical Society of America* **2008,** *123* (5), 3616.
5. Russell, D. A., Absorption coefficients and impedance. *Science and Mathematics, Department, GMI Engineering & Management Institute, www. gmi. edu, diakses Maret* **2004**.
6. Heed, C., Sound absorption and acoustic surface impedance. **2008**.
7. Muehleisen, R. T., Measurement of the acoustic properties of acoustic absorbers. *Illinois Institute of Technology, Muehleisen_plenary_acoustic_materials. pdf* **2007**.
8. Seybert, A. F. In *Notes on absorption and impedance measurements*, Noise and Vibration Conference SAE, Traverse City, 2003.
9. Yong-hua, W.; Cheng-chun, Z.; Jing, W.; Lei, S.; Xue-peng, Z.; Lu-quan, R., Analysis of sound-absorbing performance of bionic porous material *Journal of Jilin University (Engineering and Technology Edition*） **2012,** *42* (6), 1442-1447.

Chapter 3

3 The Analytical Model for One-Microphone and Three-Microphone Method

3.1 Introduction

In previous chapters, the basic concepts of acoustic damping have been introduced, including their definitions and expressions. In particular, analytical models of the Standing Wave Method[5] and Transfer Function Method[6] were discussed along with their respective advantages and disadvantages. In this chapter, two novel analytical models are developed for a fixed One-Microphone Method and a Three-Microphone Method. Both of these experimental techniques utilize the impedance tube model, this model is similar to the previously discussed methods of calculating the acoustic impedance and absorption coefficient. The theories of these two models are provided herein, along with a comparison the two methods, in addition to the two previously developed methods (SWR and TFM) which were introduced in Chapter 2.

3.2 Fixed One-Microphone Method

3.2.1 Introduction

In the Standing Wave Method, one microphone was attached to a microphone car and used to measure the acoustic pressure. For this method, only one microphone was used to measure two “specific” sound pressures at two different locations within the impedance tubes as the car moved along the horizontal axis. As discussed in Chapter 2, the Standing Wave Method is a “pseudo-one-microphone method,” which can be regarded as a special

case of the Transfer-Function Method because the Standing Wave Method measures two sound pressures at two general locations, whereas the former measures two sound pressures at two specific locations at which the maximum and minimum values take place.

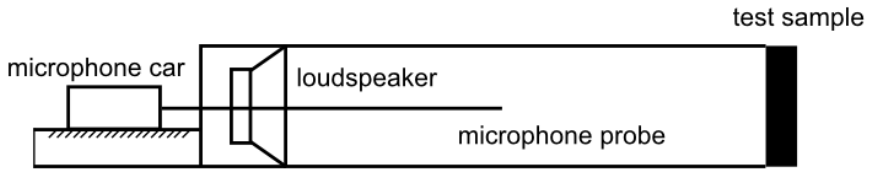

Fig 3.2.1 sketch of impedance tube with location of microphone probe fixed.

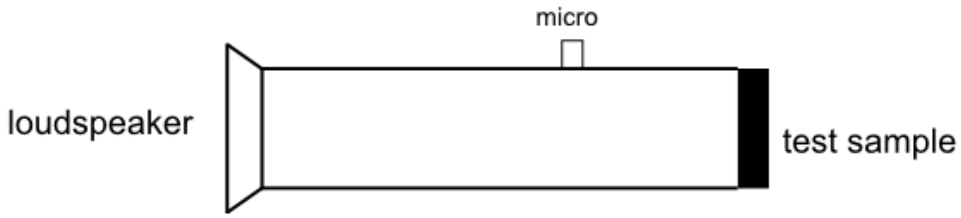

Fig 3.2.2 sketch of impedance tube with one microphone only.

The subject of this section is the discussion of a case of the one-microphone probe Standing Wave Method, where the microphone car cannot move, as shown in Fig 3.2.1. This method can also be described as being equivalent to removing one of the two microphones in the Transfer Function Method. The sketch of impedance tube with one microphone is shown in Fig 3.2.2, where the same impedance tube as used in Transfer-Function Method, but with one microphone is used to measure the sound pressure value. How should one determine the acoustic properties of the test sample when given the sound pressure with only one fixed microphone position?

3.2.2 Theory of One-Microphone Method[19 20]

For the purpose of answering the question just put forward, the analytical model of One-Microphone Method is discussed. In Fig 3.2.3, the schematic of the One-Microphone Method is presented wherein, a loudspeaker is located at the left end of the tube. The loud speaker is used to generate an incident sound wave, which travels down the tube and arrives at the test sample at the right end. Part of the sound energy will be absorbed by the material and the remaining energy will be reflected so that a reflected sound wave can be generated. This reflected sound wave will then superpose with the incident sound wave, to form a standing wave in tube. Sound pressure can be measured by the microphone that is located at the coordinate system created before, assuming that it is distance "x" between the microphone and test sample.

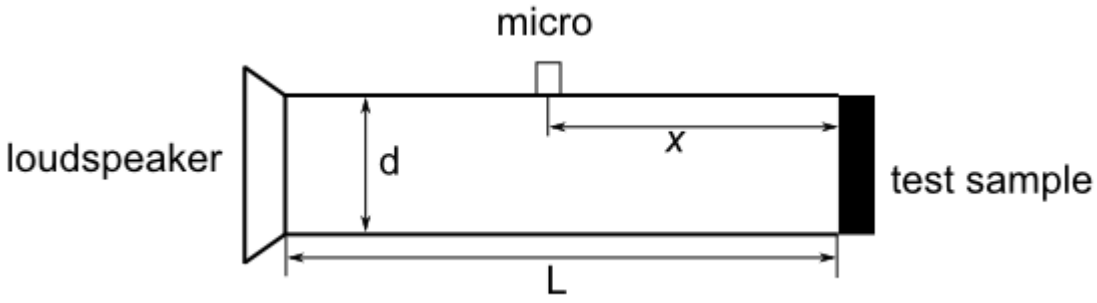

Fig 3.2.3 Schematic of the One-Microphone method

The theoretical model presented in this thesis is for a cylindrical tube, which is axisymmetric. Hence, the spatial 3-D real impedance tube can be simplified into a planar 2-D sketch, which is shown in Fig 3.2.4. In Fig. 3.2.4, "L" and "d " are the length and dimensions of the acoustic impedance tube respectively. A planar Cartesian coordinate

system was created with the origin located at the lower left corner of the sketch, where the horizontal axis spans from 0 to L, and the vertical axis spans from 0 to d.

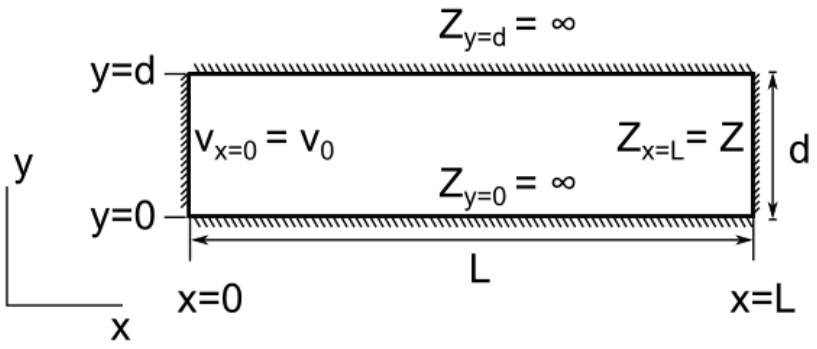

Fig 3.2.4 Sketch of analytical model of impedance tube with boundary conditions.

In this model, it is assumed that the medium in tube has density ρ and that the sound travels at a speed c. It is also assumed that the frequency of sound generated by loudspeaker is f. Hence, the governing equation that describes the sound pressure field in tube can be expressed as:

$$p(x, \omega, t) = p_i(\omega, t)e^{-ikx} + p_r(\omega, t)e^{ikx}, \tag{3.2.1}$$

where k is the wave number which is equal to $\frac{2\pi f}{c}$, ω is angular frequency, which is equal to $2\pi f$. It is also assumed that the wall of the tube is rigid, which means the impedance value of the wall is infinite:

$$Z(\, y = 0\,) = \infty;\ \ Z(\, y = d\,) = \infty. \tag{3.2.2}$$

Equation (3.2.2) represents the upper and lower boundaries of the impedance, which is approximately infinite. According to the transformed expression of the acoustic impedance in (2.2.2) :

$$v = \frac{p}{ZS} \tag{3.2.3}$$

As Z approaches to infinity, the particle velocity at the wall of the tube ($y = 0$, $y = d$) is zero:

$$v_y(\, y = 0\,) = 0 \tag{3.2.4}$$

$$v_y(\, y = d\,) = 0 \tag{3.2.5}$$

The left boundary of the domain, which is at $x = 0$, is assumed to have an initial condition where the excitation is in the positive *x* direction, with a magnitude equal to v_0. Hence, the left boundary condition can be written as:

$$v_x(\, x = 0, \omega) = v_0 \tag{3.2.6}$$

Similarly, the right boundary of the domain, which is at $x = L$, where the test sample is located, can be modeled as a absorption termination. Thus, it can be assumed that there is an absorption condition at the right boundary of the domain, which has the acoustic impedance with a magnitude equal to Z, which can be expressed as,

$$Z\ = Z(x = L, \omega). \tag{3.2.7}$$

Recall (2.2.2) with $S = 1$, the acoustic impedance can be rewritten as,

$$Z = \frac{p}{v}, \tag{3.2.8}$$

which is defined as “specific acoustic impedance”. The “specific acoustic impedance” is independent of the surface area through which an acoustic wave of frequency, f, propagates. It is also assumed in this model that the acoustic pressure at the right boundary of the domain is equal to equation (3.2.9).

$$p = p(x = L, \omega) \tag{3.2.9}$$

So the particle velocity at the $x = L$ by transforming (3.2.8) is:

$$v = \frac{p}{Z}. \tag{3.2.10}$$

After the boundary conditions expressed in equations (3.2.6) *and* (3.2.9) are substituted into equation (3.2.10), the velocity of the sound wave can be described as:

$$v_x(\, x = L, \omega) = \frac{p(x = L, \omega)}{Z(x = L, \omega)} = \frac{p(x = L, \omega)}{Z} \tag{3.2.11}$$

From Euler's equation, equation (3.2.12) can be written:

$$\rho \frac{\partial v(x, \omega, t)}{\partial t} = -\frac{\partial p(x, \omega, t)}{\partial x}\,, \tag{3.2.12}$$

where $p(x, \omega, t) = p_i(\omega, t)e^{-ikx} + p_r(\omega, t)e^{ikx}$, which is based on the governing equation (3.2.1). This PDE can be solved to obtain $v(x, \omega, t)$ which is determined to be:

$$v(x, \omega, t) = \frac{i}{\rho\omega}\frac{\partial p(x, \omega, t)}{\partial x} \tag{3.2.13}$$

By plugging (3.2.1) into(3.2.13) a revised expression for the sound wave is expressed,

$$\begin{aligned} &v(x, \omega, t) = \tfrac{i}{\rho\omega}(-ik)p_i(\omega, t)e^{-ikx} + \tfrac{i}{\rho\omega}(ik)p_r(\omega, t)e^{ikx} = \\ &\tfrac{k}{\rho\omega}p_i(\omega, t)e^{-ikx} - \tfrac{k}{\rho\omega}p_r(\omega, t)e^{ikx}. \end{aligned} \tag{3.2.13.1}$$

Recalling the wave number, k, and angular frequency, ω are equal to the following:

$$k = \tfrac{2\pi f}{c} \quad \omega = 2\pi f, \tag{3.2.13.2}$$

then the function of particle velocity can be expressed as:

$$v(x,\omega,t) = \frac{1}{\rho\frac{\omega}{k}} p_i(\omega,t)e^{-ikx} - \frac{1}{\rho\frac{\omega}{k}} p_r(\omega,t)e^{ikx} = \frac{1}{\rho c} p_i(\omega,t)e^{-ikx} - \frac{1}{\rho c} p_r(\omega,t)e^{ikx}. \quad (3.2.14)$$

By canceling factor "t" on both sides of $(3.2.1) and\ (3.2.14)$, the equations for the pressure and voltage are:

$$p(x,\omega) = p_i(\omega)e^{-ikx} + p_r(\omega)e^{ikx} \quad (3.2.15)$$

$$v(x,\omega) = \frac{1}{\rho c} p_i(\omega)e^{-ikx} - \frac{1}{\rho c} p_r(\omega)e^{ikx} \quad (3.2.16)$$

Applying the boundary condition $from\ equation$ (3.2.6), renders equation (3.2.16.1):

$$\frac{1}{\rho c} p_i(\omega) - \frac{1}{\rho c} p_r(\omega) = v_0\ , \quad (3.2.16.1)$$

which can be rewritten as:

$$p_i(\omega) - p_r(\omega) = \rho c v_0 \quad (3.2.17)$$

Then applying the boundary condition (3.2.11), the pressure can be expressed as:

$$Z * v\ (\ x = L, \omega) = p(x = L, \omega) \quad (3.2.17.1)$$

which is equivalent to:

$$\frac{Z}{\rho c} p_i(\omega)e^{-ikL} - \frac{Z}{\rho c} p_r(\omega)e^{ikL} = p_i(\omega)e^{-ikL} + p_r(\omega)e^{ikL} \quad (3.2.18)$$

To reduce the complexity and length of the expressions, variable, "z" is introduced as the specific acoustic impedance ratio[6]:

$$z = \frac{Z}{\rho c} \quad (3.2.19)$$

Thus (3.2.18) becomes:

$$z[p_i(\omega)e^{-ikL} - p_r(\omega)e^{ikL}] = p_i(\omega)e^{-ikL} + p_r(\omega)e^{ikL} \tag{3.2.20}$$

Transforming (3.2.17) to obtain:

$$p_i(\omega) = p_r(\omega) + \rho c v_0 \tag{3.2.21}$$

Plugging (3.2.21) into (3.2.20) to cancel $p_i(\omega)$ and solve $p_r(\omega)$ results in a complex expression of the pressure.

$$p_r(\omega) = \rho c v_0 \frac{(z-1)e^{ikL}}{2coskL + 2izsinkL} \tag{3.2.22}$$

Once equation (3.2.22) is substituted into equation (3.2.21), $p_i(\omega)$ can expressed as:

$$p_i(\omega) = \rho c v_0 + \rho c v_0 \frac{(z-1)(coskL - isinkL)}{2coskL + 2izsinkL} \tag{3.2.23}$$

With the substitution of equations (3.2.22) *and* (3.2.23) into the governing equation (3.2.1), the pressure can be solved for as a function of x and ω, $p(x, \omega)$ as:

$$\begin{aligned} p(x,\omega) = {} & \frac{\rho c v_0 (z-1)e^{-ik(L+x)}}{2coskL + 2izsinkL} + \frac{\rho c v_0 e^{-ikx}(2coskL + 2izsinkL)}{2coskL + 2izsinkL} \\ & + \frac{\rho c v_0 (z-1)e^{ik(x-L)}}{2coskL + 2izsinkL} \end{aligned} \tag{3.2.24}$$

Using Euler's formula and $e^{i\theta} = cos\theta + isin\theta$, and after few steps of manipulation, $p(x, \omega)$ can be expressed as:

$$p(x,\omega) = \frac{sink(L-x) - izcosk(L-x)}{coskL + izsinkL} i\rho c v_0, \tag{3.2.25}$$

which is the sound pressure function at any position in the tube. Using equation (3.2.25), equation (3.2.22) can be solved to determine z, is:

$$z = \frac{p(x,\omega)coskL - i\rho c v_0 sink(L-x)}{\rho c v_0 cosk(L-x) - ip(x,\omega)sinkL} \tag{3.2.26}$$

Recalling (3.2.17) *and* (2.3.13), the expression of specific acoustic impedance ratio $Z/\rho c$ can be written as[21]:

$$\frac{Z}{\rho c} = \frac{p(x,\omega)coskL - i\rho c v_0 sink(L-x)}{\rho c v_0 cosk(L-x) - ip(x,\omega)sinkL} \tag{3.2.27}$$

$$Z = \rho c \frac{1+r}{1-r} \tag{3.2.28}$$

Combining (3.2.27) and (3.2.28), the reflection factor, r, can be solved as:

$$r = \frac{\frac{Z}{\rho c} - 1}{\frac{Z}{\rho c} + 1} = \frac{z-1}{z+1} = \frac{\frac{p(x,\omega)coskL - i\rho c v_0 sink(L-x)}{\rho c v_0 cosk(L-x) - ip(x,\omega)sinkL} - 1}{\frac{p(x,\omega)coskL - i\rho c v_0 sink(L-x)}{\rho c v_0 cosk(L-x) - ip(x,\omega)sinkL} + 1} \tag{3.2.29}$$

Substitution of equation (3.2.29) into the expression for the absorption coefficient, α, defined in equations (2.2.6) and (3.2.29), renders the absorption coefficient α as a function of 'r', acoustic impedance, and the impedance ration, as expressed in equation (3.2.30).

$$\begin{aligned} \alpha = 1 - |r|^2 &= 1 - \left|\frac{\frac{Z}{\rho c} - 1}{\frac{Z}{\rho c} + 1}\right|^2 = \frac{z-1}{z+1} \\ &= 1 - \left|\frac{\frac{p(x,\omega)coskL - i\rho c v_0 sink(L-x)}{\rho c v_0 cosk(L-x) - ip(x,\omega)sinkL} - 1}{\frac{p(x,\omega)coskL - i\rho c v_0 sink(L-x)}{\rho c v_0 cosk(L-x) - ip(x,\omega)sinkL} + 1}\right|^2 \end{aligned} \tag{3.2.30}$$

After applying few steps of simplification, the absorption coefficient α can be re-written as:

$$\alpha = 1 - \left|\frac{p(x,\omega)coskL - \rho cv_0 cosk(L-x) + i[p(x,\omega)sinkL - \rho cv_0 sink(L-x)]}{p(x,\omega)coskL + \rho cv_0 cosk(L-x) - i[p(x,\omega)sinkL + \rho cv_0 sink(L-x)]}\right|^2 . \quad (3.2.31)$$

Thus the reflection factor r can be rewritten as:

$$r = \frac{p(x,\omega)coskL - \rho cv_0 cosk(L-x) + i[p(x,\omega)sinkL - \rho cv_0 sink(L-x)]}{p(x,\omega)coskL + \rho cv_0 cosk(L-x) - i[p(x,\omega)sinkL + \rho cv_0 sink(L-x)]} \quad (3.2.32)$$

From (3.2.31) it is clear that the absorption coefficient α, is a function of the sound pressure, *x*, sound frequency generated by loudspeaker, the properties of the medium (sound speed and medium density) and the boundary excitation value.

3.2.3 Summary for Fixed One-Microphone Method

In this chapter, Fixed One-Microphone Method was developed, wherein the acoustic impedance and absorption coefficient of the test sample was determined based on measurement of the sound pressure at one fixed location. By applying this method, it is no longer necessary to detect two specific sound pressures by moving the microphone probe in Standing Wave Ratio Method or measure two general sound pressures by using two microphones with their locations fixed in Transfer-Function Method, the One-Microphone Method.

According to the expression of reflection factor r in $(3.2.32)$, multiply both denominator and numerator by " $p(x,\omega)coskL + \rho cv_0 cosk(L-x) + i[p(x,\omega)sinkL + \rho cv_0 sink(L-x)]$", and after few steps of manipulation, the reflection factor r can be rewritten as:

$$\frac{p(x,\omega)^2 cos2kL - (\rho c v_0)^2 cos2k(L-x) + [p(x,\omega)^2 sin2kL - (\rho c v_0)^2 sin2k(L-x)]i}{p(x,\omega)^2 + (\rho c v_0)^2 + 2p(x,\omega)\rho c v_0 coskx} \quad (3.2.33)$$

When the denominator of equation becomes zero (equation3.2.34), the reflection factor r will approach positive infinity, which makes the absorption coefficient approach negative infinity, according to equation(3.2.31). This situation is called “singularity”.

$$p(x,\omega)^2 + (\rho c v_0)^2 + 2p(x,\omega)\rho c v_0 coskx = 0 \quad (3.2.34)$$

The equation(3.2.34) can be rewritten as:

$$coskx = -\frac{p(x,\omega)^2 + (\rho c v_0)^2}{2p(x,\omega)\rho c v_0}. \quad (3.2.35)$$

Thus when both the coordinate x and wave number k satisfy the relation in equation(3.2.35), the singularity situation will occur and the absorption coefficient will become negative infinite, which is implausible.

3.3 Three-Microphone Method

3.3.1 Introduction

In the Transfer Function Method, two microphones are used to measure sound pressure values at two different locations in tube. What happens if an additional one or more microphones is added to the original set of two microphones? For example, suppose there are three microphones which fixed at the wall of the impedance tube with distance from each other, as shown in Fig 3.3.1. In this section, an analytical approach for the determination of the acoustic impedance and absorption coefficient, when there are three microphones used to measure sound pressure is described.

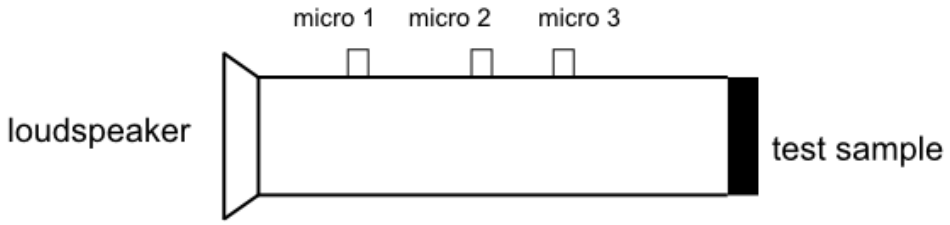

Fig 3.3.1 sketch of impedance tube with three microphones

3.3.2 Theory of Three-Microphone Method

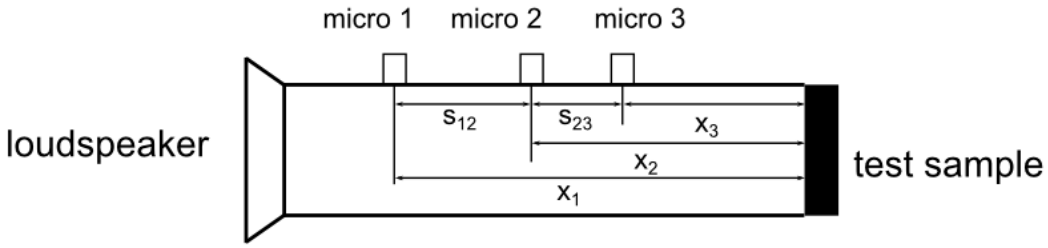

Fig 3.3.2 schematic of Three-Microphone Method

The schematic of Three-Microphone Method is shown above in Fig 3.3.2. In this figure, new coordinate system is created, where the values for x are relative to the test sample location.

The analytical model presented here is based on the TR model approach. According to (2.4.1) (2.4.2), the sound pressure p_1 at micro 1, p_2 at micro 2 and p_3 at micro 3 , can be expressed as follows:

$$p_1 = p_i e^{jkx_1} + p_r e^{-jkx_1} = p_i e^{jkx_1} + r \times p_i e^{-jkx_1}, \quad (3.3.1)$$

$$p_2 = p_i e^{jkx_2} + p_r e^{-jkx_2} = p_i e^{jkx_2} + r \times p_i e^{-jkx_2}, \text{ and} \quad (3.3.2)$$

$$p_3 = p_i e^{jkx_3} + p_r e^{-jkx_3} = p_i e^{jkx_3} + r \times p_i e^{-jkx_3}\ , \quad (3.3.3)$$

where "r" is the reflection factor, whose definition is the same as before:

$$r = \frac{p_r}{p_i} \tag{3.3.4}$$

Then (3.3.1) (3.3.2) (3.3.3) can be rewritten into matrix and vector form:

$$\begin{bmatrix} e^{jkx_1} & e^{-jkx_1} \\ e^{jkx_2} & e^{-jkx_2} \\ e^{jkx_3} & e^{-jkx_3} \end{bmatrix} \begin{Bmatrix} p_i \\ p_r \end{Bmatrix} = \begin{Bmatrix} p_1 \\ p_2 \\ p_3 \end{Bmatrix}. \tag{3.3.5}$$

By assuming that:

$$[A] = \begin{bmatrix} e^{jkx_1} & e^{-jkx_1} \\ e^{jkx_2} & e^{-jkx_2} \\ e^{jkx_3} & e^{-jkx_3} \end{bmatrix}, \tag{3.3.6}$$

$$\{X\} = \begin{Bmatrix} p_i \\ p_r \end{Bmatrix}, \text{ and} \tag{3.3.7}$$

$$\{b\} = \begin{Bmatrix} p_1 \\ p_2 \\ p_3 \end{Bmatrix}. \tag{3.3.8}$$

Equation (3.3.5) can be simplified as:

$$[A]\{X\} = \{b\}, \tag{3.3.9}$$

where $[A]$ is a 3×2 matrix, $\{X\}$ is 2×1 vector, and $\{b\}$ is 3×1 vector. If $\{X\}$ can be solved, then the reflection factor r can be obtained by (3.3.4), the absorption coefficient α by (2.2.6); and the acoustic impedance by (3.2.28). Using linear algebra,

$$\{X\} = [A]^{-1}\{b\}. \tag{3.3.10}$$

However, the inverse matrix of $[A]$ does not exist because $[A]$ is rectangular not square, (3.3.10) cannot be directly used because the linear system described by equation (3.3.9) is over-determined as described in equation (3.3.11)

$$\sum_{i=1}^{m}\sum_{j=1}^{n} A_{ij}\, X_j = \sum_{i=1}^{m} b_i, \tag{3.3.11}$$

where $[A]$ is m × n matrix with m > n. So, there are more equations than unknowns, i.e. an over-determined system. In the linear system constituted by equations $(3.3.1), (3.3.3)\ and\ (3.3.3)$ which describe the three-microphone; $m = 3, n = 2$. So m > n, which satisfies the definition of over-determined system, thus the exact solutions cannot be found. Although this kind of system does not have exact solutions, the approximate solutions which makes the error as small as possible can still be obtained by using the "Least Square Method (LSM)[22 23 24]" which will be introduced below.

Assuming the approximate solutions of the over-determined system is $\{\tilde{X}\}$, because $\{\tilde{X}\}$ is not an exact solution, the relation below must be satisfied:

$$[A]\{\tilde{X}\} \neq \{b\} \tag{3.3.12}$$

Solving equation (3.3.12) for $\{\tilde{X}\}$ renders,

$$\{\tilde{X}\} = \left[[A]^T[A]\right]^{-1}[A]^T\{b\}, \tag{3.3.13}$$

where when (3.3.6), (3.3.7), and (3.3.8) are substituted into (3.3.13) renders:

$$\begin{Bmatrix}\tilde{p}_i\\ \tilde{p}_r\end{Bmatrix} = \left[\begin{bmatrix}e^{jkx_1} & e^{-jkx_1}\\ e^{jkx_2} & e^{-jkx_2}\\ e^{jkx_3} & e^{-jkx_3}\end{bmatrix}^T\begin{bmatrix}e^{jkx_1} & e^{-jkx_1}\\ e^{jkx_2} & e^{-jkx_2}\\ e^{jkx_3} & e^{-jkx_3}\end{bmatrix}\right]^{-1}\begin{bmatrix}e^{jkx_1} & e^{-jkx_1}\\ e^{jkx_2} & e^{-jkx_2}\\ e^{jkx_3} & e^{-jkx_3}\end{bmatrix}^T\begin{Bmatrix}p_1\\ p_2\\ p_3\end{Bmatrix} \tag{3.3.14}$$

The components in (3.3.14) can be calculated as follows:

$$[A]^T = \begin{bmatrix}e^{jkx_1} & e^{-jkx_1}\\ e^{jkx_2} & e^{-jkx_2}\\ e^{jkx_3} & e^{-jkx_3}\end{bmatrix}^T = \begin{bmatrix}e^{jkx_1} & e^{jkx_2} & e^{jkx_3}\\ e^{-jkx_1} & e^{-jkx_2} & e^{-jkx_3}\end{bmatrix} \tag{3.3.15}$$

$$[A]^T[A] = \begin{bmatrix}e^{2jkx_1} + e^{2jkx_2} + e^{2jkx_3} & 3\\ 3 & e^{-2jkx_1} + e^{-2jkx_2} + e^{-2jkx_3}\end{bmatrix} \tag{3.3.16}$$

Taking the inverse matrix of equation (3.3.16) renders,

$$\left[[A]^T[A]\right]^{-1}$$

$$= \begin{bmatrix} e^{2jkx_1} + e^{2jkx_2} + e^{2jkx_3} & 3 \\ 3 & e^{-2jkx_1} + e^{-2jkx_2} + e^{-2jkx_3} \end{bmatrix}^{-1}$$

$$= \frac{\begin{bmatrix} e^{-2jkx_1} + e^{-2jkx_2} + e^{-2jkx_3} & -3 \\ -3 & e^{2jkx_1} + e^{2jkx_2} + e^{2jkx_3} \end{bmatrix}}{\det\begin{bmatrix} e^{2jkx_1} + e^{2jkx_2} + e^{2jkx_3} & 3 \\ 3 & e^{-2jkx_1} + e^{-2jkx_2} + e^{-2jkx_3} \end{bmatrix}} \quad (3.3.17)$$

After substituting equations (3.3.17), (3.3.15), and (3.3.8) back into equations (3.3.14) and (3.3.14) results in:

$$\begin{Bmatrix} \tilde{p}_i \\ \tilde{p}_r \end{Bmatrix} =$$

$$\frac{\begin{bmatrix} e^{-2jkx_1} + e^{-2jkx_2} + e^{-2jkx_3} & -3 \\ -3 & e^{2jkx_1} + e^{2jkx_2} + e^{2jkx_3} \end{bmatrix}}{\det\begin{bmatrix} e^{2jkx_1} + e^{2jkx_2} + e^{2jkx_3} & 3 \\ 3 & e^{-2jkx_1} + e^{-2jkx_2} + e^{-2jkx_3} \end{bmatrix}} \begin{bmatrix} e^{jkx_1} & e^{jkx_2} & e^{jkx_3} \\ e^{-jkx_1} & e^{-jkx_2} & e^{-jkx_3} \end{bmatrix} \begin{Bmatrix} p_1 \\ p_2 \\ p_3 \end{Bmatrix}$$

$$= \frac{\begin{bmatrix} e^{-2jkx_1} + e^{-2jkx_2} + e^{-2jkx_3} & -3 \\ -3 & e^{2jkx_1} + e^{2jkx_2} + e^{2jkx_3} \end{bmatrix}}{(e^{2jkx_1} + e^{2jkx_2} + e^{2jkx_3})(e^{2jkx_1} + e^{2jkx_2} + e^{2jkx_3}) - 3^2} \begin{bmatrix} e^{jkx_1} & e^{jkx_2} & e^{jkx_3} \\ e^{-jkx_1} & e^{-jkx_2} & e^{-jkx_3} \end{bmatrix} \begin{Bmatrix} p_1 \\ p_2 \\ p_3 \end{Bmatrix}$$

(3.3.18)

From (3.3.18) the sound pressures measured by the three microphones, can be used to determine the incident sound pressure and reflected sound pressure, where the approximate value for the reflection factor, $\tilde{r}$, can be calculated by

$$\tilde{r} = \frac{\tilde{p}_r}{\tilde{p}_i}, \quad (3.3.19)$$

Also, the approximate absorption factor, $\tilde{\alpha}$ can be obtained using approximate reflection factor, $\tilde{r}$,

$$\tilde{\alpha} = 1 - |\tilde{r}|^2 \quad (3.3.20)$$

Approximate specific acoustic impedance Z can be obtainedusing approximate reflection factor $\tilde{r}$:

$$Z = \rho c \frac{1+\tilde{r}}{1-\tilde{r}} \tag{3.3.21}$$

where the density of medium in tube ρ and sound speed in medium is c, were defined in previous chapters.

3.3.3 Summary for Three-Microphone Method

According to the expression of $\{\tilde{X}\}$ in (3.3.13), the premise that inverse matrix of (3.3.13) exists is:

$$\det([A]^T[A]) \neq 0 \tag{3.3.22}$$

Then, when the inverse matrix of (3.3.16) does not exist:

$$\det([A]^T[A]) = 0 \tag{3.3.23}$$

$$\det\begin{bmatrix} e^{2jkx_1}+e^{2jkx_2}+e^{2jkx_3} & 3 \\ 3 & e^{-2jkx_1}+e^{-2jkx_2}+e^{-2jkx_3} \end{bmatrix} = 0, \tag{3.3.35}$$

which is equivalent to:

$$(e^{2jkx_1}+e^{2jkx_2}+e^{2jkx_3}) * \left(e^{-2jkx_1}+e^{-2jkx_2}+e^{-2jkx_3}\right) - 3^2 = 0 \tag{3.3.24}$$

If the condition in equation (3.3.24) is met, there will be a large error in the solution $\{\tilde{X}\}$, which also makes the approximate reflection factor $\tilde{r}$ and approximate absorption factor $\tilde{\alpha}$ implausible.

In Three-Microphone Method, there are totally three equations to describe the sound pressure field which generated by the superposition of the incident and reflect sound wave in impedance tube. In the Three-Microphone Method, the extra microphone means

adding one more equation to the equation set to describe the sound pressure field, resulting in three equations with two unknowns, which makes the equation set over-determined. It takes much more time to solve the over-determined equations set than the determined equations set because the approximate solutions need to be obtained, to make the residual error as small as possible. Although two equations created in Transfer-Function Method can have "exactly" solutions, according to literatures, some singularities may occur during the process of calculation and make the solutions implausible[24]. Adding one more microphone, that is to add one more measuring point, the amount of singularities will be less than the situation that there is only two measuring points. For the measurement with multiple microphones, there will be wider frequency range and increased precision[25]. Theoretically, the more measuring point, the fewer singularities there will be and the more convergent the solutions will become.

3.4 Discussion

By comparing the One-microphone Method, Transfer-Function Method and Three-Microphone Method, the advantage of the One-microphone Method it requires only one measurement of the sound pressure using one microphone at one arbitrary location. However, the One-microphone Method requires people to investigate the analytical model of the impedance tube by investigating the governing equation and boundary conditions, which is not necessary for the Transfer-Function Method and Three-microphone Method to do so. Also, the acoustic impedance of the test sample should be determined first when using the One-microphone Method, which makes this approach unrealistic for cases where this information desired. According to this method, the

absorption coefficient can be subsequently calculated by reflection factor after the acoustic impedance is provided. The reflection factor is also derived from the acoustic impedance of sample obtained. On the other hand, when the Transfer-Function Method and Three-microphone Method are used, the reflection factor will be determined first, then the absorption coefficient and finally the acoustic impedance.

References

1. ISO, ISO 10534-1, Acoustics---Determination of sound absorption coefficient and impedance in impedance tubes---Part 1: Method using standing wave ratio. International Standards Organisation. 1996.
2. ISO, ISO 10534-2, Acoustics-Determination of sound absorption coefficient and impedance in impedance tubes-Part 2: Transfer-function method. 1998.
3. Software, F. M., kundt's Tube-Rigid Termination *Actran Student Edition Tutorial*.
4. Software, F. M., Kundt's Tube-Absorbing Termination. *Actran Student Edition Tutorial*.
5. Chu, W. T., Transfer function technique for impedance and absorption measurements in an impedance tube using a single microphone. *The Journal of the Acoustical Society of America* **1986,** *80* (2), 555-560.
6. Oulu, U. o. 5.5. overdetermined system, least squares method. http://s-mat-pcs.oulu.fi/~mpa/matreng/ematr5_5.htm.
7. Oulu, U. o. Example 1: The least squares method. http://s-mat-pcs.oulu.fi/~mpa/matreng/eem5_5-1.htm.
8. Jang, S.-H.; Ih, J.-G., On the multiple microphone method for measuring in-duct acoustic properties in the presence of mean flow. *The journal of the acoustical society of America* **1998,** *103* (3), 1520-1526.
9. Dickens, P.; Smith, J.; Wolfe, J., Improved precision in measurements of acoustic impedance spectra using resonance-free calibration loads and controlled error distribution. *The Journal of the Acoustical Society of America* **2007,** *121* (3), 1471-1481.

Chapter 4

4 The Simulation of Impedance Tube Method using Finite Element Modeling

4.1 Introduction

In Chapters 2 and 3, four analytical methods for the determination of acoustic impedance and absorption coefficient were presented. In all four of the methods, the assumptions and derivations are based on the fact that an impedance tube is used to measure the acoustic properties of the test sample. In this chapter, a virtual impedance tube using a finite element model is presented. This model will be used in the validation of the analytical models described in the previous chapter. The acoustic impedance tube is modeled using ACTRAN 14 Student Edition.

4.2 Introduction to Acoustic Property of Porous Absorption Materials

The acoustic properties of materials can be divided into two types: macroscopic and microstructural properties. As the discussion made in Chapter 1, acoustic impedance and absorption coefficient together belong to the macroscopic properties of absorption materials. Also, within the category of porous absorption materials, are those materials with rigid or elastic frames. In this thesis, only acoustic materials with rigid frames will be investigated. Hence, the finite element method described herein is based on assumption that the solid material has a rigid structure, where the sound energy dissipates via viscous friction and heat transfer.

4.3 Microstructural Properties for Porous Materials with Rigid Frame

To investigate the reason why the porous materials can absorb sound energy, it is necessary to introduce microstructural properties of sound absorption materials. The microscopic properties of the sound absorbing material can be categorized according to the material's porosity, flow resistivity, tortuosity and characteristic lengths. In this model, the properties of a porous foam, where the fluid is air, is modeled in ACTRAN 14 Student Edition.

4.3.1 Porosity $\emptyset$

Porosity is a basic microstructural parameter for porous absorption materials, which can be defined as "the ratio of interconnected void volume to total volume of a material"[4]. The interconnected void volume can also be assumed to be the air volume, and the porosity determined from equation (4.3.1)[26]:

$$\emptyset = \frac{V_{air}}{V} = \frac{V - V_{frame}}{V} = 1 - \frac{V_{frame}}{V}, \tag{4.3.1}$$

where V_{air} is interconnected void volume, V is total volume of a material, V_{frame} is the volume, which the frame occupies in V. The expression for total volume can be written as:

$$V = V_{frame} + V_{air}. \tag{4.3.2}$$

Usually absorption materials with good performance have high porosity.[27] In general, these porosities can range from 95% to 98% for common porous materials. Measuring the open cell foams can be awkward because it is difficult to determine which cells are really open and interconnected. It is also unrealistic to measure for fibrous absorption

materials because accurately measuring the exact volume of a compressible sample can be arduous.[4] Methods for measuring porosity of materials have been proposed by several researchers: Zwikker and Kosten [28],Champoux, et al. [29] and Beranek [30].

4.3.2 Flow Resistivity σ

Flow resistivity is defined as the ratio of the static pressure differential, ΔP, to the normal steady flow through a small sample with velocity, v; where the thickness of the sample is d and is mathematically by Muehleisen [4] and by Cox and D'antonio [27]. These researchers state that the flow resistivity is the measurement of how easily air can enter a porous material, and the resistance that air flow encounters within a structure. The sketch of this flow interaction is shown in Fig 4.3.1,[26] and the expression for flow resistivity is given in (4.3.3):[31]

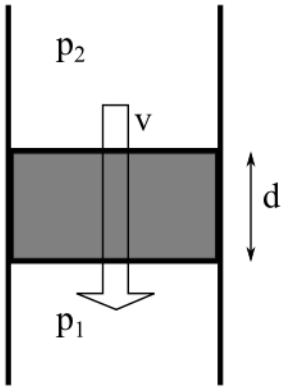

Fig 4.3.1 Sketch of flow resistivity for a certain material with thickness, d.

$$\sigma = \frac{\Delta P}{vd} = \frac{p_2 - p_1}{vd}. \tag{4.3.3}$$

Flow resistivity is one of the most crucial parameters in determining the absorption performance of acoustic material that is porous. In addition to the other researchers, flow

resistivity of materials can be measured using the methodology described by EN [32]. This parameter can also be measured according to ASTMC522-03(2009)e1 [13].

4.3.3 Tortuosity α

Tortuosity can be defined as a measurement of the pore structure, which is not straight in the porous material[4]. The more complex the path, the more time a wave is in contact with the absorption material[4]. Tortuosity α is expressed as[26] :

$$\alpha = \frac{\sigma_t}{\sigma_s} = \frac{1}{cos^2\theta}. \quad (4.3.4)$$

In equation (4.3.4), N is the number of cylindrical pores within a porous material, r, is the radius of the cylindrical pores, and d , is the thickness of the pore. Also, in equation (4.3.4), σ_s is the flow resistivity of porous material with a pore normal to its surface, and σ_t is the flow resistivity of the porous material with an angle θ between the axis of pore and the surface normal. A detailed description of the methodology used to measure the tortuosity of materials is provided in Fellah, et al. [33] and Umnova, et al. [34].

4.3.4 Characteristic Length

Two other significant microstructural properties used to describe a sound absorbing material are the characteristic viscous length, Λ, and the thermal length, Λ', which are closely related to viscous and thermal losses respectively.

4.3.4.1 Thermal Length Λ'

Mathematically, the thermal length Λ' is defined as two times the ratio of volume to surface area in connected pores, this parameter can be measured directly because it is based on the geometry of the sample[4]. Equation (4.3.5)4 provide the expression for this value.

$$\Lambda' = 2\frac{\int dV}{\int dS} = \frac{V_{sample}}{S_{pore\ walls}} \tag{4.3.5}$$

4.3.4.2 Viscous Length Λ

The viscous length, Λ, is similar to the thermal length Λ', as shown in equation (4.3.6).[4] However, this parameter cannot be measured directly because each integral is weighted by the square of the fluid velocity in the pore[4].

$$\Lambda = 2\frac{\int {v^2}_{fluid} dV}{\int {v^2}_{fluid} dS} \tag{4.3.6}$$

4.4 Finite Element Modeling in ACTRAN 14 Student Edition

4.4.1 Introduction

The acoustic parameters which dominate the absorption performance of porous materials have been introduced successively in previous sections. Hence, the porous materials can be modeled in finite element software according to the aforementioned acoustic parameters which have been determined above. Next, a description of the methodology for producing the finite element model of the virtual impedance tube using finite element software “ACTRAN 14 Student Edition” is provided.

4.4.2 Pre-processing

4.4.2.1 Determine the regions

This section describes the boundary conditions for the finite element model. The area surrounded by the wall of the impedance tube can be treated as an isolated region by ignoring the influence or disturbance from outside environment. The first region which can be regarded as area surrounded by four boundaries is shown in Fig 3.2.4. The dimensions of the real impedance tube in our laboratory which is cylindrical, are length $L = 2.5\text{ft} \approx 0.762\text{m}$, inner diameter $d = 1.25\text{inch} \approx 0.032\text{m}$. Thus, the first region (grey area in Fig.4.4.1) is a cylindrical one with height L and diameter d and filled up by a certain acoustic medium (e.g. air) inside. The thickness of the test sample, $= 1\text{ inch} \approx 0.025\text{m}$. The second region (green area in Fig.4.4.1) is also a cylindrical one with height equal to "t" and a diameter equal to "d" but filled up by a certain porous absorption material inside.

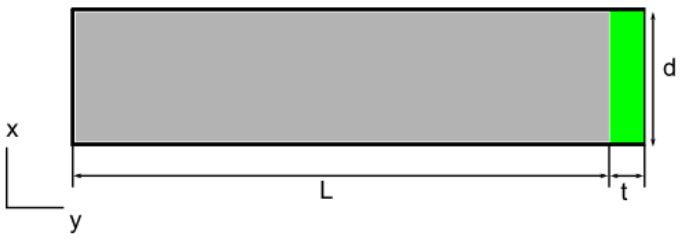

Fig 4.4.1 Sketch of the Regions to be analyzed

A *x*-*y* coordinate system in Fig.4.4.1 is set up for regions which need to be analyzed. The grey region and the green region are separated by circular surface at $y = L$. The two cylindrical regions together can be merged into one cylindrical region which is axisymmetric, that is to say this 3-D merged region can be obtained by rotating a 2-D region which is shown in Fig.4.4.2 about the axis of symmetry of cylinder in Fig.4.4.1 by

360 degrees. Hence, it is not necessary to analyze the 3-D region because a 2-D simplified region is well enough to represent the previous 3-D one due to fact that the geometry of the problem is axisymmetric. Hence, the solution can be solved on a 2D mesh representing a generator of the 3D geometry, which transfers a 3-D finite element modeling to a 2-D finite element modeling.[35]

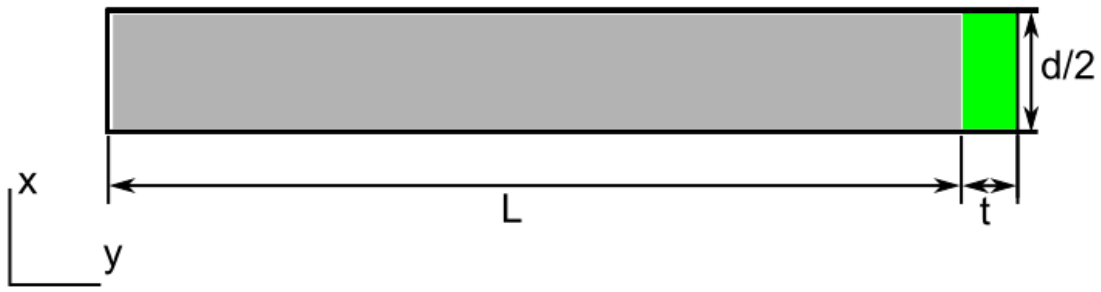

Fig 4.4.2 Sketch of the 2-D simplified Regions

The region for the acoustic medium is grey. The length of the medium is described in terms of the x coordinate, where the range is $[0, d/2]$. The range for the *y* coordinate is $[0, L]$. The region for the porous absorption material is green, and the *x* coordinate range is $[0, d/2]$, while for the y coordinate the range is $[L, L + t]$.

4.4.2.2 Meshing the Regions

After determining the regions that need to be analyzed, the next step is to mesh the two regions partitioned in last section respectively using quadratic elements.

To capture the fluctuation of sound wave in acoustic medium, it is highly recommended to use at least 4 quadratic elements per wavelength for the concern of

precision[19 20]. In first region filled by acoustic medium, based on the prerequisite that the frequency generated by loudspeaker ranges from 0Hz to 5000Hz, thus the maximum frequency is:

$$f_{max} = 5000Hz \tag{4.4.1}$$

According to the relation between wave speed and wave length λ:

$$c = \lambda f, \tag{4.4.2}$$

where c is the sound speed in acoustic medium, so the minimum wave length can be obtained as:

$$\lambda_{min} = \frac{c}{f_{max}} \tag{4.4.3}$$

Thus the largest element length in the mesh can be calculated as:

$$L_{max} = \frac{\lambda_{min}}{4} = \frac{c}{4 \times f_{max}} \tag{4.4.4}$$

Assuming that acoustic medium in our finite element model is air, so $\mathrm{c} = 340\mathrm{m/s}$, which is the sound speed in air, plugging that together with (4.4.1) into (4.4.4):

$$L_{max} = 0.017m \tag{4.4.5}$$

According to the dimension of the impedance tube, take $\Delta x = \Delta y = 0.008\mathrm{m}$ in first region filled by acoustic medium, similarly based on dimension of the test sample, take $\Delta x = 0.008\mathrm{m}$ $\Delta \mathrm{y} = 0.004\mathrm{m}$, both satisfy (4.4.5), hence there are $2 \times 95.25 = 195.5$ elements in first region and $2 \times 6.25 = 12.5$ elements in second region. According to Fig.4.4.2 with $\mathrm{L} \approx 0.762\mathrm{m}, \mathrm{d}/2 \approx 0.016\mathrm{m}, \mathrm{t} \approx 0.025\mathrm{m}$, the meshing in ACTRAN 14 is shown in Fig.4.4.3.

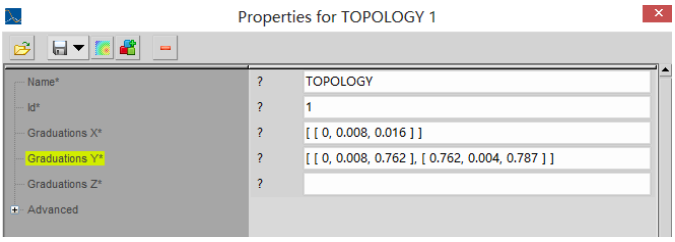

Fig 4.4.3 meshing two regions in ACTRAN 14

4.4.2.3 Adding a New Domain for the Air

After finish meshing the regions, the next step is to add a new domain that represents the air in tube. In figure 4.4.4, the two dimensional new domain has been named as “Air” and its interpolation has been set as quadratic, the range of this domain in *x* coordinate (vertical) is from 0m to 0.016m, and in *y* coordinate (horizontal) it ranges from 0m to 0.762m.

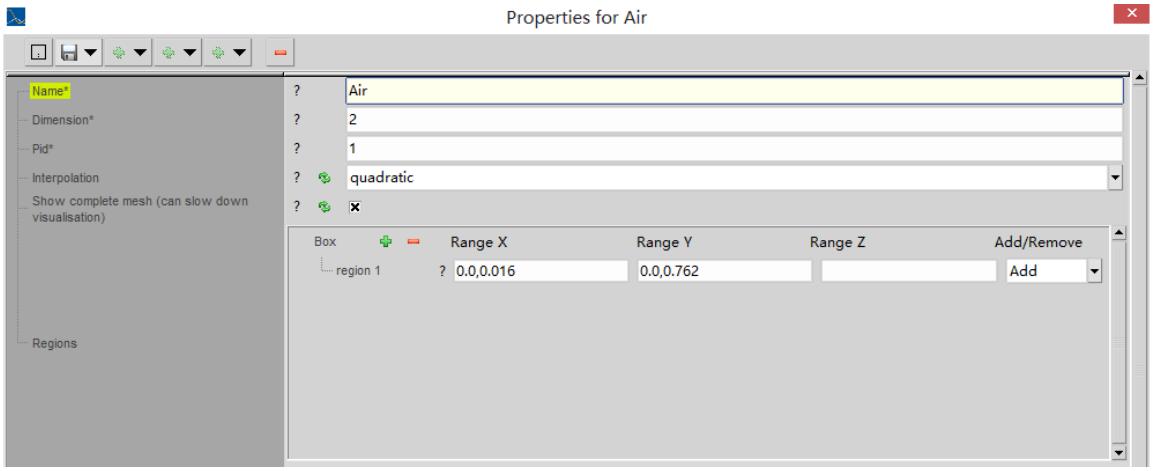

Fig 4.4.4 Add and fill the properties of a new domain named “Air” for the air (1)

In figure 4.4.5, which is preview view, the area that in red color is the new domain for air, one can image that the red area is filled with air molecules.

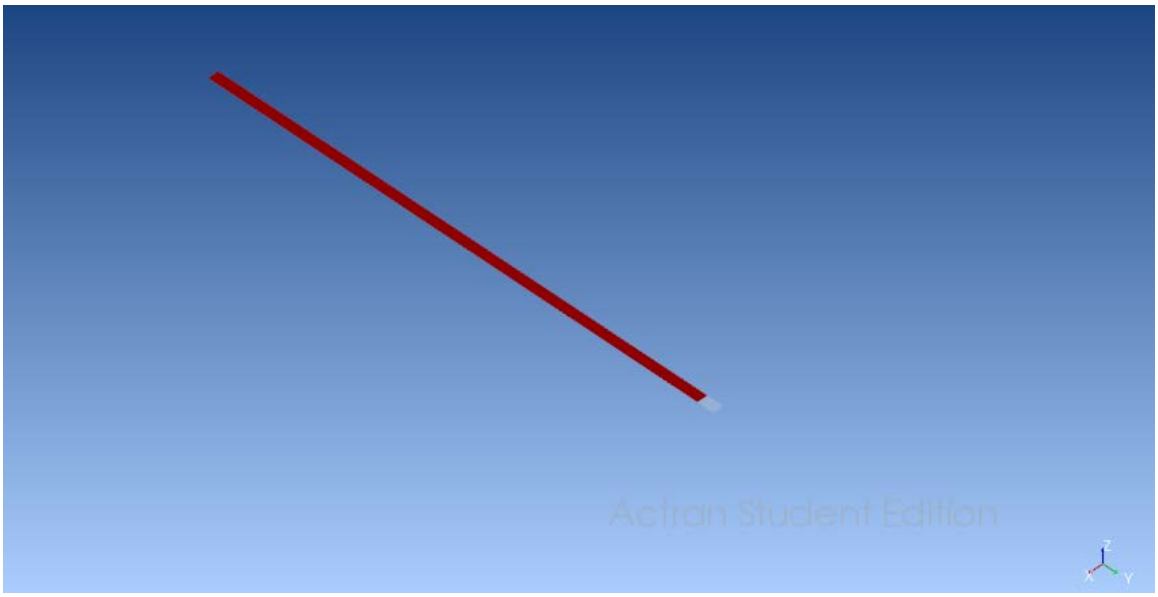

Fig 4.4.5 Add and fill the properties of a new domain named “Air” for the air (2)

4.4.2.4 Adding a New Domain for the Porous Absorption Material

After finish adding a new domain that represents the air in tube, the next step is to add a new domain that represents the porous absorption material located at one end of tube. In figure 4.4.6, the two dimensional new domain has been named as “porous absorption material” and its interpolation has also been set as quadratic, the range of this domain in *x* coordinate (vertical), which is the same as the air domain, is from 0m to 0.016m, and in *y* coordinate (horizontal) it ranges from 0.762m to 0.787m.

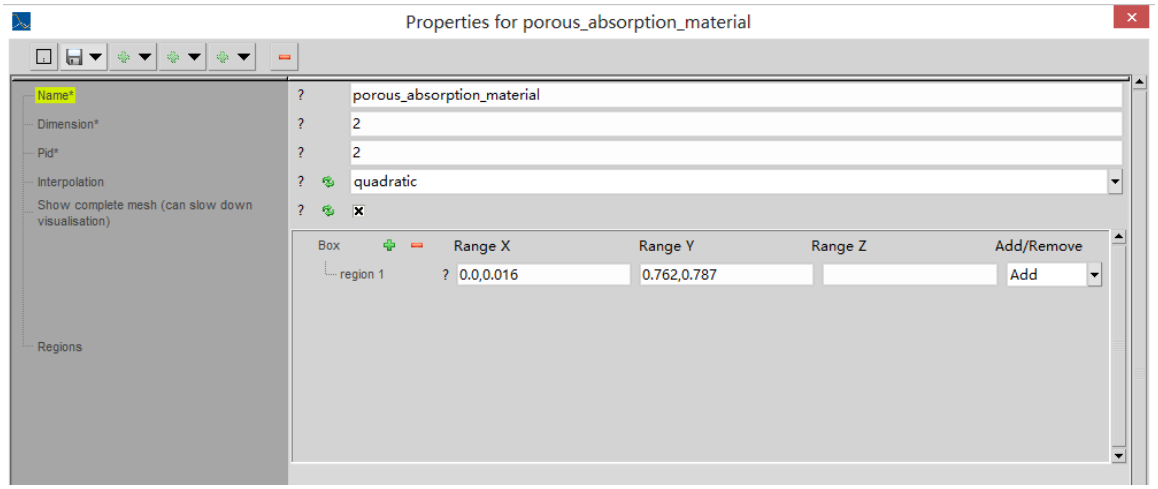

Fig 4.4.6 Add and fill the properties of a new domain named “porous absorption material” for the porous absorption material (1)

In figure 4.4.7, which is preview view, the area that in red color is the new domain for porous absorption material, one can also image that the red area is filled with porous absorption material, and this new domain constitutes one boundary condition of this finite element model.

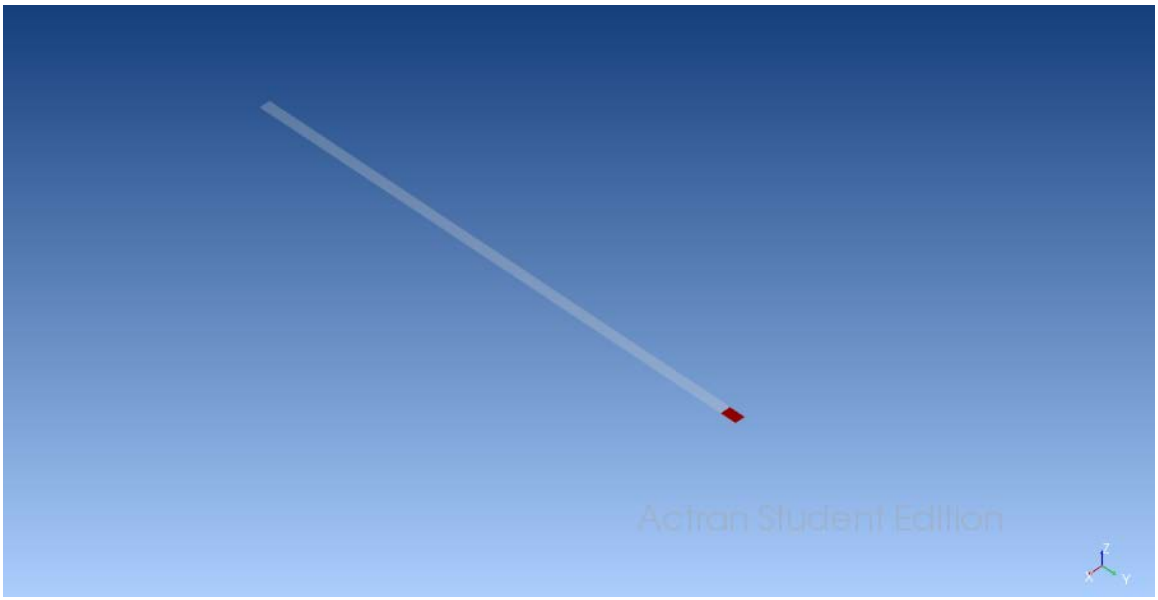

Fig 4.4.7 Add and fill the properties of a new domain named “porous absorption material” for the porous absorption material (2)

4.4.2.5 Adding a New Domain for the Boundary Excitation

After adding a new domain that represents porous absorption material located at one end of tube, there is still one boundary condition at the other end of tube which needs to be determined, so the next step is to add a new domain that represents the velocity boundary excitation applied at the other end of tube. In figure 4.4.8, the one dimensional new domain has been named as “Boundary Excitation” and its interpolation has also been set as quadratic, the range of this domain in *x* coordinate (vertical), which is the same as the air domain and domain of porous absorption material, is from 0 m to 0.016 m, and in *y* coordinate (horizontal) it locates at 0 m.

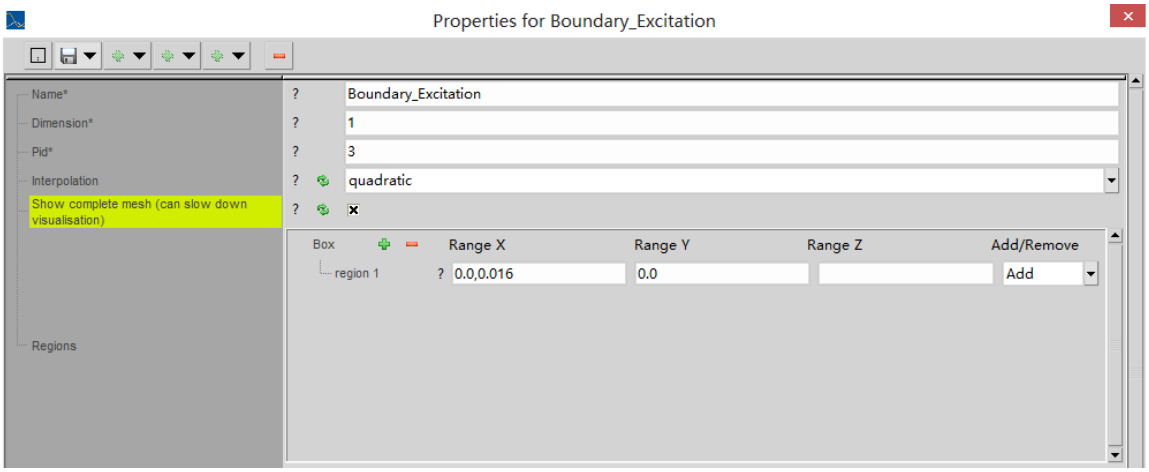

Fig 4.4.8 Add and fill the properties of a new domain named “Boundary Excitation” for the boundary excitation (1)

In figure 4.4.9, which is preview view, the line that in red color is the new domain for velocity boundary excitation, one can also image that the red line is a loudspeaker which generates vibration and causes the air molecules move forward, and this new domain constitutes the other boundary condition of this finite element model.

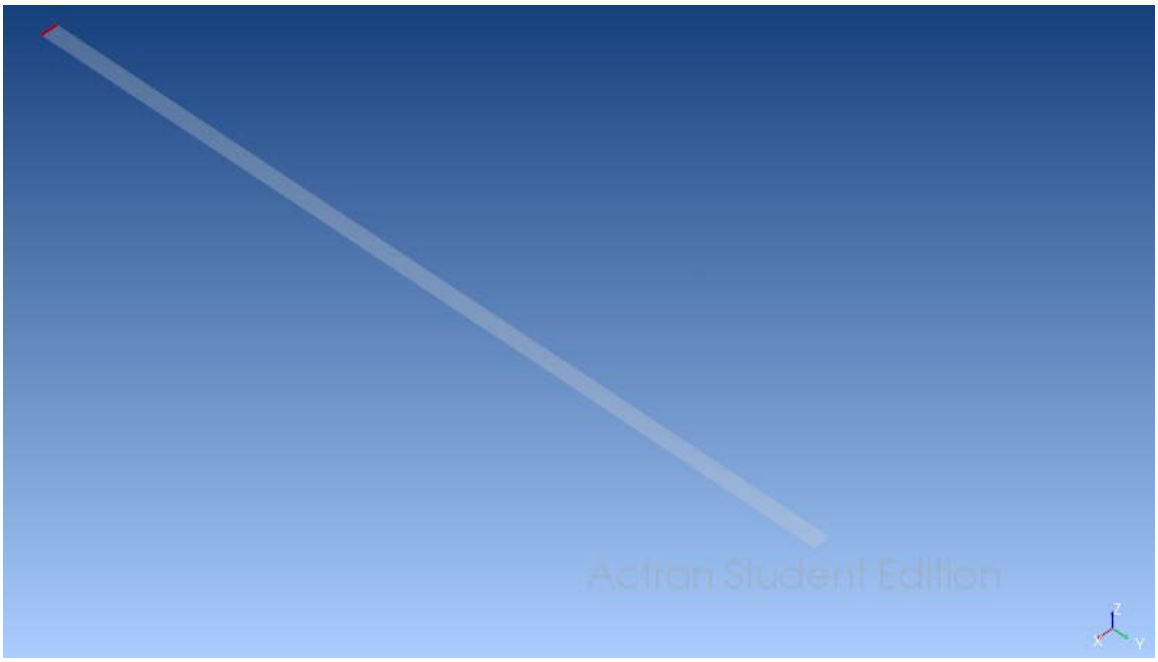

Fig 4.4.9 Add and fill the properties of a new domain named “Boundary Excitation” for the boundary excitation (2)

4.4.2.6 Create the Frequency Analysis and Define Axisymmetry

To generate plane wave in tube, the highest frequency must satisfy that[9]:

$$f_{max} \approx \frac{101}{r} \approx \frac{101}{d/2} \approx \frac{202}{d} \tag{4.4.6}$$

, where d is the diameter of the tube,

$$d = 1.25in = 0.031m \tag{4.4.7}$$

Thus the maximum frequency can be calculated using (4.4.6):

$$f_{max} \approx 6516Hz \tag{4.4.8}$$

Considering the maximum frequency which loudspeaker could generate is $5000\,\mathrm{Hz}$, which satisfies (4.4.8):

$$5000Hz \leq f_{max} = 6516Hz \tag{4.4.9}$$

Thus the range of frequency can be specified from 20Hz to 5000Hz with a step of 1 Hz, shown in Fig.4.4.10.

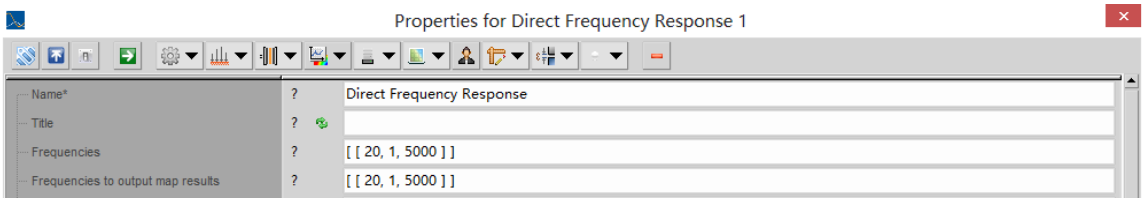

Fig 4.4.10 Specify the frequency range

For the reason that ACTRAN model is 2-Dimensional axisymmetric model, the axisymmetry order should be set to 0, which specifies a constant solution with varied azimuthal angle in the tube cross[20], shown in Fig 4.4.11.

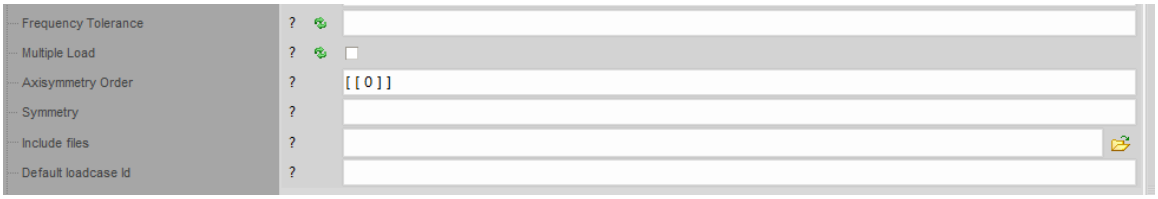

Fig 4.4.11 define the axisymmetric order

4.4.2.7 Create the Finite Fluid Component

The next step is to add a finite fluid component and name it “Acoustic”, which is shown in Fig.4.4.12.

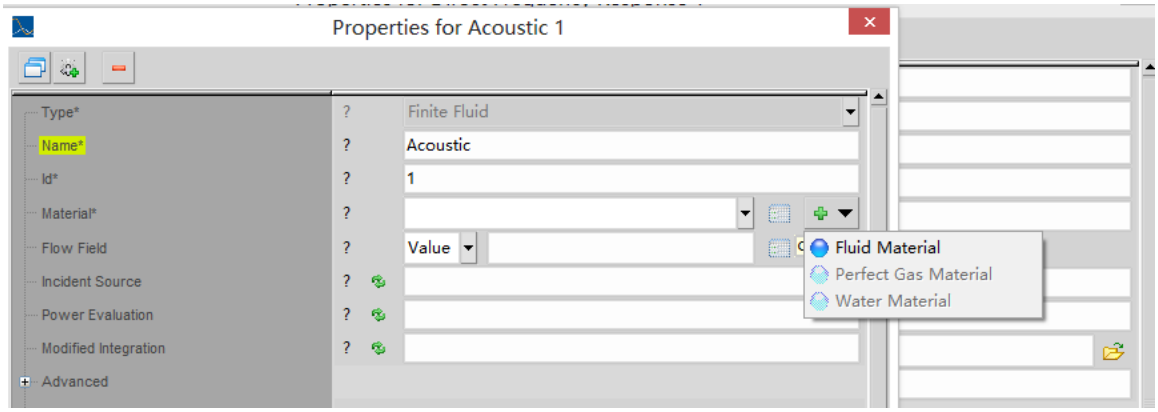

Fig 4.4.12 Add a finite fluid component named “Acoustic”

Then set up the fluid material and name it “Air”, the standard properties of air, which are sound speed and fluid density, need to be specified as 340 $\mathrm{m/s}$ and 1.225 kg/m^3 respectively, which is shown in Fig 4.4.13.

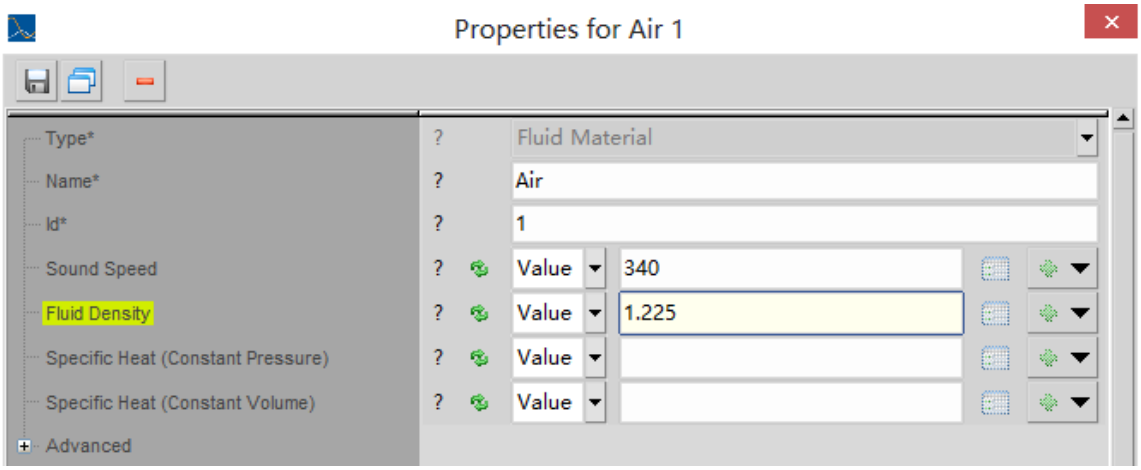

Fig 4.4.13 Create a new fluid material named “Air” and specify standard properties of Air

In Fig 4.4.14, with the scope selector, the Air domain is assigned to the Acoustic component.

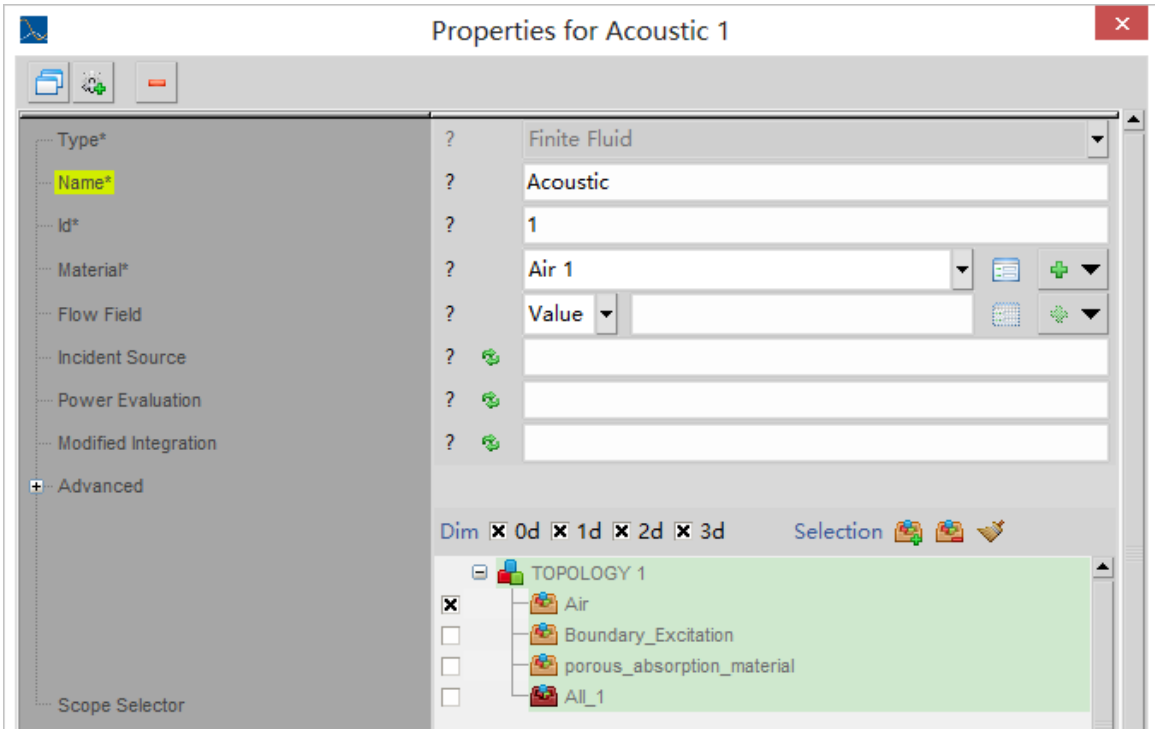

Fig 4.4.14 Assign the finite fluid component to “Air” domain

4.4.2.8 Create the Porous Rigid Component

The next step is to add a porous rigid component and name it “porous material”, then specify the power evaluation to “1” to activate the computation of the dissipated power, which is shown in Fig 4.4.15.

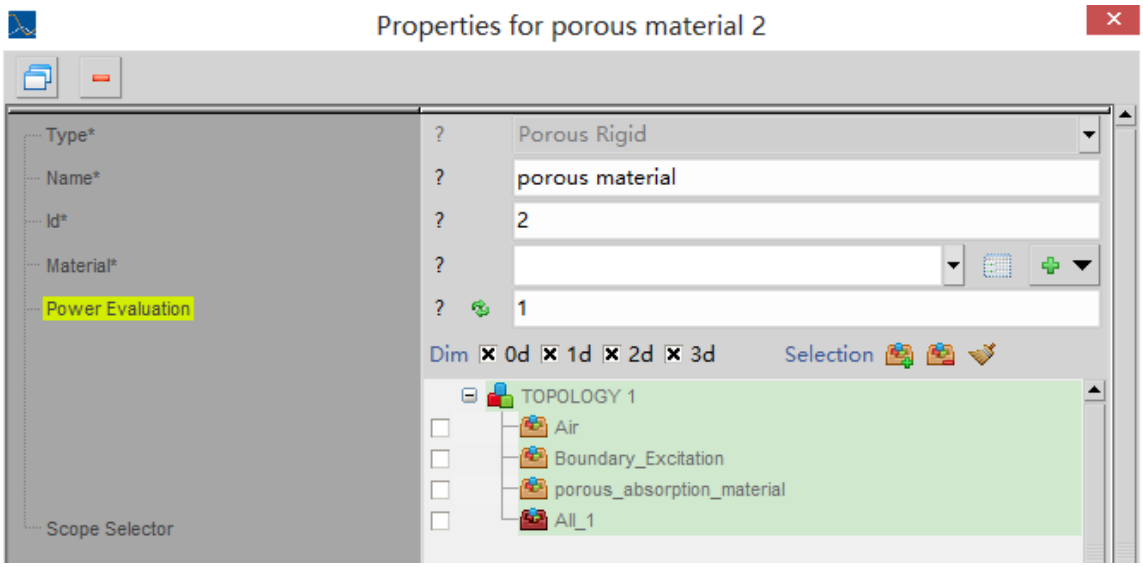

Fig 4.4.15 Add a porous rigid component named “porous material”

Then set up the porous material and name it “Foam”, the properties of foam, which are porosity, flow resistivity, tortuosity, viscous length and thermal length, can be specified as 0.94, 10000 N. s/m^4, 1.06, 3e − 5 m and 8e − 5 m respectively, which is shown in Fig 4.4.16.

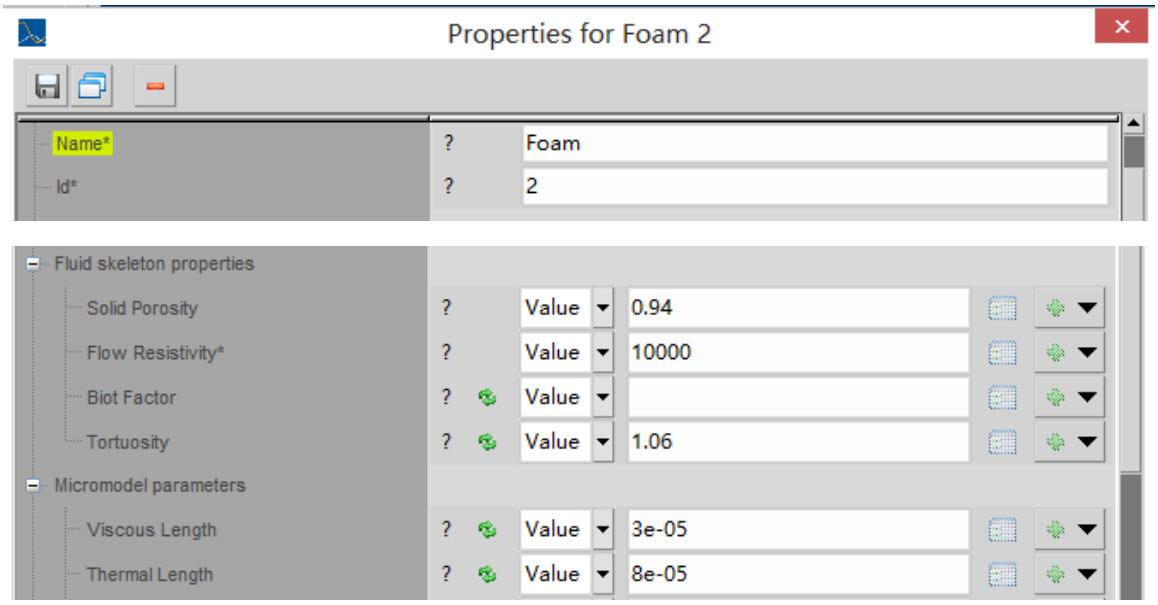

Fig 4.4.16 Create a new porous material named “Foam” and specify acoustic parameters of Foam

In Fig 4.4.17, with the scope selector, the porous absorption material domain is assigned to the porous material component.

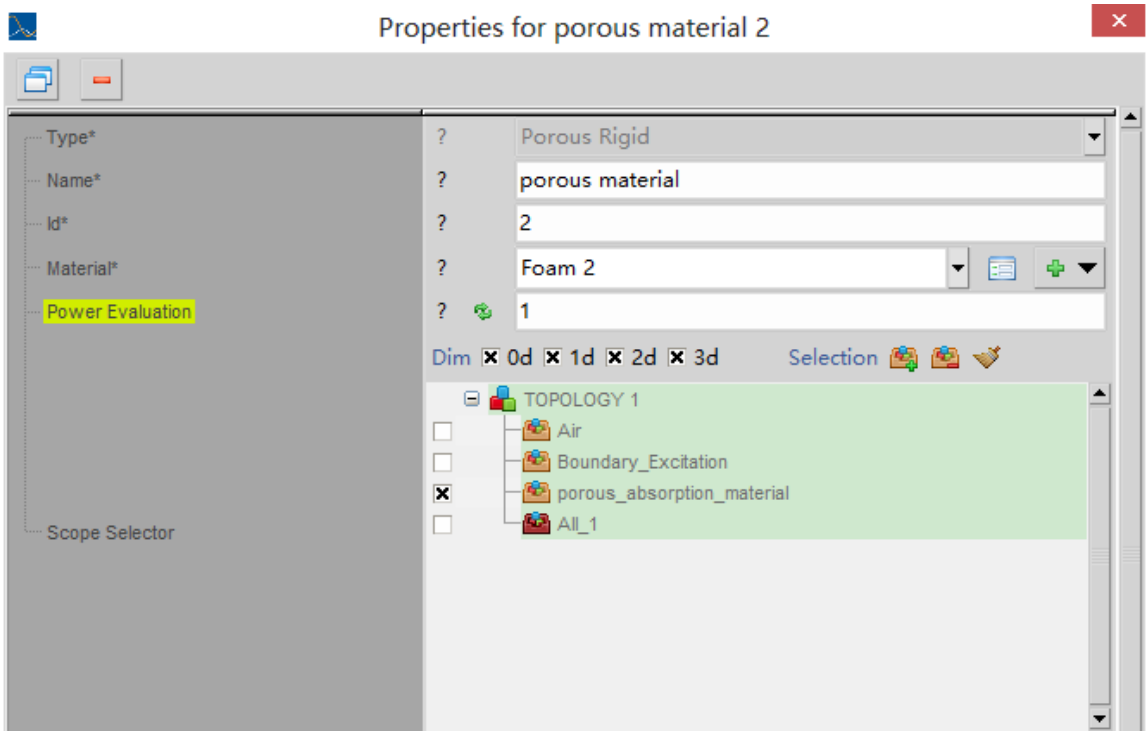

Fig 4.4.17 assign the porous rigid component to “porous absorption material” domain

4.4.2.9 Create the Velocity Boundary Condition

The next step is to create a new velocity boundary condition and name it “Velocity”, which is also called boundary excitation. The value of this boundary condition can be specified as 1m/s and the direction is along the Y direction, which is shown in Fig 4.4.18 and with the scope selector, the porous absorption material domain is assigned to the Velocity component.

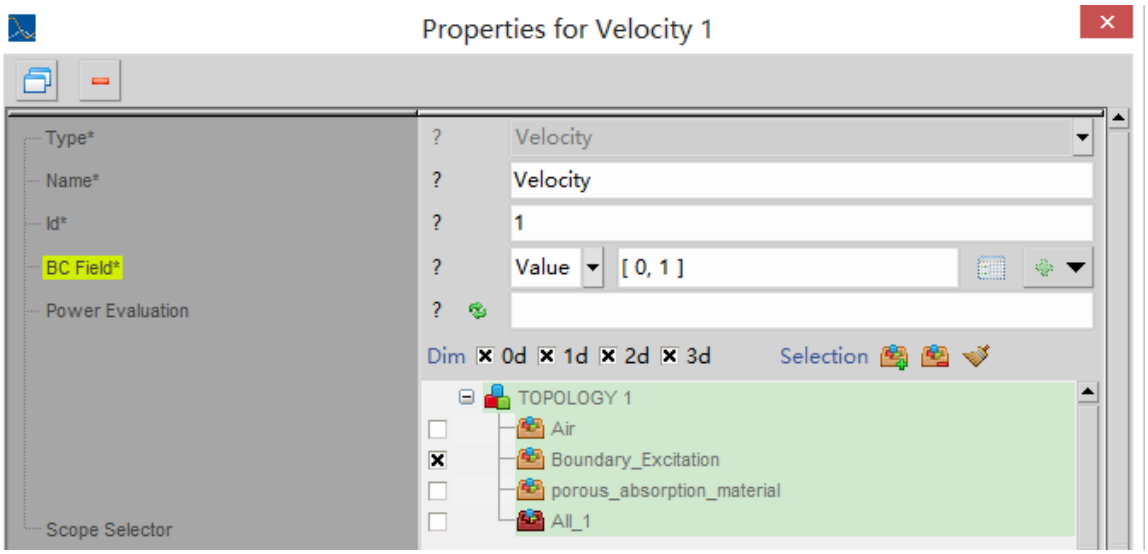

Fig 4.4.18 Specify the value of the boundary condition and assign the velocity boundary condition to “Boundary Excitation” domain

4.4.2.10 Specify the Solver

The next step is to define the solver of the analysis, Krylov solver cannot be used because a porous component is used, so the Mumps is selected as the solver[35], which is shown in Fig 4.4.19.

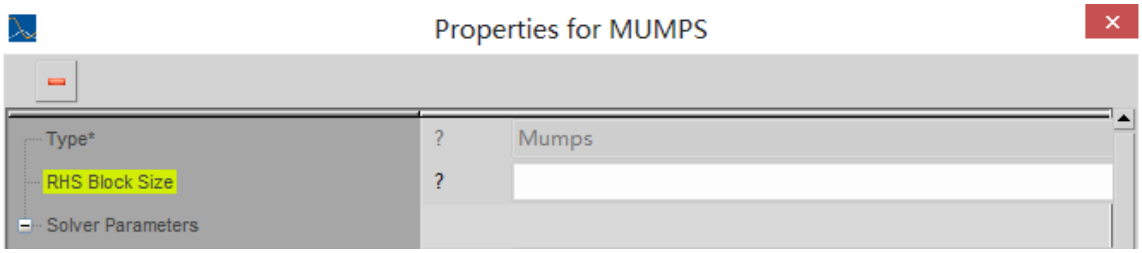

Fig 4.4.19 Define the solver of the analysis as MUMPS solver

4.4.2.11 Create the Field Points

After specifying the solver, the next step is to create the field points in finite element model which represent the microphones in real impedance tube, the positions of three microphones in the air domain which is shown in Fig 4.4.21, need to be specified in the tube coordinate created previously, according to the dimension in Fig 4.4.20.

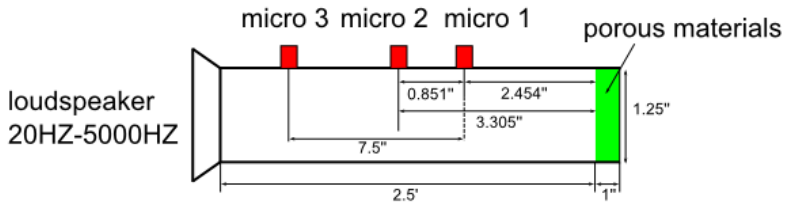

Fig 4.4.20 Sketch of positions of three microphones which plug in real impedance tube.

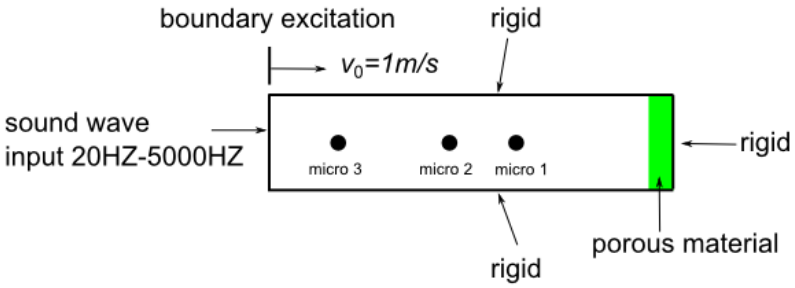

Fig 4.4.21 Sketch of positions of three field points which represent three microphones in real impedance tube.

By transferring inch into meter, the coordinates of microphone 1, 2, 3 can be determined and entered as[0.008,0.700,0],[0.008,0.678,0], [0.008,0.509,0] respectively, which is shown in Fig.4.4.22, the three red points indicate three microphones.

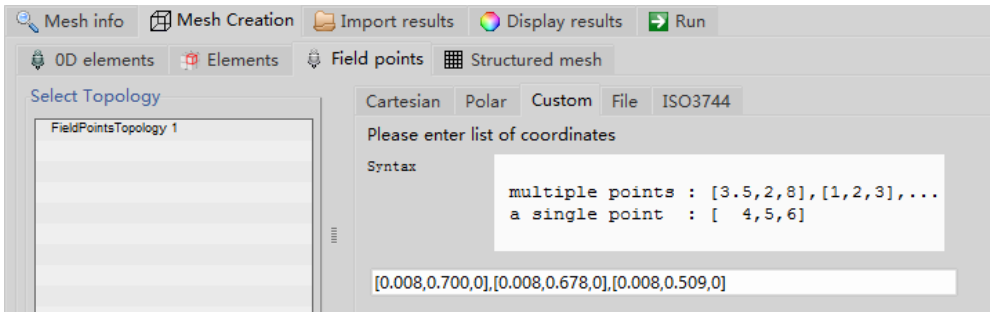

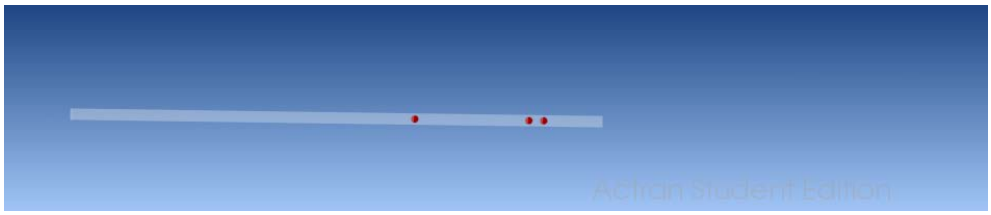

Fig 4.4.22 Create three field points in air domain of finite element model.

4.4.3 Solve

After finishing the pre-processing, the next step is to export the analysis file and launch the computation in ACTRAN. “End of computation job” in Fig 4.4.23, which is auncher window, indicates that the computation has finished.

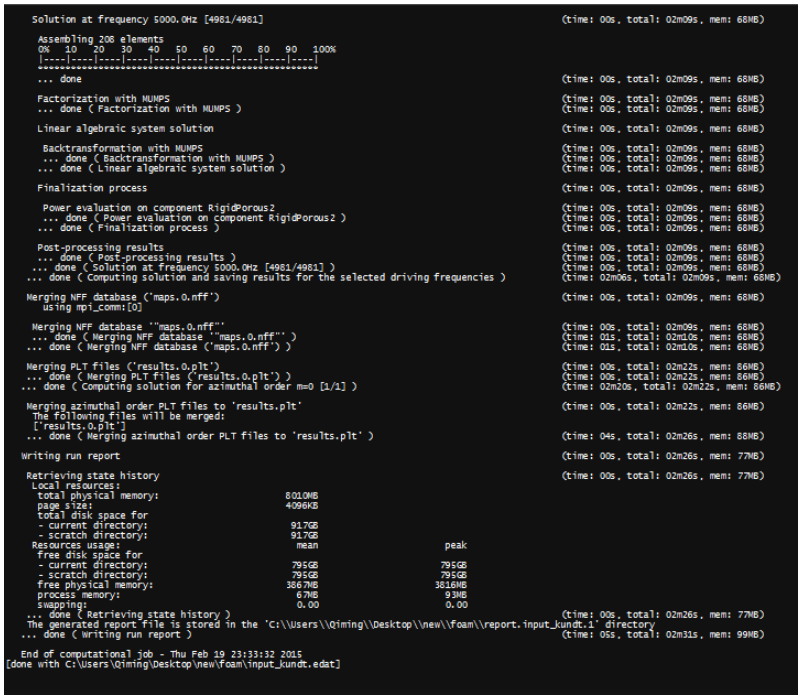

Fig 4.4.23 Launcher window.

4.4.4 Post-processing

In the post-processing section, the primary purpose is to obtain the sound pressure values detected by three field points, the three field points represent the three

microphones in real impedance tube, and then plot the graphs of sound pressure values of three microphones (dB) vs. frequencies from 20 Hz to 5000Hz which are shown in Fig 4.4.24, Fig 4.4.25 and Fig 4.4.26, respectively.

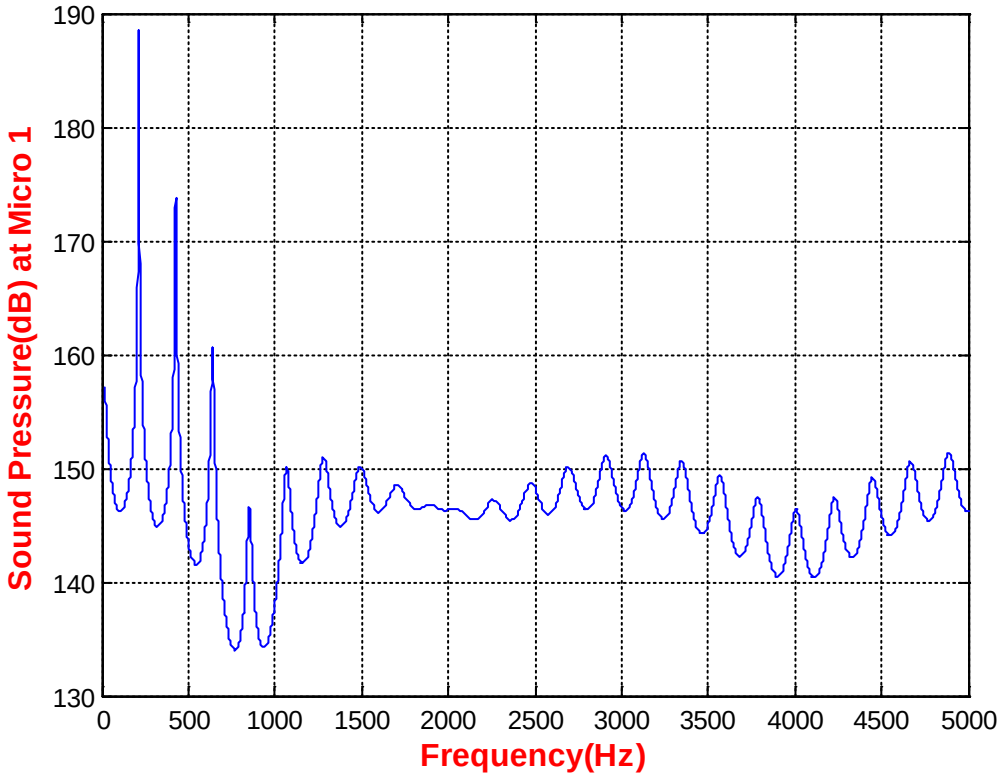

Fig 4.4.24 Sound Pressure (dB) vs. Frequencies (20 Hz to 5000Hz) measured at Micro 1 (reference pressure is 2e-05Pa)

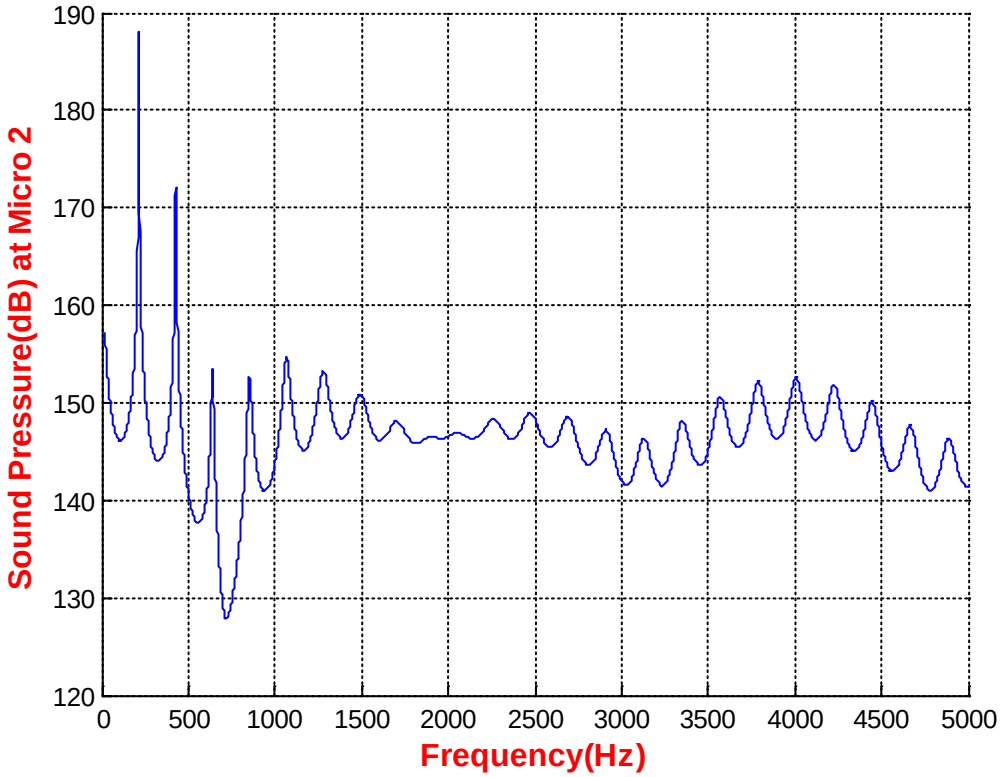

Fig 4.4.25 Sound Pressure (dB) vs. Frequencies (20 Hz to 5000Hz) measured at Micro 2 (reference pressure is 2e-05Pa)

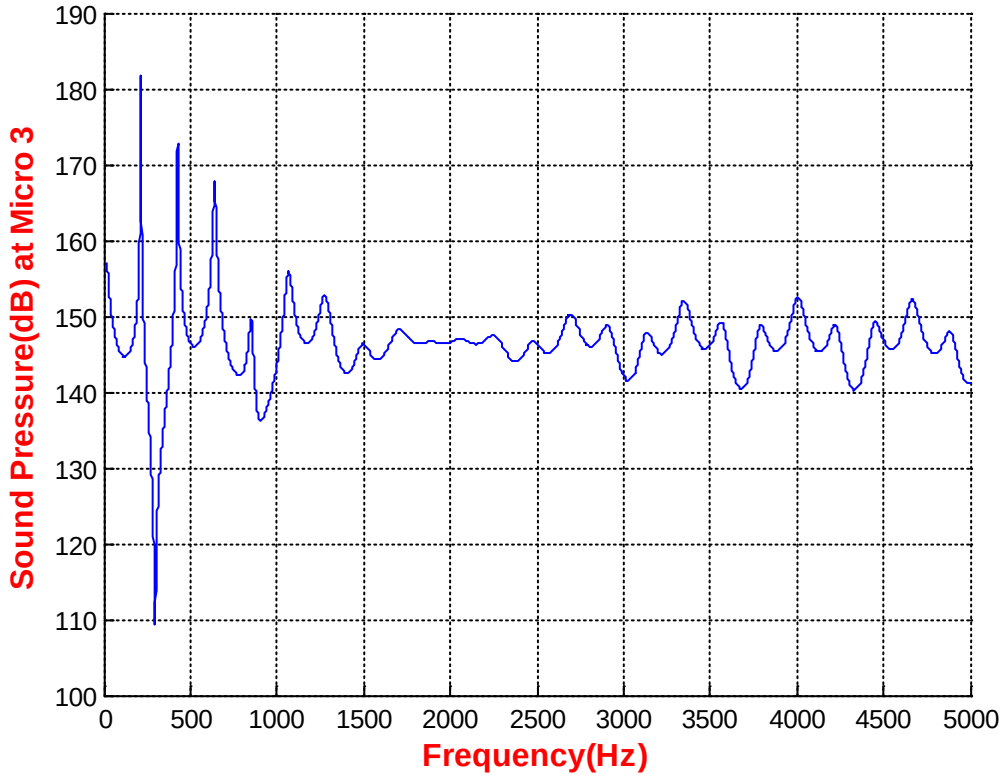

Fig 4.4.26 Sound Pressure (dB) vs. Frequencies (20 Hz to 5000Hz) measured at Micro 3 (reference pressure is 2e-05Pa)

The data file of real part and imaginary part of sound pressure (Pa) vs. frequencies (Hz) can be obtained and exported as a txt format. Fig.4.4.27 is an example of part of data file, which is the real part sound pressure vs. frequencies (Hz) measured by microphone 1 and Fig.4.4.28 is another example of part of data file, which is the imaginary part sound pressure vs. frequencies (Hz) measured by microphone 1. Similarly, the real and imaginary part of sound pressure (Pa) vs. frequencies (Hz) at Micro 2 and Micro 3 can be obtained in the same way. The data file can also be imported into MATLAB to do the further calculation and analysis, which will be introduced in Chapter 5.

#	"freq"	"POINT_1 3"
	20	0.2318924
	21	0.2318102
	22	0.2317223
	23	0.2316285
	24	0.2315286
	25	0.2314222
	26	0.231309
	27	0.2311888
	28	0.2310612
	29	0.2309259
	30	0.2307825
	31	0.2306307
	32	0.2304701
	33	0.2303003
	34	0.2301207
	35	0.2299311
	36	0.229731
	37	0.2295197
	38	0.2292969
	39	0.2290621
	40	0.2288146
	41	0.2285538
	42	0.2282793
	43	0.2279903
	44	0.2276863

Fig.4.4.27 real part of sound pressure (Pa) vs. frequencies (Hz) at Micro 1

#	"freq"	"POINT_1 3"
	20	-1437.453
	21	-1370.948
	22	-1310.583
	23	-1255.559
	24	-1205.208
	25	-1158.97
	26	-1116.371
	27	-1077.007
	28	-1040.532
	29	-1006.649
	30	-975.0976
	31	-945.6539
	32	-918.1205
	33	-892.3245
	34	-868.1132
	35	-845.3513
	36	-823.9188
	37	-803.7084
	38	-784.6244
	39	-766.5808
	40	-749.5001
	41	-733.3126
	42	-717.9551
	43	-703.3705

Fig.4.4.28 imaginary part of sound pressure (Pa) vs. frequencies (Hz) at Micro 1

4.5 Summary

In this chapter, the process of finite element modeling of impedance tube terminated by porous absorption material in ACTRAN has been introduced in details. The process mainly contains three parts: pre-processing, solve and post-processing. A real experiment can be simulated in ACTRAN by finite element modeling, which in other words, a

numerical experiment. In the next chapter, sound pressure data obtained from the finite element model in this chapter will be further processed according to the analytical models introduced in Chapter 2 and Chapter 3 using MATLAB.

References

1. Muehleisen, R. T., Measurement of the acoustic properties of acoustic absorbers. *Illinois Institute of Technology, Muehleisen_plenary_acoustic_materials. pdf* **2007**.

2. Turo, D.; Vignola, J.; Glean, A. Characteristic impedance, wavenumber and porous material design. School of Engineering ,Department of Mechanical Engineering,The Catholic University of America 2012.
3. Cox, T. J.; D'antonio, P., *Acoustic absorbers and diffusers: theory, design and application*. CRC Press: 2009.
4. Zwikker, C.; Kosten, C. W., *Sound absorbing materials*. Elsevier: 1949.
5. Champoux, Y.; Stinson, M. R.; Daigle, G. A., Air‐based system for the measurement of porosity. *The Journal of the Acoustical Society of America* **1991,** *89* (2), 910-916.
6. Beranek, L. L., Acoustic impedance of porous materials. *The Journal of the Acoustical Society of America* **1942,** *13* (3), 248-260.
7. Kuczmarski, M. A.; Johnston, J. C., Acoustic Absorption in Porous Materials. **2011**.
8. EN, B., 29053 "Acoustics—Materials for acoustical applications. *Determination of airflow resistance* **1993**.
9. ASTMC522-03(2009)e1, Standard Test Method for Airflow Resistance of Acoustical Materials, ASTM International, West Conshohocken, PA, 2009, www.astm.org.
10. Fellah, Z. E. A.; Berger, S.; Lauriks, W.; Depollier, C.; Aristegui, C.; Chapelon, J.-Y., Measuring the porosity and the tortuosity of porous materials via reflected waves at oblique incidence. *The Journal of the Acoustical Society of America* **2003,** *113* (5), 2424-2433.
11. Umnova, O.; Attenborough, K.; Shin, H.-C.; Cummings, A., Deduction of tortuosity and porosity from acoustic reflection and transmission measurements on thick samples of rigid-porous materials. *Applied Acoustics* **2005,** *66* (6), 607-624.
12. ACOUSTICS, A. T., Workshop 7 – Virtual Kundt's Tube. *Hi-Key Technology*.
13. Software, F. M., kundt's Tube-Rigid Termination *Actran Student Edition Tutorial*.
14. Software, F. M., Kundt's Tube-Absorbing Termination. *Actran Student Edition Tutorial*.
15. Russell, D. A., Absorption coefficients and impedance. *Science and Mathematics, Department, GMI Engineering & Management Institute, www. gmi. edu, diakses Maret* **2004**.

Chapter 5

5 Results and Discussion

5.1 Introduction

This chapter summarizes the results predicted from the analytical models derived in Chapters 2 and 3, and the results predicted from the finite element models. In Sections 5.2 to 5.4, the computed results for the absorption coefficient and specific acoustic impedance (Pa·m^{-1}·s) are plotted as a function of frequency (Hz) for the Fixed One-Microphone Method, Transfer-Function Method and Three-Microphone Method. Also the calculated values for the materials; porosity, flow resistivity, tortuosity, viscous length and thermal length of the porous absorption material determined by the methodology described in Chapter 4 are used to define the boundary conditions for the finite element model. The results for this model are also presented in this chapter.

5.2 Singularity Analyses[25] [24]

In Chapter 3, the singularity analyses of One-Microphone Method and Three-Microphone Method have been investigated respectively, shown in (3.2.34) and (3.3.36) :

$$p(x,\omega)^2 + (\rho c v_0)^2 + 2p(x,\omega)\rho c v_0 cos kx = 0 \qquad (3.2.34)$$

$$(e^{2jkx_1} + e^{2jkx_2} + e^{2jkx_3}) * \left(e^{-2jkx_1} + e^{-2jkx_2} + e^{-2jkx_3}\right) - 3^2 = 0 \qquad (3.3.24)$$

And based on the previous analyses on singularity in Chapter 3, if one of the two equations above is satisfied, the norm of complex reflection factor r calculated from the corresponding analytical model will become positive infinite, so according to the relationship between reflection factor r and absorption coefficient α which was shown in (2.2.6):

$$\alpha = 1 - |r|^2 = 1 - \left|\frac{p_r}{p_i}\right|^2 \tag{2.2.6}$$

, therefore the absorption coefficient will become negative infinite, which makes the result implausible.

According to Jang and Ih and also it can be deduced from (3.3.36) that when there are $n(n \geq 2)$ microphones and with coordinates of microphones denoted as x_1, x_2, x_3, x_4, x_5 ... x_n, the singularity condition in (3.3.36) for three microphones can be deduced to express the n microphones situation:

$$(\sum_{i=1}^{n} e^{2jkx_i}) * (\sum_{i=1}^{n} e^{-2jkx_i}) - n^2 = 0 \quad (n \geq 2) \tag{5.1.1}$$

The singularity condition of Transfer-Function Method, which is also called as Two-Microphone Method, is a special case of the n microphones, so in (3.3.36) “3” can be substitute by “2” and “n” can be assigned as “2”, thus the singularity condition for the analytical model of Transfer-Function Method can be obtained:

$$(e^{2jkx_1} + e^{2jkx_2}) * \left(e^{-2jkx_1} + e^{-2jkx_2}\right) - 2^2 = 0 \tag{5.1.2}$$

Then (5.1.2) can be rewritten and simplified according to Euler's formula $e^{i\theta} = cos\theta + isin\theta$:

$$\cos(2k|x_2 - x_1|) = 1 \tag{5.1.3}$$

And according to properties of cosine function, (5.1.3) can be further expressed as:

$$2k|x_2 - x_1| = 2n\pi \qquad n = 1,2,3 \ldots \tag{5.1.4}$$

There is another method to obtain the singularity condition of Transfer-Function Method which is to refer to the expression of reflection factor r in (2.4.12):

$$r = \frac{H_{21} - e^{-jks}}{e^{jks} - H_{21}} e^{2jkx_1} \tag{2.4.12}$$

The complex reflection factor r will become infinite if the denominator of RHS of (2.4.12) is approximate to zero, that is:

$$e^{jks} - H_{21} = 0 \tag{5.1.5}$$

s and H_{21} are two parameters which have been defined previously in Chapter 2 and their expressions are $s = x_1 - x_2$ and $H_{21} = p_2/p_1$, (5.1.5) is equivalent to (5.1.2), (5.1.3) and (5.1.4).

Therefore the singularity conditions of analytical models are obtained so far and shown in (3.2.24) (5.1.2) and (3.3.36) for One-Microphone Method, Transfer-Function Method and Three-Microphone Method, respectively. Once these conditions are satisfied, the results will change abruptly or become unreasonable.

5.3 Plots of the Absorption Coefficient as a function of Frequency

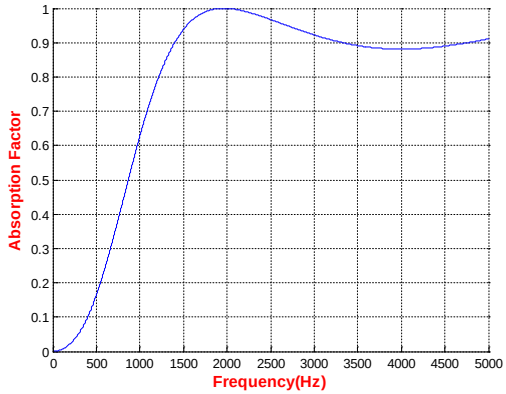

Fig 5.2.1 Absorption coefficient vs. Frequencies (Hz) obtained from Transfer-Function Method using Micro 1 and Micro 2

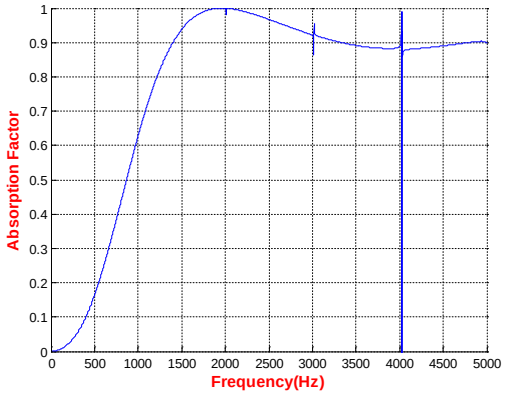

Fig 5.2.2 Absorption coefficient vs. Frequencies (Hz) obtained from Transfer-Function Method using Micro 2 and Micro 3

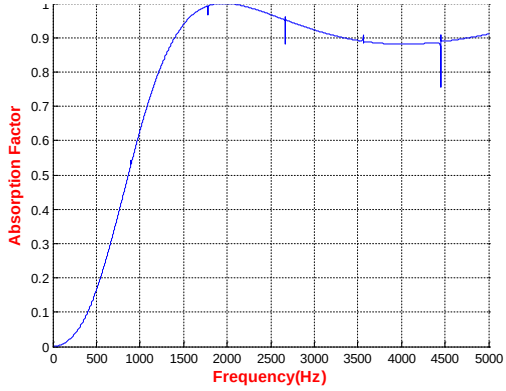

Fig 5.2.3 Absorption coefficient vs. Frequencies (Hz) obtained from Transfer-Function Method using Micro 1 and Micro 3

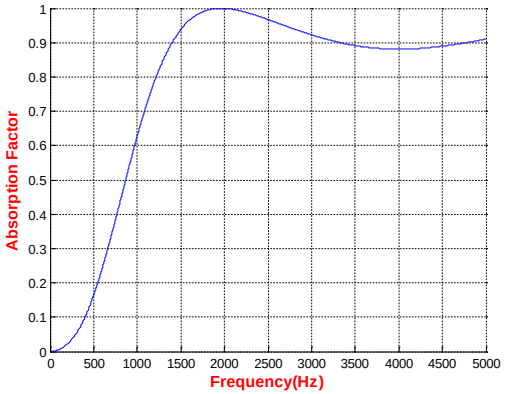

Fig 5.2.4 Absorption coefficient vs. Frequencies (Hz) obtained from Three-Microphone Method using Micro 1 Micro 2 and Micro 3

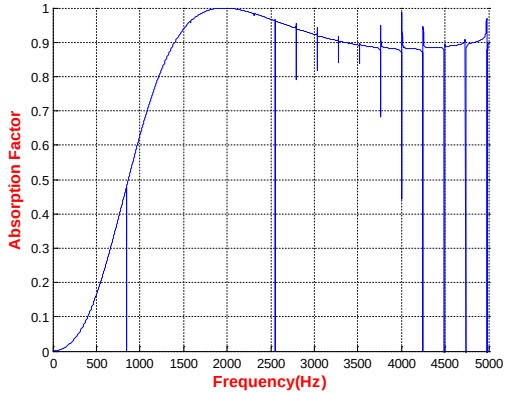

Fig 5.2.5 Absorption coefficient vs. Frequencies (Hz) obtained from One-Microphone Method using Micro 1

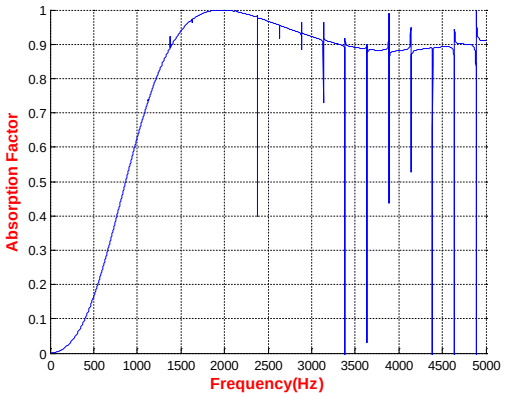

Fig 5.2.6 Absorption coefficient vs. Frequencies (Hz) obtained from One-Microphone Method using Micro 2

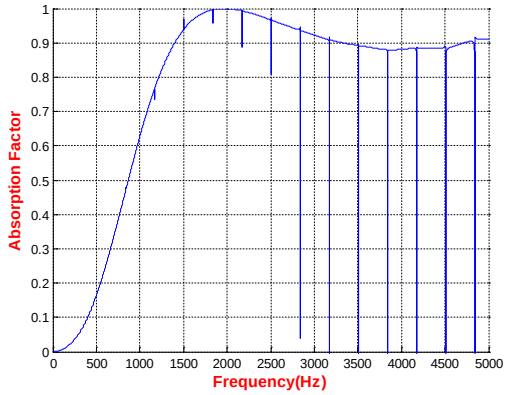

Fig 5.2.7 Absorption coefficient vs. Frequencies (Hz) obtained from One-Microphone Method using Micro 3

5.4 Plots of the Real Part of Specific Acoustic Impedance as a function of Frequency

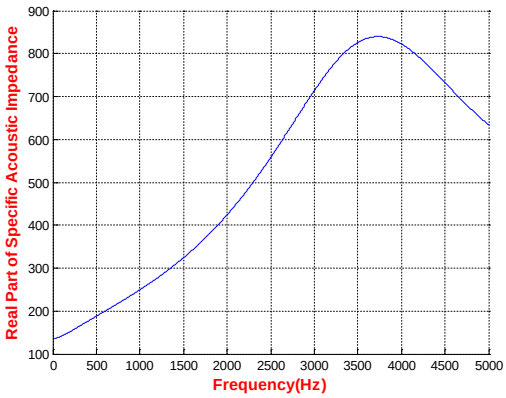

Fig 5.3.1 Real Part of Specific Acoustic Impedance ($Pa \cdot m^{-1} \cdot s$) vs. Frequencies (Hz) obtained from Transfer-Function Method using Micro 1 and Micro 2

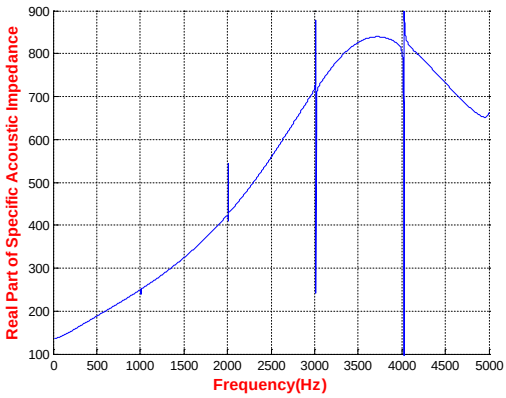

Fig 5.3.2 Real Part of Specific Acoustic Impedance ($Pa \cdot m^{-1} \cdot s$) vs. Frequencies (Hz) obtained from Transfer-Function Method using Micro 2 and Micro 3

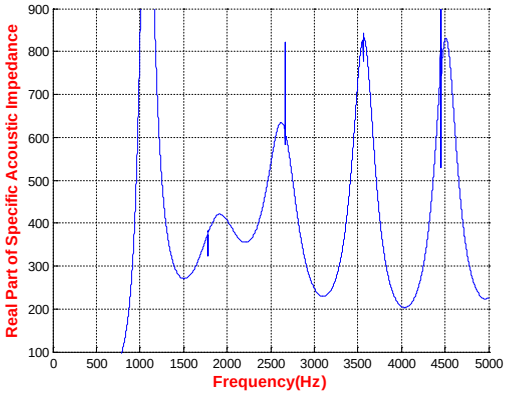

Fig 5.3.3 Real Part of Specific Acoustic Impedance ($Pa \cdot m^{-1} \cdot s$) vs. Frequencies (Hz) obtained from Transfer-Function Method using Micro 1 and Micro 3

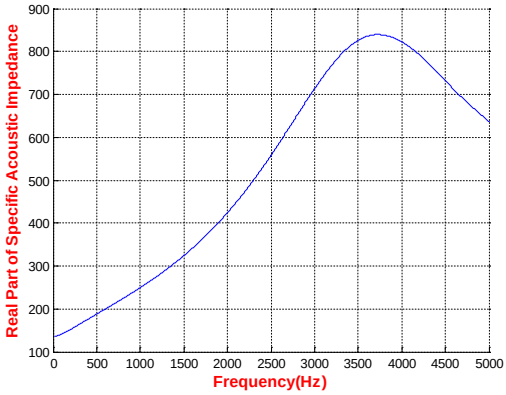

Fig 5.3.4 Real Part of Specific Acoustic Impedance ($Pa \cdot m^{-1} \cdot s$) vs. Frequencies (Hz) obtained from One-Microphone Method using Micro 1, Micro 2 and Micro 3

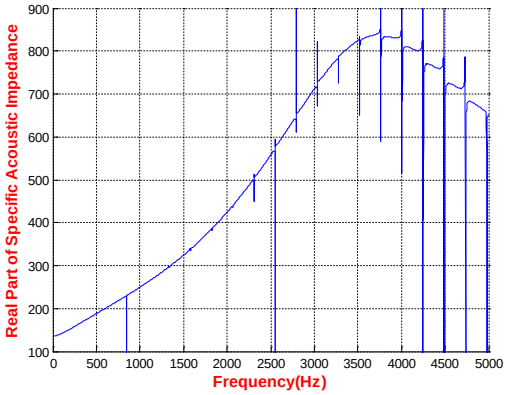

Fig 5.3.5 Real Part of Specific Acoustic Impedance ($Pa \cdot m^{-1} \cdot s$) vs. Frequencies (Hz) obtained from One-Microphone Method using Micro 1

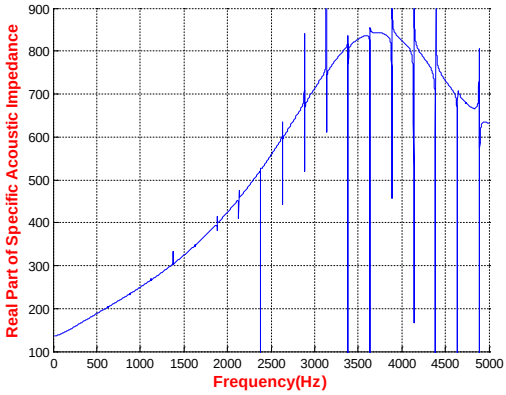

Fig 5.3.6 Real Part of Specific Acoustic Impedance ($Pa \cdot m^{-1} \cdot s$) vs. Frequencies (Hz) obtained from One-Microphone Method using Micro 2

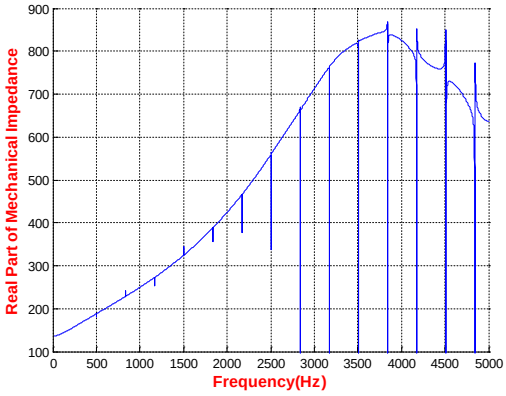

Fig 5.3.7 Real Part of Specific Acoustic Impedance ($Pa \cdot m^{-1} \cdot s$) vs. Frequencies (Hz) obtained from One-Microphone Method using Micro 3

5.5 Plots of the Imaginary Part of Specific Acoustic Impedance as a function of Frequency

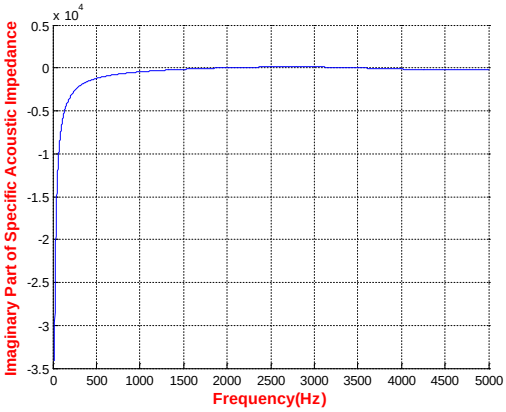

Fig 5.4.1 Imaginary Part of Specific Acoustic Impedance ($Pa \cdot m^{-1} \cdot s$) vs. Frequencies (Hz) obtained from Transfer-Function Method using Micro 1 and Micro 2

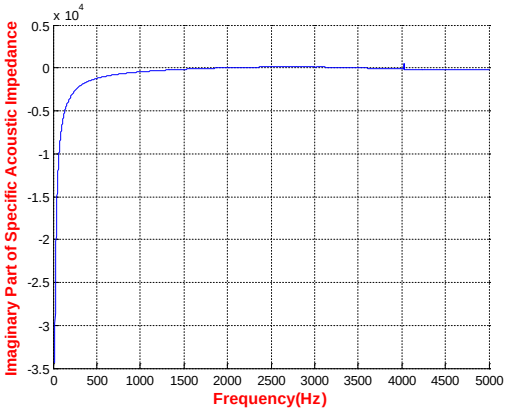

Fig 5.4.2 Imaginary Part of Specific Acoustic Impedance ($Pa \cdot m^{-1} \cdot s$) vs. Frequencies (Hz) obtained from Transfer-Function Method using Micro 2 and Micro 3

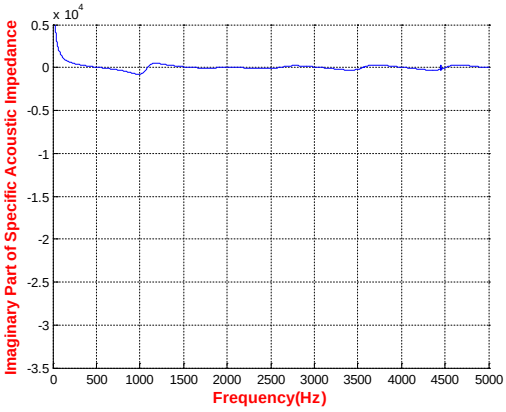

Fig 5.4.3 Imaginary Part of Specific Acoustic Impedance ($Pa \cdot m^{-1} \cdot s$) vs. Frequencies (Hz) obtained from Transfer-Function Method using Micro 1 and Micro 3

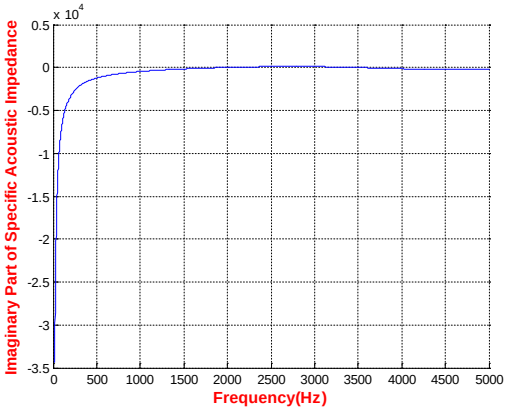

Fig 5.4.4 Imaginary Part of Specific Acoustic Impedance ($Pa \cdot m^{-1} \cdot s$) vs. Frequencies (Hz) obtained from One-Microphone Method using Micro 1, Micro 2 and Micro 3

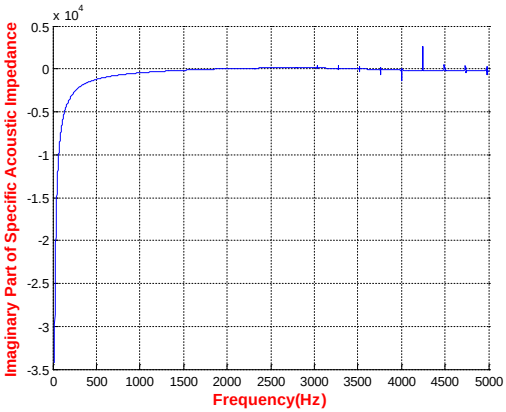

Fig 5.4.5 Imaginary Part of Specific Acoustic Impedance ($Pa \cdot m^{-1} \cdot s$) vs. Frequencies (Hz) obtained from One-Microphone Method using Micro 1

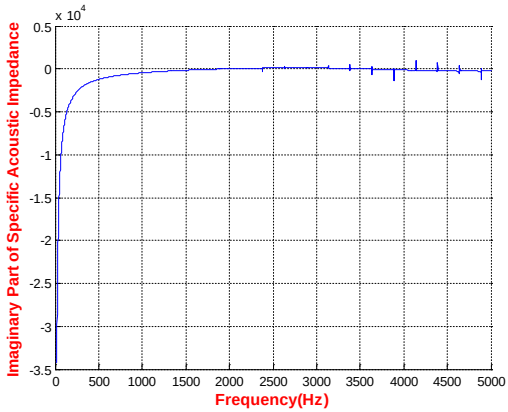

Fig 5.4.6 Imaginary Part of Specific Acoustic Impedance ($Pa \cdot m^{-1} \cdot s$) vs. Frequencies (Hz) obtained from One-Microphone Method using Micro 2

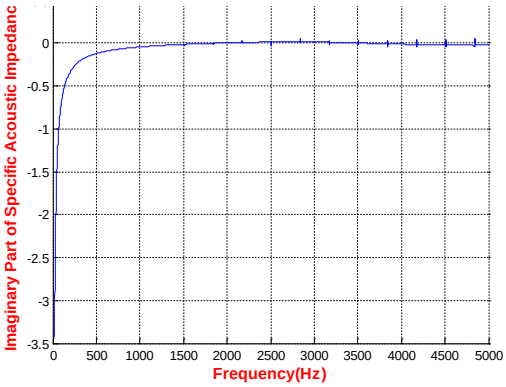

Fig 5.4.7 Imaginary Part of Specific Acoustic Impedance ($Pa \cdot m^{-1} \cdot s$) vs. Frequencies (Hz) obtained from One-Microphone Method using Micro 3

5.6 Residual Error vs. Frequencies by Three-Microphone Method

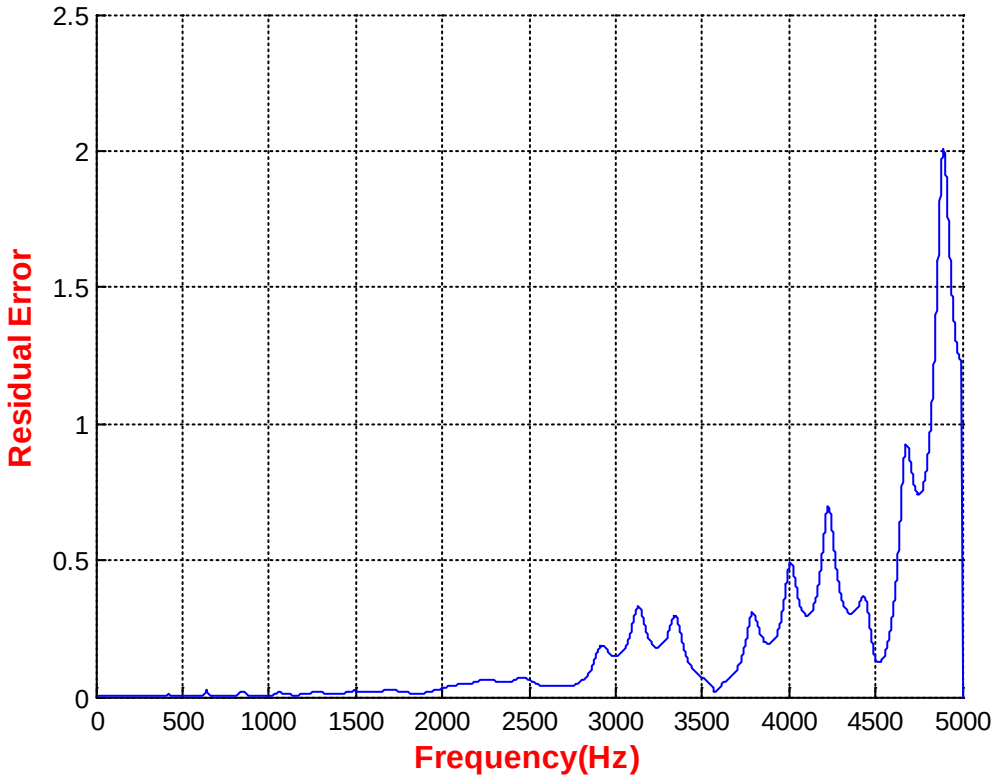

Fig 5.5.1 Residual Error vs. Frequencies (Hz) obtained from Three-Microphone Method using Micro 1, Micro 2 and Micro 3

5.7 Discussions of results

In Fig 5.2.1, Fig 5.2.2, Fig 5.2.3, Fig 5.3.4, Fig 5.3.5, Fig 5.3.6 and Fig 5.4.7, which are the graphs of absorption coefficient vs. frequencies, it can be seen that the absorption coefficient increases with the growth of sound frequency from 0 Hz, when the sound frequency reaches about 2000 Hz, the absorption coefficient obtains its maximum value, approximately equals to 1, after sound frequency continued growing beyond 2000 Hz, the absorption coefficient begins to decrease slightly, however, when the sound frequency exceeds about 4000 Hz, the absorption coefficient will be increasing again and finally reaches about 0.92 when sound frequency is 5000 Hz.

In Fig 5.3.1, Fig 5.3.2, Fig 5.3.4, Fig 5.3.5, Fig 5.3.6 and Fig 5.3.7, which are the graphs of real part of specific acoustic impedance vs. frequencies, according to Section 1.2 in Chapter 1 and Section 2.2.1 in Chapter 2, the real part of acoustic impedance, which is also called the resistive part, represents the energy transfer of an acoustic wave, and only the resistive part is related to energy loss, it can be seen that the real acoustic impedance increases with the growth of sound frequency from 0Hz, when the sound frequency reaches about 3750Hz, the real acoustic impedance obtains its maximum value, about 840 $\mathrm{Pa{\cdot}m^{-1}{\cdot}s}$, after sound frequency continued growing beyond 3750Hz, the real acoustic impedance begins to decrease and finally reaches about 640 $\mathrm{Pa{\cdot}m^{-1}{\cdot}s}$ when sound frequency is 5000Hz.

In Fig 5.4.1, Fig 5.4.2, Fig 5.4.4, Fig 5.4.5, Fig 5.4.6 and Fig 5.4.7, which are the graphs of imaginary part of specific acoustic impedance vs. frequencies, according to 1.2 in Chapter 1 and 2.2.1 in Chapter 2, the imaginary part of acoustic impedance, which is also called the reactive part, represents pressure that is out of phase with the motions of molecules which constitute the acoustic medium and causes no average energy transfer, thus the reactive part is not related to energy loss. It can be seen that with the growth of sound frequency from 0Hz to 5000 Hz, the real acoustic impedance increases from about -3.4×10^4 $\mathrm{Pa{\cdot}m^{-1}{\cdot}s}$ and approached to 0 $\mathrm{Pa{\cdot}m^{-1}{\cdot}s}$ approximately.

Based on the singularities analyses in Section 5.5, the abrupt changes of the results will occur in Two-Microphone Method when using Micro 2 and Micro 3, similar situations will always appear when using One Microphone Method, regardless of which microphone is using. However, there are no abrupt changes when using Two-Microphone Method with Micro 1 and Micro 2 and Three-Microphone Method, it is apparently that in

Fig 5.3.3 and Fig 5.4.3, the results of the acoustic impedance vs. frequencies obtained by using Two-Microphone Method with Micro 1 and Micro 3 are unreasonable.

We conclude that the results obtained by Two-Microphone Method are easily to be influenced by the microphone spacing. Good microphone spacing can generate reasonable results and with no singularities, fair microphone spacing can generate reasonable results but with singularities and poor microphone spacing can generate results with singularities or unreasonable.

It is obviously that the abrupt changes will occur in high frequency and periodically, in low frequency, it will be less apparent which can be neglected.

Although there are no encountered singularities and no unreasonable results occurring when using Three-Microphone Method, the solutions obtained from that method are not exact solutions but approximate ones according to Section 3.3.2. Thus it is necessary to consider residual error when using that method. The residual error vs. frequencies (Hz) is plotted in Fig 5.5.1, when frequency is from 0 Hz to about 2000 Hz, the residual error is small enough so that it can be neglected, whereas with the growth of sound frequency, the residual error will increase and cannot be ignored, when sound frequency reached 4874Hz, the residual error obtained its maximum value. Therefore the Three-Microphone Method is more reliable in low frequency range than in high frequency range.

References

1. Arenas, J. P.; Crocker, M. J., Recent trends in porous sound-absorbing materials. *Sound & vibration* **2010,** *44* (7), 12-18.
2. Theebe, M. A., Planes, trains, and automobiles: the impact of traffic noise on house prices. *The Journal of Real Estate Finance and Economics* **2004,** *28* (2-3), 209-234.

3. Wolfe, J. In *Aeronautics Research Mission Directorate Update with emphasis on Integrated Systems Research*, 48th AIAA Aerospace Science Meeting, Orlando, Florida, Orlando, Florida, 2010.
4. Muehleisen, R. T., Measurement of the acoustic properties of acoustic absorbers. *Illinois Institute of Technology, Muehleisen_plenary_acoustic_materials. pdf* **2007**.
5. ISO, ISO 10534-1, Acoustics---Determination of sound absorption coefficient and impedance in impedance tubes---Part 1: Method using standing wave ratio. International Standards Organisation. 1996.
6. ISO, ISO 10534-2, Acoustics-Determination of sound absorption coefficient and impedance in impedance tubes-Part 2: Transfer-function method. 1998.
7. ASTMC384-04(2011), Standard Test Method for Impedance and Absorption of Acoustical Materials by Impedance Tube Method, ASTM International, West Conshohocken, PA, 2011, www.astm.org.
8. ASTME1050-10, Standard Test Method for Impedance and Absorption of Acoustical Materials Using A Tube, Two Microphones and A Digital Frequency Analysis System, ASTM International, West Conshohocken, PA, 2010, www.astm.org.
9. Russell, D. A., Absorption coefficients and impedance. *Science and Mathematics, Department, GMI Engineering & Management Institute, www. gmi. edu, diakses Maret* **2004**.
10. ISO, ISO 354 Acoustics--Measurement of sound absorption in a reverberation room. 2003; Vol. 2003.
11. ASTM, ASTM C423-02a Standard Test Method for Sound Absorption and Sound Absorption Coefficients by the Reverberation Room Method. ASTM International: 2002.
12. Suhanek, M.; Jambrosic, K.; Domitrovic, H., Student project of building an impedance tube. *Journal of the Acoustical Society of America* **2008,** *123* (5), 3616.
13. ASTMC522-03(2009)e1, Standard Test Method for Airflow Resistance of Acoustical Materials, ASTM International, West Conshohocken, PA, 2009, www.astm.org.
14. Everest, F. A.; Pohlmann, K., *Master Handbook of Acoustics*. McGraw-Hill Education: 2009.
15. Wikipedia, Acoustic impedance-Mathematical definitions. 2014.
16. Heed, C., Sound absorption and acoustic surface impedance. **2008**.
17. Seybert, A. F. In *Notes on absorption and impedance measurements*, Noise and Vibration Conference SAE, Traverse City, 2003.
18. Yong-hua, W.; Cheng-chun, Z.; Jing, W.; Lei, S.; Xue-peng, Z.; Lu-quan, R., Analysis of sound-absorbing performance of bionic porous material *Journal of Jilin University (Engineering and Technology Edition）* **2012,** *42* (6), 1442-1447.
19. Software, F. M., Kundt's Tube-Rigid Termination *Actran Student Edition Tutorial*.
20. Software, F. M., Kundt's Tube-Absorbing Termination. *Actran Student Edition Tutorial*.
21. Chu, W. T., Transfer function technique for impedance and absorption measurements in an impedance tube using a single microphone. *The Journal of the Acoustical Society of America* **1986,** *80* (2), 555-560.
22. Oulu, U. o. 5.5. overdetermined system, least squares method. http://s-mat-pcs.oulu.fi/~mpa/matreng/ematr5_5.htm.

23. Oulu, U. o. Example 1: The least squares method. http://s-mat-pcs.oulu.fi/~mpa/matreng/eem5_5-1.htm.
24. Jang, S.-H.; Ih, J.-G., On the multiple microphone method for measuring in-duct acoustic properties in the presence of mean flow. *The journal of the acoustical society of America* **1998,** *103* (3), 1520-1526.
25. Dickens, P.; Smith, J.; Wolfe, J., Improved precision in measurements of acoustic impedance spectra using resonance-free calibration loads and controlled error distribution. *The Journal of the Acoustical Society of America* **2007,** *121* (3), 1471-1481.
26. Turo, D.; Vignola, J.; Glean, A. Characteristic impedance, wavenumber and porous material design. School of Engineering ,Department of Mechanical Engineering,The Catholic University of America 2012.
27. Cox, T. J.; D'antonio, P., *Acoustic absorbers and diffusers: theory, design and application*. CRC Press: 2009.
28. Zwikker, C.; Kosten, C. W., *Sound absorbing materials*. Elsevier: 1949.
29. Champoux, Y.; Stinson, M. R.; Daigle, G. A., Air‐based system for the measurement of porosity. *The Journal of the Acoustical Society of America* **1991,** *89* (2), 910-916.
30. Beranek, L. L., Acoustic impedance of porous materials. *The Journal of the Acoustical Society of America* **1942,** *13* (3), 248-260.
31. Kuczmarski, M. A.; Johnston, J. C., Acoustic Absorption in Porous Materials. **2011**.
32. EN, B., 29053 "Acoustics—Materials for acoustical applications. *Determination of airflow resistance* **1993**.
33. Fellah, Z. E. A.; Berger, S.; Lauriks, W.; Depollier, C.; Aristegui, C.; Chapelon, J.-Y., Measuring the porosity and the tortuosity of porous materials via reflected waves at oblique incidence. *The Journal of the Acoustical Society of America* **2003,** *113* (5), 2424-2433.
34. Umnova, O.; Attenborough, K.; Shin, H.-C.; Cummings, A., Deduction of tortuosity and porosity from acoustic reflection and transmission measurements on thick samples of rigid-porous materials. *Applied Acoustics* **2005,** *66* (6), 607-624.
35. ACOUSTICS, A. T., Workshop 7 – Virtual Kundt's Tube. *Hi-Key Technology*.

Chapter 6

6 Concluding Remarks and Future Research Directions

6.1 Introduction

This chapter summarizes the work performed for this thesis, the results predicted from the novel analytical models and their subsequent validation via comparison with predictions from previously derived models and a finite element model.

6.2 Concluding Remarks

According to singularity analyses of the analytical models of One-Microphone Method, Transfer-Function Method and Three-Microphone Method in Chapter 5, the singularities can make the results unreasonable and will occur if the parameters of the analytical model satisfy the singularity condition.

By looking at the results obtained from the analytical models in Chapter 5, the singularities are always occurring when using One-Microphone Method, regardless of which microphone is used to measure sound pressure. The singularities are more apparent in high frequencies than in low frequencies and appear almost periodically.

When obtaining results from the analytical model of Two-Microphone Method, the results are easily influenced by the microphone spacing. Poor microphone spacing can generate unreasonable results. Therefore, to assure that a results are reasonable and with no singularities using that model, good microphone spacing is vital.

There are no singularities and no unreasonable results occurring when using analytical model of Three-Microphone Method. This model is not influenced by microphone selection or by the microphone spacing. Thus this model is much more reliable when compared with the other two analytical models, even though there is residual error, which increases in the high frequencies when using this model.

In summary, by comparing the analytical model of Three-Microphone Method with the other two analytical models, this model is preferable and is recommended to use as model to avoid singularities and unreasonable results.

6.3 Future Research Directions

It will be interesting to look at when there are n ($n \geq 3$) microphones to be used to measure sound pressure in duct, which can be called as Multiple-Microphone Method when the number of microphone is greater than three, to explore how the number of microphones can influence the quality of results and residual error. In addition, a comparison between experimental results and the analytical predictions is recommended for the validation of the the analytical models in described in Chapter 3 and Chapter 5.

Appendix

7 Appendix (MATLAB Codes)

1. Calculate the complex sound pressure values at Micro 1, Micro 2 and Micro 3

```
f=[20 21 22 23...5000]; %frequency 20Hz-5000Hz step 1 Hz
%import values of real and imaginary part of sound pressure
at three microphones' locations from ACTRAN
p1real=[ 0.2318924   0.2318102   0.2317223... -58.6791];
p1image=[ -1437.453  -1370.948   -1310.583... -402.5237];
p2real=[0.2323837   0.232353    0.2323193... 220.1406];
p2image=[-1436.995  -1370.467   -1310.078... 85.18557];
p3real=[0.2356436   0.2359553   0.2362825... -223.4915];
p3image=[-1430.317  -1363.444   -1302.711... -45.4722];
%calculate the complex sound pressure values at locations
of three microphones
p1=p1real+p1image*1i; % complex sound pressure at micro 1
p2=p2real+p2image*1i; % complex sound pressure at micro 2
p3=p3real+p3image*1i; % complex sound pressure at micro 3
```

2. Plot Sound Pressure Level (SPL) at Micro 1, Micro 2 and Micro 3

```
%plot Sound Pressure Level (SPL)
p1d=20*log10(abs(p1)/(2e-05)); %reference pressure is 2e-
05Pa
plot(f,p1d);xlabel('Frequency(Hz)','FontSize',12,'FontWeigh
t','bold','Color','r');ylabel('Sound Pressure(dB) at Micro
1','FontSize',12,'FontWeight','bold','Color','r');
grid on
hold on
p2d=20*log10(abs(p2)/(2e-05)); %reference pressure is 2e-
05Pa
plot(f,p2d);xlabel('Frequency(Hz)','FontSize',12,'FontWeigh
t','bold','Color','r');ylabel('Sound Pressure(dB) at Micro
2','FontSize',12,'FontWeight','bold','Color','r');
grid on
hold on
p3d=20*log10(abs(p3)/(2e-05)); %reference pressure is 2e-
05Pa
plot(f,p3d);xlabel('Frequency(Hz)','FontSize',12,'FontWeigh
```

```
t','bold','Color','r');ylabel('Sound Pressure(dB) at Micro
3','FontSize',12,'FontWeight','bold','Color','r');
grid on
```

3. Calculations by Analytical Model of Transfer-Function Method

```
%calculate transfer functions
H21=p2./p1;H32=p3./p2;H31=p3./p1;
%plot transfer function vs frequency
plot(f,H21);
grid on
hold on
plot(f,H32);
grid on
hold on
plot(f,H31);
grid on

%locations of micro 1 micro 2 and micro 3 in old coordinate
x1=0.700; %micro 1
x2=0.678; %micro 2
x3=0.509; %micro 3
l=0.762; %length of tube
%coordinate transformation
X1=l-x1;
X2=l-x2;
X3=l-x3;
%space between each two microphones
s1=X1-X2;
s2=X2-X3;
s3=X1-X3;
c=340; %sound speed in air
w=2*pi*f; %angular frequency
k=w/c; %wave number
A1=exp(-1i*k*s1);B1=exp(1i*k*s1);C1=exp(2i*k*X1);
A2=exp(-1i*k*s2);B2=exp(1i*k*s2);C2=exp(2i*k*X2);
A3=exp(-1i*k*s3);B3=exp(1i*k*s3);C3=exp(2i*k*X3);
%reflection factor calculated by micro 1 and micro 2
r1=(H21-A1)./(B1-H21).*C1;
%reflection factor calculated by micro 2 and micro 3
r2=(H32-A2)./(B2-H32).*C2;
%reflection factor calculated by micro 1 and micro 3
r3=(H31-A3)./(B3-H31).*C3;
%norm of reflection factor r1 r2 r3
X=abs(r1);
Y=abs(r2);
```

```
Z=abs(r3);

%calculate and plot absorption coefficient vs frequency (Hz)
by micro 1 and micro 2
a1=ones(1,4981)-X.^2;
plot(f,a1);xlabel('Frequency(Hz)','FontSize',12,'FontWeight
','bold','Color','r');ylabel('Absorption
Factor','FontSize',12,'FontWeight','bold','Color','r');
grid on
hold on
%calculate and plot absorption coefficient vs frequency (Hz)
by micro 2 and micro 3
a2=ones(1,4981)-Y.^2;
plot(f,a2);xlabel('Frequency(Hz)','FontSize',12,'FontWeight
','bold','Color','r');ylabel('Absorption
Factor','FontSize',12,'FontWeight','bold','Color','r');
grid on
hold on
%calculate and plot absorption coefficient vs frequency (Hz)
by micro 1 and micro 3
a3=ones(1,4981)-Z.^2;
plot(f,a3);xlabel('Frequency(Hz)','FontSize',12,'FontWeight
','bold','Color','r');ylabel('Absorption
Factor','FontSize',12,'FontWeight','bold','Color','r');
grid on

D=0.016; % inner diameter of tube (sample)
R=D/2; %inner radius of tube (sample)
s0=pi*R^2; %cross-section area of sample
dens=1.225; %density of air in tube

%micro 1 and micro 2
ZM1=dens*c*s0*(ones(1,4981)+r1)./(ones(1,4981)-
r1);%calculate mechanical impedance
ZS1=dens*c*(ones(1,4981)+r1)./(ones(1,4981)-r1); %calculate
specific acoustic impedance

ZMR1=real(ZM1); %obtain real part of mechanical impedance
ZMI1=imag(ZM1); %obtain imaginary part of mechanical
impedance
ZSR1=real(ZS1); %obtain real part of specific acoustic
impedance
ZSI1=imag(ZS1); %obtain imaginary part of specific acoustic
impedance

%plot real part of mechanical impedance vs frequency (Hz)
by micro 1 and micro 2
```

```
plot(f,ZMR1);xlabel('Frequency(Hz)','FontSize',12,'FontWeig
ht','bold','Color','r');ylabel('Real Part of Mechanical
Impedance','FontSize',12,'FontWeight','bold','Color','r');
grid on
hold on
%plot imaginary part of mechanical impedance vs frequency
(Hz) by micro 1 and micro 2
plot(f,ZMI1);xlabel('Frequency(Hz)','FontSize',12,'FontWeig
ht','bold','Color','r');ylabel('Imaginary Part of
Mechanical
Impedance','FontSize',12,'FontWeight','bold','Color','r');
hold on
%plot real part of specific acoustic impedance vs frequency
(Hz) by micro 1 and micro 2
plot(f,ZSR1);xlabel('Frequency(Hz)','FontSize',12,'FontWeig
ht','bold','Color','r');ylabel('Real Part of Specific
Acoustic
Impedance','FontSize',12,'FontWeight','bold','Color','r');
grid on
hold on
%plot imaginary part of specific acoustic impedance vs
frequency (Hz) by micro 1 and micro 2
plot(f,ZSI1);xlabel('Frequency(Hz)','FontSize',12,'FontWeig
ht','bold','Color','r');ylabel('Imaginary Part of Specific
Acoustic
Impedance','FontSize',12,'FontWeight','bold','Color','r');


%micro 2 and micro 3
ZM2=dens*c*s0*(ones(1,4981)+r2)./(ones(1,4981)-r2);
%calculate mechanical impedance
ZS2=dens*c*(ones(1,4981)+r2)./(ones(1,4981)-r2); %calculate
specific acoustic impedance

ZMR2=real(ZM2); %obtain real part of mechanical impedance
ZMI2=imag(ZM2); %obtain imaginary part of mechanical
impedance
ZSR2=real(ZS2); %obtain real part of specific acoustic
impedance
ZSI2=imag(ZS2); %obtain imaginary part of specific acoustic
impedance

%plot real part of mechanical impedance vs frequency (Hz)
by micro 2 and micro 3
plot(f,ZMR2);xlabel('Frequency(Hz)','FontSize',12,'FontWeig
ht','bold','Color','r');ylabel('Real Part of Mechanical
Impedance','FontSize',12,'FontWeight','bold','Color','r');
```

```
grid on
hold on

%plot imaginary part of mechanical impedance vs frequency
(Hz) by micro 2 and micro 3
plot(f,ZMI2);xlabel('Frequency(Hz)','FontSize',12,'FontWeig
ht','bold','Color','r');ylabel('Imaginary Part of
Mechanical
Impedance','FontSize',12,'FontWeight','bold','Color','r');
hold on

%plot real part of specific acoustic impedance vs frequency
(Hz) by micro 2 and micro 3
plot(f,ZSR2);xlabel('Frequency(Hz)','FontSize',12,'FontWeig
ht','bold','Color','r');ylabel('Real Part of Specific
Acoustic
Impedance','FontSize',12,'FontWeight','bold','Color','r');
grid on
hold on

%plot imaginary part of specific acoustic impedance vs
frequency (Hz) by micro 2 and micro 3
plot(f,ZSI2);xlabel('Frequency(Hz)','FontSize',12,'FontWeig
ht','bold','Color','r');ylabel('Imaginary Part of Specific
Acoustic
Impedance','FontSize',12,'FontWeight','bold','Color','r');


%micro 1 and micro 3
ZM3=dens*c*s0*(ones(1,4981)+r3)./(ones(1,4981)-r3);
%calculate mechanical impedance
ZS3=dens*c*(ones(1,4981)+r3)./(ones(1,4981)-r3); %calculate
specific acoustic impedance

ZMR3=real(ZM3); %obtain real part of mechanical impedance
ZMI3=imag(ZM3); %obtain imaginary part of mechanical
impedance
ZSR3=real(ZS3); %obtain real part of specific acoustic
impedance
ZSI3=imag(ZS3); %obtain imaginary part of specific acoustic
impedance

%plot real part of mechanical impedance vs frequency (Hz)
by micro 1 and micro 3
plot(f,ZMR3);xlabel('Frequency(Hz)','FontSize',12,'FontWeig
ht','bold','Color','r');ylabel('Real Part of Mechanical
Impedance','FontSize',12,'FontWeight','bold','Color','r');
```

```
grid on
hold on

%plot imaginary part of mechanical impedance vs frequency
(Hz) by micro 1 and micro 3
plot(f,ZMI3);xlabel('Frequency(Hz)','FontSize',12,'FontWeig
ht','bold','Color','r');ylabel('Imaginary Part of
Mechanical
Impedance','FontSize',12,'FontWeight','bold','Color','r');
hold on

%plot real part of specific acoustic impedance vs frequency
(Hz) by micro 1 and micro 3
plot(f,ZSR3);xlabel('Frequency(Hz)','FontSize',12,'FontWeig
ht','bold','Color','r');ylabel('Real Part of Specific
Acoustic
Impedance','FontSize',12,'FontWeight','bold','Color','r');
grid on
hold on

%plot imaginary part of specific acoustic impedance vs
frequency (Hz) by micro 1 and micro 3
plot(f,ZSI3);xlabel('Frequency(Hz)','FontSize',12,'FontWeig
ht','bold','Color','r');ylabel('Imaginary Part of Specific
Acoustic
Impedance','FontSize',12,'FontWeight','bold','Color','r');
```

4. Calculations by Analytical Model of One-Microphone Method

```
v=1; %boundary excitation
%micro 1
z1=(p1.*cos(k*l)-
1i*dens*c*v*sin(k*X1))./(dens*c*v*cos(k*X1)-
p1.*sin(k*l)*1i); %calculate specific acoustic impedance
ratio
Z1=z1*(dens*c*s0); %calculate mechanical impedance
R1=(z1-1)./(z1+1); %calculate reflection factor
alpha1=ones(1,4981)-abs(R1).^2; %calculate absorption
coefficient
%plot absorption coefficient vs frequency (Hz)
plot(f,alpha1,'g');xlabel('Frequency(Hz)','FontSize',12,'Fo
ntWeight','bold','Color','r');ylabel('Absorption
Factor','FontSize',12,'FontWeight','bold','Color','r');

Z1R=real(Z1); %obtain real part of mechanical impedance
Z1I=imag(Z1); %obtain imaginary part of mechanical
```

```
impedance
ZS1R=real(Z1/s0); %obtain real part of specific acoustic
impedance
ZS1I=imag(Z1/s0); %obtain imaginary part of specific
acoustic impedance

%plot real part of mechanical impedance vs frequency (Hz)
by micro 1
plot(f,Z1R);xlabel('Frequency(Hz)','FontSize',12,'FontWeigh
t','bold','Color','r');ylabel('Real Part of Mechanical
Impedance','FontSize',12,'FontWeight','bold','Color','r');
grid on
hold on
%plot imaginary part of mechanical impedance vs frequency
(Hz) by micro 1
plot(f,Z1I);xlabel('Frequency(Hz)','FontSize',12,'FontWeigh
t','bold','Color','r');ylabel('Imaginary Part of Mechanical
Impedance','FontSize',12,'FontWeight','bold','Color','r');
grid on
hold on

%plot real part of specific acoustic impedance vs frequency
(Hz) by micro 1
plot(f,ZS1R);xlabel('Frequency(Hz)','FontSize',12,'FontWeig
ht','bold','Color','r');ylabel('Real Part of Specific
Acoustic
Impedance','FontSize',12,'FontWeight','bold','Color','r');
grid on
hold on
%plot imaginary part of specific acoustic impedance vs
frequency (Hz) by micro 1
plot(f,ZS1I);xlabel('Frequency(Hz)','FontSize',12,'FontWeig
ht','bold','Color','r');ylabel('Imaginary Part of Specific
Acoustic
Impedance','FontSize',12,'FontWeight','bold','Color','r');


%micro 2
z2=(p2.*cos(k*l)-
1i*dens*c*v*sin(k*X2))./(dens*c*v*cos(k*X2)-
p2.*sin(k*l)*1i); %calculate specific acoustic impedance
ratio
Z2=z2*(dens*c*s0); %calculate mechanical impedance
R2=(z2-1)./(z2+1); %calculate reflection factor
alpha2=ones(1,4981)-abs(R2).^2; %calculate absorption
coefficient
```

```
%plot absorption coefficient vs frequency (Hz)
plot(f,alpha2,'y');xlabel('Frequency(Hz)','FontSize',12,'Fo
ntWeight','bold','Color','r');ylabel('Absorption
Factor','FontSize',12,'FontWeight','bold','Color','r');

Z2R=real(Z2); %obtain real part of mechanical impedance
Z2I=imag(Z2); %obtain imaginary part of mechanical
impedance
ZS2R=real(Z2/s0); %obtain real part of specific acoustic
impedance
ZS2I=imag(Z2/s0); %obtain imaginary part of specific
acoustic impedance

%plot real part of mechanical impedance vs frequency (Hz)
by micro 2
plot(f,Z2R);xlabel('Frequency(Hz)','FontSize',12,'FontWeigh
t','bold','Color','r');ylabel('Real Part of Mechanical
Impedance','FontSize',12,'FontWeight','bold','Color','r');
grid on
hold on

%plot imaginary part of mechanical impedance vs frequency
(Hz) by micro 2
plot(f,Z2I);xlabel('Frequency(Hz)','FontSize',12,'FontWeigh
t','bold','Color','r');ylabel('Imaginary Part of Mechanical
Impedance','FontSize',12,'FontWeight','bold','Color','r');
grid on
hold on

%plot real part of specific acoustic impedance vs frequency
(Hz) by micro 2
plot(f,ZS2R);xlabel('Frequency(Hz)','FontSize',12,'FontWeig
ht','bold','Color','r');ylabel('Real Part of Specific
Acoustic
Impedance','FontSize',12,'FontWeight','bold','Color','r');
grid on
hold on

%plot imaginary part of specific acoustic impedance vs
frequency (Hz) by micro 2
plot(f,ZS2I);xlabel('Frequency(Hz)','FontSize',12,'FontWeig
ht','bold','Color','r');ylabel('Imaginary Part of Specific
Acoustic
Impedance','FontSize',12,'FontWeight','bold','Color','r');


%micro 3
```

```
z3=(p3.*cos(k*l)-
1i*dens*c*v*sin(k*X3))./(dens*c*v*cos(k*X3)-
p3.*sin(k*l)*1i); %calculate specific acoustic impedance
ratio
Z3=z3*(dens*c*s0); %calculate mechanical impedance
R3=(z3-1)./(z3+1); %calculate reflection factor
alpha3=ones(1,4981)-abs(R3).^2; %calculate absorption
coefficient

%plot absorption coefficient vs frequency (Hz)
plot(f,alpha3,'b');xlabel('Frequency(Hz)','FontSize',12,'Fo
ntWeight','bold','Color','r');ylabel('Absorption
Factor','FontSize',12,'FontWeight','bold','Color','r');

Z3R=real(Z3); %obtain real part of mechanical impedance
Z3I=imag(Z3); %obtain imaginary part of mechanical
impedance
ZS3R=real(Z3/s0); %obtain real part of specific acoustic
impedance
ZS3I=imag(Z3/s0); %obtain imaginary part of specific
acoustic impedance

%plot real part of mechanical impedance vs frequency (Hz)
by micro 3
plot(f,Z3R);xlabel('Frequency(Hz)','FontSize',12,'FontWeigh
t','bold','Color','r');ylabel('Real Part of Mechanical
Impedance','FontSize',12,'FontWeight','bold','Color','r');
grid on
hold on

%plot imaginary part of mechanical impedance vs frequency
(Hz) by micro 3
plot(f,Z3I);xlabel('Frequency(Hz)','FontSize',12,'FontWeigh
t','bold','Color','r');ylabel('Imaginary Part of Mechanical
Impedance','FontSize',12,'FontWeight','bold','Color','r');
grid on
hold on

%plot real part of specific acoustic impedance vs frequency
(Hz) by micro 3
plot(f,ZS3R);xlabel('Frequency(Hz)','FontSize',12,'FontWeig
ht','bold','Color','r');ylabel('Real Part of Mechanical
Impedance','FontSize',12,'FontWeight','bold','Color','r');
grid on
hold on

%plot imaginary part of specific acoustic impedance vs
```

```
frequency (Hz) by micro 3
plot(f,ZS3I);xlabel('Frequency(Hz)','FontSize',12,'FontWeig
ht','bold','Color','r');ylabel('Imaginary Part of Specific
Acoustic
Impedance','FontSize',12,'FontWeight','bold','Color','r');
```

5. Calculations by Analytical Model of Three-Microphone Method

```
n=1; % set count n as 1
ALPHA=zeros(1,4981); %empty matrix to store absorption
coefficient values
RS=zeros(1,4981); %empty matrix to store reflection factor
values

while n<4982; % end condition of loop
A=[exp(1i*k(n)*2*X1)+exp(1i*k(n)*2*X2)+exp(1i*k(n)*2*X3),3;
3,exp(1i*k(n)*2*(-X1))+exp(1i*k(n)*2*(X2))+exp(1i*k(n)*2*(-
X3))]; % [A]'*[A] matrix
AA=[exp(1i*k(n)*X1),exp(1i*k(n)*X2),exp(1i*k(n)*X3);exp(1i*
k(n)*(-X1)),exp(1i*k(n)*(-X2)),exp(1i*k(n)*(-X3))];
% [A]' matrix
AAA=inv(A)*AA*[p1(n);p2(n);p3(n)];
r=AAA(2)/AAA(1); %reflection factor
RS(n)=r; % put reflection factor into empty matrix which
store reflection factor values
alpha=1-(real(r))^2-(imag(r))^2; %absorption coefficient
ALPHA(n)=alpha; % put absorption coefficient into empty
matrix which store absorption coefficient values
n=n+1;
end

%plot absorption coefficient vs frequency (Hz)
plot(f,ALPHA,'r');xlabel('Frequency(Hz)','FontSize',12,'Fon
tWeight','bold','Color','r');ylabel('Absorption
Factor','FontSize',12,'FontWeight','bold','Color','r');

ZM=dens*c*s0*(ones(1,4981)+RS)./(ones(1,4981)-RS);
%calculate mechanical impedance
ZS=dens*c*(ones(1,4981)+RS)./(ones(1,4981)-RS); %calculate
specific acoustic impedance

ZMR=real(ZM); %obtain real part of mechanical impedance
ZMI=imag(ZM); %obtain imaginary part of mechanical
impedance
ZSR=real(ZS); %obtain real part of specific acoustic
```

```
impedance
ZSI=imag(ZS); %obtain imaginary part of specific acoustic
impedance

%plot real part of mechanical impedance vs frequency (Hz)
plot(f,ZMR);xlabel('Frequency(Hz)','FontSize',12,'FontWeigh
t','bold','Color','r');ylabel('Real Part of Mechanical
Impedance','FontSize',12,'FontWeight','bold','Color','r');
grid on
hold on

%plot imaginary part of mechanical impedance vs frequency
(Hz)
plot(f,ZMI);xlabel('Frequency(Hz)','FontSize',12,'FontWeigh
t','bold','Color','r');ylabel('Imaginary Part of Mechanical
Impedance','FontSize',12,'FontWeight','bold','Color','r');
grid on
hold on

%plot real part of specific acoustic impedance vs frequency
(Hz)
plot(f,ZSR);xlabel('Frequency(Hz)','FontSize',12,'FontWeigh
t','bold','Color','r');ylabel('Real Part of Specific
Acoustic
Impedance','FontSize',12,'FontWeight','bold','Color','r');
grid on
hold on

%plot imaginary part of specific acoustic impedance vs
frequency (Hz)
plot(f,ZSI);xlabel('Frequency(Hz)','FontSize',12,'FontWeigh
t','bold','Color','r');ylabel('Imaginary Part of Specific
Acoustic
Impedance','FontSize',12,'FontWeight','bold','Color','r');

%error analysis of Three-Microphone Method
m=1; % set count m as 1
RESIDUL=zeros(1,4981); %empty matrix to store residual
error values
while m<4981; % end condition of loop
residul=[p1(m);p2(m);p3(m)]-[exp(1i*k(m)*X1),exp(1i*k(m)*(-
X1));exp(1i*k(m)*X2),exp(1i*k(m)*(-
X2));exp(1i*k(m)*X3),exp(1i*k(m)*(-X3))]*AAA; %calculate
residual error
RESIDUL(m)=sqrt(abs(residul(1))^2+abs(residul(2))^2+abs(res
idul(3))^2); % put residual error into empty matrix which
store residual error values
```

```
m=m+1;
end

%plot residual error vs frequency (Hz)
plot(f,RESIDUL);xlabel('Frequency(Hz)','FontSize',12,'FontW
eight','bold','Color','r');ylabel('Residual
Error','FontSize',12,'FontWeight','bold','Color','r');
```